



**UNIVERSITY OF  
KWAZULU-NATAL**

---

**INYUVESI  
YAKWAZULU-NATALI**

**DYNAMIC STABILITY AND BUCKLING OF VISCOELASTIC PLATES  
AND NANOBAMS SUBJECT ED TO DISTRIBUTED AXIAL FORCES**

BY

MOUAFO TEIFOUE T Arman d Robinson 213574523

Submitted in fulfilment of the academic requirements for the degree of Doctor of

Philosophy in Mechanical Engineering

School of Engineering

College of Agriculture, Engineering and Science

University of KwaZulu-Natal

Durban

South Africa

August 2016

SUPERVISOR: Professor SARP Adali

## SUPERVISOR' S DECLARAT ION

As the candidate's supervisor, I agree/do not agree to the submission of this thesis.

Signed \_\_\_\_\_ Date \_\_\_\_\_

Professor SARP Ad ali

## DECLAR ATION 1: PLAGIARISM

I, MOUAFO TEIFOUET Ar mand Robi nson declare that:

(i) The research reported in this dissertation, except where otherwise indicated, is my original work.

(ii) This dissertation has not been submitted for any degree or examination at any university.

(iii) This dissertation does not contain other person's data, pictures, graphs or other information, unless specifically acknowledged as being sourced from other persons.

(iv) This dissertation does not contain other person's writing, unless specifically acknowledged as being sourced from other researchers. Where written sources have been quoted, then:

a) their words have been re-written but the general information attributed to them has been referenced;

b) where their exact words have been used, their writing has been placed inside quotation marks, and referenced.

(v) Where I have reproduced a publication of which I am an author, co-author or editor, I have indicated in detail which part of the publication was actually written by myself alone and have fully referenced such publication.

(vi) This dissertation does not contain text, graphics or tables copied and pasted from the Internet, unless specifically acknowledged, and the source being detailed in the dissertation and in the References sections.

Signed \_\_\_\_\_ Date \_\_\_\_\_

MOUAFO TEIFOUET Arm and Robi nson

## DECLARATION 2: PUBLICATIONS

### Conference:

Mouafo Teifouet and Sarp Adali, Variational formulation and solution for buckling of elastically restrained nonlocal carbon nanotubes under distributed axial loads, 7th World Nano conference, June 20-21, 2016, Cape Town, South Africa. poster

### Journal publications

Mouafo Teifouet Armand Robinson, Sarp Adali, Nonconservative stability of viscoelastic rectangular plates with free edges under uniformly distributed follower force, International Journal of Mechanical Sciences, 107 (2016) 150-159.

Mouafo Teifouet Armand Robinson and Sarp Adali, Nonconservative stability of viscoelastic rectangular plates subjected to triangularly distributed tangential follower loads, submitted to Journal of Theoretical and Applied Mechanics.

Mouafo Teifouet Armand Robinson and Sarp Adali, Dynamic stability of viscoelastic plates under axial flow by differential quadrature method, accepted to be published in Engineering Computations

Mouafo Teifouet Armand Robinson, Sarp Adali, Variational solution for buckling of nonlocal carbon nanotubes under uniformly and triangularly distributed axial loads, Composite Structures 156 (2016) 101–107

Mouafo Teifouet Armand Robinson, Sarp Adali, Buckling of nonuniform carbon nanotubes under concentrated and distributed axial loads with application to nanocones, submitted to Mechanics Research and Communications.

Mouafo Teifouet Armand Robinson and Sarp Adali, Variational formulation and solution for buckling of elastically restrained nonlocal carbon nanotubes under distributed axial loads, in preparation.

Signed \_\_\_\_\_ Date \_\_\_\_\_

MOUAFO TEIFOUET Armand Robinson

## ABSTRACT

Plates and beams are typical examples of structures that must be analyzed and understood. Buckling and vibration represent for such structures a potential source of fatigue and damage. Damage and fatigue are often caused by axial forces. The current research uses differential quadrature method to study the stability of viscoelastic plate subjected to follower forces in one hand, and the Rayleigh-Ritz method to analyze the buckling of Carbone nanotubes subjected to point and axial load in other hand.

For plate, the 3D relation of viscoelastic is used to derive the equation of vibration of viscoelastic rectangular plate subjected to follower force. This equation is solved numerically by differential quadrature method, then the dynamic stability analysis is done by plotting the eigenvalues versus the follower force.

We employ the Euler Bernoulli beam theory and the nonlocal theory to derive the equation of equilibrium of Carbone nanotubes subjected to point and axial loads. Rayleigh-Ritz method is used to calculate buckling loads, and the effects of equation's parameters on that buckling loads are analysed properly.

Frequencies of vibration of viscoelastic plates and critical load obtained by using differential quadrature method are compared to other results with good satisfaction. The same satisfaction is observed when the buckling load values of Carbone nanotubes obtained using the Rayleigh-Ritz methods are compared to those existing in the literature.

The cantilever viscoelastic plate undergoes flutter instability only and the delay time appears to influence that instability more than other parameters. The SFSF plate undergoes divergence instability only. The both types of instability are observed CSCS plate subjected to uniformly follower load but the flutter instability disappears in presence of triangular follower load. The values of the mentioned critical loads increase with triangular follower load for all boundary conditions. The aspect ratio has a large influence on the divergence and flutter critical load values and little influence on the instability quality. The laminar friction coefficient of the flowing fluid increases the critical fluid velocity but its effect on the stability of viscoelastic plate behavior is minor.

The nonlocal parameter appears to decrease buckling load considerably. Buckling is more sensitive to the magnitude of the tip load for the clamped-free boundary conditions. The application of the present theory to a non-uniform nanocone shows that the buckling loads increases with radius ratio and decreases with small scale constants.

## RESUME (In French)

Les plaques et les poutres sont des exemples typiques de structures qui doivent être analysées et comprises. Le flambement et les vibrations représentent pour de telles structures une source potentielle de fatigue et de dommages. Ces dommages et fatigue sont souvent causés par des forces axiales. La présente étude utilise la méthode de la quadrature différentielle pour étudier la stabilité de la plaque viscoélastique soumise à des forces axiales nonconservatives d'une part, et la méthode de Rayleigh-Ritz pour analyser le flambement des nanotubes de Carbone soumis à la charge ponctuelle et axiale d'autre part.

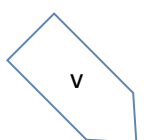
Pour la plaque, la relation 3D de la viscoélasticité est utilisée pour dériver l'équation de vibration de la plaque rectangulaire viscoélastique soumise à la force nonconservative. Cette équation est résolue numériquement par la méthode de quadrature différentielle, ensuite l'analyse de stabilité dynamique est étudiée en traçant l'évolution des valeurs propres de la fréquence en fonction des charges.

Nous utilisons la théorie des poutres d'Euler Bernoulli et la théorie non locale pour dériver l'équation d'équilibre des nanotubes de Carbone soumis à des charges ponctuelles et axiales. La méthode de Rayleigh-Ritz est utilisée pour calculer les charges de flambage et les effets des paramètres de l'équation sur les charges de flambage sont analysés correctement.

Les fréquences de vibration des plaques viscoélastiques et de la charge critique obtenues en utilisant la méthode de quadrature différentielle sont comparées à d'autres résultats avec une bonne satisfaction. La même satisfaction est observée lorsque les valeurs de charge de flambage des nanotubes de carbone obtenus en utilisant les méthodes de Rayleigh-Ritz sont comparées à celles existant dans la littérature.

La plaque viscoélastique en porte-à-faux ne subit que l'instabilité dynamique alors que la viscosité semble influencer cette instabilité plus que d'autres paramètres. La plaque SFSF subit une instabilité divergence seulement. Les deux types d'instabilité sont observés sur la plaque CSCS soumise à des forces uniformément réparties, mais l'instabilité dynamique disparaît en présence de charge nonconservative triangulaire. Les valeurs des charges critiques augmentent avec la charge triangulaire pour toutes les conditions aux limites considérées. Le rapport des dimensions de la plaque a une grande influence sur les charges de divergence et de charges critiques du flottement et peu d'influence sur la qualité de l'instabilité. Le coefficient de frottement laminaire du fluide s'écoulant augmente la vitesse critique du fluide mais son effet sur la stabilité du comportement de la plaque viscoélastique est mineur.

Le paramètre non local semble diminuer considérablement la charge de flambage. Ce flambage est plus sensible à l'amplitude de la charge ponctuelle pour les conditions aux limites encastre-libre. L'application de la présente théorie aux nanocône non uniforme montre que les charges de flambement augmentent avec le rapport de rayons et diminuent avec des constantes non locales.



## ACKNOWLEDGMENTS

Many people encouraged me, helped me and supported me from the time I applied for PhD at UKZN till this day of its completion. This is reason why for me, it could be a less majesty keep the mouth shut about what everyone has done.

First of all, I like to thank my supervisor Prof ADALI, who accepted to supervise this thesis despite his very busy schedule. My deepest gratitude also goes to my parents, brothers and sisters who supported me financially, and morally. It was a big deal at the beginning, but we can say "thank you" to our ancestors who made everything possible. To my lovely wife Dongmo, I will say love makes two people very close despite distance. Thanks for your love and your affection. At the University of DSCHANG I will first of all say thanks to the Vice Chancellor Professor TSAFACK NANFOSSO who understood me and permitted me to take a study leave for PhD research. Many thanks to what you have been doing to PhD students since you arrived at UDS. Thanks to Professor NGAMENI, the Dean of the faculty of Sciences at UDS for his kindness and expeditious reaction about signing my documents. I really appreciated your way of management. To Mme ZEBAZE Jenatus, the Dean's secretary, I will say thanks dear sister for all the priceless advices. Thanks to my colleagues Dr KAMDEM and Dr KOUMETIO for all their encouragements. I am very grateful to Pravesh Moodley for his help during the first step of my registration at UKZN. Many thanks to his Majesty FOSSOKENG SOLEFACK Simon, the chief of Batsengla community for all his help. You are the community chief who always care about all his people. My heartfelt thanks to Professor TAPAMO Jules Raymond for all his advices and encouragements during this work. I would finally be thankful to the International student office of UKZN for their contributions concerning my first trip to South Africa.

## TABLE OF CO NTENTS

SUPERVISOR’S DECLARATION.....	ii
DECLARATION 1: PLAGIARISM.....	ii
DECLARATION 2: PUBLICATIONS.....	iii
ABSTRACT.....	iv
RESUME (In French).....	v
ACKNOWLEDGMENTS.....	vi
TABLE OF CONTENTS.....	vii
LIST OF TABLES.....	ix
LIST OF FIGURES.....	ix
NOMENCLATURE.....	x
ABBREVIATIONS.....	xii
CHAPTER1: INTRODUCTION.....	1
1.1-Motivations and aims.....	1
1.2-Objective.....	2
1.3-Thesis structure.....	3
CHAPTER 2: LITERAURE REVIEW.....	4
2.1-Follower forces.....	4
2.2-The Differential quadrature method (DQM).....	7
2.3-Carbon Nanotubes.....	8
2.4-Rayleigh-Ritz method.....	9
2.5-References.....	11
CHAPTER 3: BASIC CONCEPTS FOR RECTANGULAR PLATES THEORY, VISCOELASTICITY AND DIFFERENTIAL QUADRATURE METHOD.....	18
3.1-Introduction.....	18
3.2-Basic definitions.....	18
3.3-Basic assumptions.....	19
3.4-Constitutive relations and equation of vibration.....	19
3.4.1-The displacement and strain.....	19
3.4.2-Stress, resultant and stress couples.....	21

3.4.3-Moments and shear forces.....	22
3.5-Viscoelastic plate subjected to follower force $T(x)$ and transversal force $p$ .....	23
3.5.1-The viscoelasticity.....	23
3.5.2- The viscoelastic equation.....	24
3.6-Differential quadrature method.....	26
3.6.1-The form of weighting coefficients.....	26
3.6.2-The choice of discrete points: The $\delta$ -technics.....	27
3.6.3-Treatment of boundary conditions.....	28
3.6.3a-Modification of weighting coefficient matrices.....	28
3.6.3b-Coupling boundary conditions with general Equation (CBCGE=general approach).....	29
3.7-References.....	29
 CHAPTER4-PAPER 1: NONCONSERVATIVE STABILITY OF VISCOELASTIC RECTANGULAR PLATES WITH FREE EDGES UNDER UNIFORMLY DISTRIBUTED FOLLOWER FORCE.....	31
 CHAPTER 5-PAPER 2: NONCONSEVATIVE STABILITY OF VISCOELASTIC RECTANGULAR PLATES SUBJECTED TO TRIANGULARLY DISTRIBUTED TANGENTIAL FOLLOWER LOADS.....	42
 CHAPTER 6-PAPER 3: DYNAMIC STABILITY OF VISCOELASTIC PLATES UNDER AXIAL FLOW BY DIFFERENTIAL QUADRATURE METHOD.....	58
 CHAPTER 7: BUCKLING OF NONLOCAL NANOBEAM.....	76
7.1-Introduction.....	76
7.2-The basic definitions and origin of Carbon nanotubes.....	76
7.3-Equation of buckling of the CNT considered as nanobeam.....	79
7.3.1-displacement and stress distribution on the nanobeam.....	79
7.3.1a-The displacement.....	79
7.3.1b-The stress of nanobeam.....	79
7.4-Equilibrium equation of axially loaded of nanobeam.....	81
7.5-Weak form derivation for axially loaded elastically restrained nanobeam.....	82
7.6-The Rayleigh-Ritz method on solving buckling of CNT.....	83
7.7-References.....	83

CHAPTER 8-PAPER 4: VARIATIONAL SOLUTION FOR BUCKLING OF NONLOCAL CARBON NANOTUBES UNDER UNIFORMLY AND TRIANGULARLY DISTRIBUTED AXIAL LOADS.....	85
CHAPTER 9-PAPER 5: BUCKLING OF NONUNIFORM CARBON NANOTUBES UNDER CONCENTRATED AND DISTRIBUTED AXIAL LOADS WITH APPLICATION TO NANOCONES.....	93
CHAPTER 10: GENERAL CONCLUSION AND FUTURE PROSPECTS.....	103
10.1-Conclusion.....	103
10.2-Future prospects.....	106

### LIST OF TAB LES

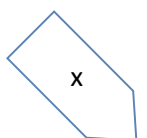
Tab. 7.1. Comparison of Thermal and electrical conductivity of CNT with some materials.....	77
---	----

### LIST OF FIGU RES

Fig. 3.1: Displacement and strain of rectangular plate.....	20
Fig. 3.2: Stress repartition on the plate’s slice.....	21
Fig. 3.3: Moments and shear forces on a rectangular plate’s slice.....	22
Fig. 3.4: (a) Creep response, (b)relaxation response, (c) hysteresis loop of viscoelastic solid material.....	23
Fig.3.5: Viscoelastic models: (a) Kelvin-Voigt , (b) Maxwell (c) Solid standard .....	23
Figure 3.6: Differential quadrature domain discretization for rectangular plate.....	29
Fig.7.1: Schematic diagrams of (a) single-wall nanotube (SWNT) and (b) multi-wall nanotube (MWNT).....	76
Fig.7.2: Free body diagram of nanobeam.....	79

## NOMEN CLATUR E

$\alpha$	Nonlocal kernel function
$\sigma(t)$	Time dependant stress
$\sigma_0$	Initial Stress
$\varepsilon(t)$	Time dependant strain
$\varepsilon_0$	Initial Strain
$\eta$	Viscoelasticity coefficient
$\varepsilon_s$	Static strain
$\varepsilon_d$	Dynamic strain
$\rho$	Mass density of plate's material
$\nu$	Poisson's coefficient
$\delta_{ij}$	Kronecker symbol
$\omega$	Eigenfrequency of viscoelastic rectangular plate.
$\lambda$	Aspect ratio of rectangular plate
$\lambda_L, \mu_L$	Lame parameters
$\mu$	Dimensionless small scale parameter of nanobeams
$\phi_j$	Approximating function of Rayleigh-Ritz method
$\Delta$	Laplacian
a, b	Dimensions of rectangular plate on X and y axe respectively
$A_j, B_j$	Weighting coefficients along X and Y direction respectively
$C_j$	Coefficients of Rayleigh-Ritz series
$e_{ij}, \varepsilon_{ii}$	Deviatoric and spherical component of strain tensor respectively



$E$	Young's modulus
$f_j$	Body force for nonlocal nanobeam
$G, K$	Shear modulus and bulk modulus respectively
$h$	Width of rectangular plate
$H$	Dimensionless viscoelasticity coefficient
$L$	Length of carbon nanotube
$M_{nl}$	Moment for nonlocal nanobeams
$N_x$	Axial force acting on nonlocal nanobeams
$N, M$	Number of discretized domain of plate along $X$ and $Y$ direction respectively
$\bar{P}_0, \bar{Q}_0, \bar{Q}_1$	Laplace transformation of reduced viscoelastic operators
$q$	Dimensionless follower force acting on plate
$S_{bd}, S_{bb}$	Matrices of boundary domain of differential quadrature method
$S_{db}, S_{dd}$	Matrices of interior (working domain) in differential quadrature method
$s_{ij}, \sigma_{ii}$	Deviatoric and spherical component of stress tensor respectively
$t$	Time
$T_x$	Generalised follower force
$u, v, w$	Plate displacement component with respect to $x, y, z$ respectively
$V$	Nano body volume
$W_b, W_d$	Displacement vectors of boundary and working domain respectively in differential quadrature method.
$W_{ij}$	Discretized displacement of rectangular plate.
$(x, y, z)$	Cartesian coordinates
$X_i, Y_j$	Discretized points of rectangular plate along $X$ and $Y$ respectively

## ABBREVIATIONS

1D	One dimensional
2D	Two dimensional
3D	Three Dimensions
CBGE	Coupling boundary conditions with general equation
CFFF	Plate with one edge Clamped and three others free
CNT	Carbon nanotube
CSCS	Plate with two opposite edges simply supported and two others clamped
CTP	Classical plate theory
DQM	Differential Quadrature Method
FEDQM	Finite element differential quadrature method
FDDQM	Finite difference differential quadrature method
HDQM	Harmonic Differential quadrature method
MGDQM	Modified generalized differential quadrature method
MWNT	Multi-walled nanotube
RBS-DQ	Radius-based differential quadrature
SDQM	Spline-based differential quadrature method
SFSF	Plate with two opposite edges simply supported and two others free
SSSS	Simply supported plate in its four edges
SWNT	Single walled nanotube

## CHAPTER 1: INTRODUCTION

### 1.1-Motivations and aims

In the present work the subjects studied are the dynamic stability of viscoelastic rectangular plates subjected to distributed follower forces, and the effect of point and axial forces on the buckling of uniform and nonuniform nanotubes.

Plate structures have been found to be very useful in many domains of modern technology like aeronautic, automotive, and offshore structures. During the evolution of science, some new materials have been discovered which can reinforce the above mentioned plates structures to make them more strong. These new materials are carbon nanotubes, considered nowadays as the strongest material and therefore very attractive to scientists because of their wide usefulness even for African countries. For example nano filters produced with CNTs are useful for water purification which reduces many illnesses, increasing therefore the life expectancy of poor population. CNTs are also useful for solar cell production for electricity generation, very useful for villages with lack of electricity.

Both plate and CNT in their respective environment of existence may be subjected to many forces which are able to change their behaviours characteristics or even create damage. Among them the follower forces can be named. Defined as forces which change with the deformation of structure on which they act, viz., which "follow" the behaviour of that structure, follower forces have been classified as nonconservative because their work are path dependant. The structures on which they act are nonconservative systems. One can found this kind of forces in many domain in real life. These domains include aeronautic (Engine thrust action on the wings of aircraft during flight), automobile industry (Force acting on rotating disk for automobile's disk brake), biological system (Forces acting on lumbar spine for human being when standing), civil engineering (cantilever pipe conveying fluid)...etc. Past researchers have demonstrated that such forces can generate vibration of system on which they act as well as buckling which are risky most of the time in structural engineering.

It is known also that the type of force, the characteristics of the structure where the forces act, the structure's geometry, the support conditions highly influence their sensitivity to vibration and buckling, reason why it is always important to identify the characteristics which influence the most the behaviour of these structures in order to optimise final products during the manufacturing processes.

For nonconservative viscoelastic rectangular plate, many parameters have been identified to influence their instability, and among them one important has found to be boundary conditions. The boundary conditions have been discovered to play a crucial role as they may change qualitatively and /or quantitatively the type of instability which occurs. Many works have been presented in the past in this regard and only the combined simply supported and clamped boundary conditions were considered. Free boundary has not yet been studied and it is understandable, because here the mathematical formulation depends on two space variables and consequently not easy to implement numerically. In this thesis free boundary conditions will be taken into account and their effect on instability will be studied in details. The triangular follower force as well as fluid deducted follower force is also carry out with many considerations.

On the other hand, it has been proved that CNTs can buckle on the effect of follower forces or point forces. Contrarily to other existing structures where buckling is just destructive, it appears to be also beneficial for CNTs as it increases their thermal conductivity. Many studies have been done concerning the CNTs but, only vibration has carry attention of researchers, contrarily to buckling which has been very pettily drawn their attention. Furthermore, the buckling of non-uniform or elastically restrained CNTs subjected to follower forces have not yet been studied. This research will try to break the previously lacks, precisely by focussing on the effects of combined tip forces and follower forces on the buckling of non-uniform and elastically restrained CNTs, as well as the influence of boundary conditions.

## 1.2-Objectives

The main objectives of this thesis are:

First study the dynamic stability of viscoelastic rectangular plates subjected to distributed follower force and evaluate the accuracy of differential quadrature method for such problem. The second objective is to study the combined effect of point and axial loads on the buckling of CNTs, as well as accuracy of Rayleigh-Ritz method. Many steps must be followed as enumerated below:

1-Implementing free boundary condition in the differential quadrature method in order to solve two dimensional plate instability problem.

2-Investigate the effect of triangular follower forces on the rectangular plate and compare its effects with uniform follower forces.

3- Study in detail the role played by the flowing fluid induced follower forces as well as its velocity in the stability of viscoelastic rectangular plate.

4-Analyze the effects of combined tip forces and follower forces on the buckling of CNTs considered as one dimensional nanobeams.

5- Compare the accuracy of Rayleigh-Ritz method on the study of buckling of non-uniform CNTs with existing results as well as the effects of elastic restrains.

### 1.3-Thesis structure

For the total comprehension about what is developed in this thesis the following structure is adopted:

Chapter 1 Introduces the thesis by enlightening the motivation, objectives, aims and the plan of the thesis. Chapter 2 presents the literature survey. In Chapter 3, we firstly establish the mathematical equation governing the viscoelastic rectangular plate subjected to tangential follower force. Secondly, the differential quadrature's domain discretisation and implementation of boundary condition are explained in details. Chapter 4 is a research paper 1 which studies the instability analysis of nonconservative rectangular plate with free edges using differential quadrature method. It is followed by Chapter 5 which is research paper 2. In this chapter, we compare the effect of uniform and triangular follower loads on the vibration behaviour of viscoelastic rectangular plate. Chapter 6 is Paper 3 presenting flow generated follower loads on the vibration of viscoelastic rectangular plate.

Chapter 7 consists firstly of the global presentation of the carbon nanotubes, followed by the establishment of the mathematic equations governing the buckling of Carbon nanotubes, considered as nanobeams, by using the nonlocal theory. Thirdly, the weak formulation principle is explained for the nanobeam with general boundary conditions and subjected to follower forces. This chapter ends with the explanation of how to solve the buckling problem of CNTs via Rayleigh-Ritz method. Chapter 8 is Paper 4, devoted to the study of buckling of carbon nanotubes subjected to point load, uniform distributed and triangular follower loads.

Chapter 9 or Paper 5 studies the buckling of non-uniform Carbon nanotubes subjected to point, uniformly distributed and triangular distributed loads. This thesis ends up with Chapter 10, where the general conclusion of the whole work as well as future prospects are presented.

## CHAPTER 2: LITERATURE REVIEW

### 2.1-Follower forces

Bolotin [1] was among one of the first authors who studied the follower forces. He considered them as nonconservative forces because that kind of forces have no potential. He extended the Euler theory of elasticity, on the study of such compressive forces applied on the bar, which rotate together with the end section of that bar, and remain tangential to its deformed axis. He left the question of existence of such "Follower" forces open as he questioned himself about their existences in real life although their completely known mathematical formulations. He stated that the energy supply of systems subjected to above mentioned forces could come from two sources: The change with time of angle between the deformed and initial axis of the bar, or its linear displacement. Nevertheless, Bolotin attributed the behaviour of some existing forces in engineering systems, the term "follower forces": These are for example the system formed the reaction of jet attached at the end of the bar, in case the system is undamped and when inertia effects are absent. He carefully explained also that, all his assumptions about follower forces and other previous studies were done without any experiment, and proposed that, further, every researcher should try as soon as he can, to make the theory of follower forces accurately representing the existing forces in real practices. He was followed by Hermann [2] who studied some mechanical models of one dimensional structures subjected to follower forces. Those systems include two degree of freedom and some models were built in order to compare their behaviours with existing mathematical models. This can be found also in the book written later by Leipholz [3] who thought that flutter instability [4] is not just present for time-dependant forces, but can be present also for time independent forces like follower forces. Following that approach, Smith and Herrmann [5], Sundararajan [6], Celep [7], Sinha and Pawlowski [8], Kim et al. [9], Djondjorov and Vassilev [10] investigated the stability of beams and columns subjected to follower forces including effects of elastic foundation on the stability of systems. In these studies, boundary conditions of beams, plates and columns play a great role in the stability. Among them the cantilever beams (clamped-free) was widely studied, because of its more practical aspects. Precisely, De Rosa and Franciosi [11] carried out research on intermediate support on Beck's, Leipholz's, Hauger's and Pfluger's rods. Obtained eigenvalues were solved and the results obtained for critical divergence or flutter loads converge for every considered case with the existing one. Also flutter or divergence instability may depend on where the intermediate support is situated along the considered rod. In 2007 Shvartsman

[12] studied the stability of spring-hinged large deflexion beams subjected to tip follower force, normal to the beams. He used the non-iterative method to solve a problem and concluded of the existence of only flutter instability on such system. He concluded in [13] that flutter instability appears to be the only instability type which is found on cantilevered beam subjected to intermediate follower forces and it is independent on the angle between the follower force's angle of inclination; idea which was followed later by Mutyalarao et al. [14]. Stability of cracked beams [15] or nonlinear beams [16, 17] subjected to follower forces was also studied.

Although it's worth mentioning all scientists who spent many years studying systems subjected to follower forces, let say that, this subject of research has not been unanimously accepted , creating therefore a controversy.

In fact Koiter [18] in 1996 published a titled "unrealistic follower forces", demonstrating that such forces were not existent practically and proposed "elimination of the abstraction of follower forces as external loads from the physical and engineering literature on elastic stability" while Sugiyama et al [19] replied by the paper titled "realistic follower forces" emphasizing on the existence of follower forces, and citing some physical systems where such forces can be observed, after have recognised the lack of experimental on the subject. For example he said that the follower forces can be observed in a hose in a pool, he also qualified a squeezing force acting on a rotating disk as nonconservative follower forces. Some other systems were cited such as rocket and pipe conveying fluids or aerospace systems. Following the same idea, Langthjem [20] firstly emphasized that, the feasible system to realize follower forces is cantilever pipe conveying fluids, but recognised that although many theoretical and inapplicable research were carried out about the follower loads, many problems of structural stability found solutions through the above study. Beck's, Reut's, Leipholz's and Hauger's columns were studied in detail, with experimental analysis for Beck's and Reut's columns. This analysis showed that, experimental results were close to the analytical ones. He recognised Leipholz's column of being realized in an automobile brake system, where noise due to dynamic or parametric instability (brake squeal) is a well-known environmental problem.

The above mentioned divergence between Koiter and Sugiyama permitted Elishakoff [21] to first remind the majority of researchers who published about follower forces, and tried his best to clarify each one's results. Nevertheless, he recognised that some experiments were realized by Willems [22], who obtained his experimental value for Beck's column close to theoretical one, only for 94% difference and said that experiment could have described a

theory if the experiment was carried accurately. He emphasized that follower force may be considered as useful model to describe some other forces, such as pipe conveying fluid, widely studied by Paidoussis et al. [23,24]. In conclusion, the author advised researchers to be careful in the using of some words, as "Beck's column", which, for him must represent Euler cantilevered columns, and not follower force, because experiments have not yet give their proof that Beck's columns are follower forces because, to be taken like that, there must be something tricky ("angel") in the consideration which role is to show how the direction of force must "follow" structure's deformation. Beck's columns for the present author has never been used to design structures, which doesn't mean they are inexistent but because it is not representing a well-known concrete model. After all these scientific battles, the study of follower forces continued, because many PhD thesis have been produced concerning the subject [25-27] and their effects have even extended to two dimensional structures like plates.

About plates, Datta and Biswas [28] recognized the existence of follower forces on vibrating aerospace structures like flexible wing panels subjected to jet thrust, considered here as plate-like structures. They added that, follower forces were nonconservative, and that their effect on the dynamic stability of aerostructures may depend on load direction control parameter, damping, or ply orientation for composites. Before this, many theoretical studies had already been performed on conservative rectangular plates. They include Zuo and Schreyer [29] who studied the stability of nonconservative simply supported rectangular plate and concluded that it experienced divergence stability which depends on the aspect ratio and on Poisson's coefficient. Kim and Park [30] studied the intermediate follower forces on rectangular plate and come out with the conclusion that, the region of application of the follower forces and aspect ratio had considerable influence on their stability. Adali [31] analytically studied the behaviour of 2D rectangular thin plate, subjected to non-conservative and conservative forces. He found out the existence of static and dynamic instabilities for both considered force's type. In his studies it appeared that, aspect ratio has a great effect on stability boundaries, physically and numerically. The effect of elastic foundation was also studied in his research, and what came out was that, the frequency parameter increases with elastic modulus. Poisson's coefficient found himself to increase, decrease or maintain the flutter frequency dependently on the values of aspect ratio or axial load magnitude. Gopal and Struthers [32] examined the effect of aspect ratio, follower force and the boundary conditions on buckling mode and buckling load for orthotropic plates subject to follower

forces and concluded that the orthotropic coefficient affects only the magnitude of the buckling load and the size of the stability regions.

Effect of viscoelasticity on the instability of plates subjected to follower forces was studied by Wang et al. [33] in details. He considered two boundary conditions: Simply supported and two opposite edges simply supported and two other clamped. For the simply supported plate, only divergence instability was observed, and its value highly depends on aspect ratio. For the plate with two opposite edges simply supported and other clamped, both divergence and flutter instabilities appear for squared plate and for small delay-time, contrarily to the plate with high aspect ratio who experiences only divergence instability. When the viscoelastic parameter increases, it significantly affects the plate with two opposite edges simply supported and others clamped, than the simply supported viscoelastic plate. Teifouet [34] extended the result by considering the nonlinear model of Wang et al. [33] and examined the effect of nonlinear parameter on the stability.

## 2.2-The Differential quadrature method (DQM)

Like finite element method or finite difference method the differential quadrature method is one of the most used numerical methods nowadays for solving problems in structural engineering, especially those dealing with plates and beams. It is important to recall that DQM was created in the 1970s by Bellman and Casti [35]. Knowing that the continued integration can be approximated by discrete sum, Bellman with his research team extended the theory for the expression of first derivative, which could therefore be expressed as linear sum including a so-called matrix coefficients, and then called it “differential quadrature” method. Later it was shown how this method could be suitable for solving linear and nonlinear partial differential equations [35-37] and, DQM rapidly became a preferred numerical method for solving problems involving higher order differential equations even for multidimensional domains [38,39]. This is why Faruk and Sliepcevich [40] published the paper titled "Differential Quadrature for Multi-dimensional Problems", where they applied the method to two and three dimensional problems in convection-diffusion and obtained good results. These results were very satisfactory after a comparison with those existing in the literature. Weighting coefficients obtained in DQM were centro-symmetric or skew symmetric as in [41,42]. Since they are the key of the method, their calculations need therefore to be done carefully. In fact, Du et al. [43] successfully overcame the drawback of existing calculations of weighting coefficients by introducing the Lagrange-based interpolating functions. The above mentioned functions allow henceforth to use the

differential quadrature method for solving any structural problem, with any number of grid points which can be distributed anyhow. He consequently solved problems previously encountered by Bellman et al. [44], who used the Legendre interpolating functions. Boundary conditions also could then be implemented well for any chosen problem, but accuracy for some problems particularly those including clamped and free boundaries will appear later to have some specifications about their treatments. This is why Bert and Malik [45] and Shu and Du [46] overcame the situation about the method of Boundary conditions implementation for structural 1D and 2D problems. Application to some system by Bert and Malik [47] like heat diffusion in a sphere, heat conduction, cooling/heating by combined convection and radiation were carried out and the obtained results were close to those existing in literature.

After overcoming the drawbacks existing in this methods in terms of weighting coefficients, number of grid points, implementation of boundary conditions, the utilization of DQM became easier for solving problems, particularly those involving 1D and 2D structures. Many versions of DQM were derived and they include Krowiak [48] who used spline –based interpolation functions (SDQM), and the obtained results were compared with those obtained, using Classical DQM. It appeared that SDQM may be more convergent when high degree polynomial functions are used for spline approximation. Civalek et al. [49] developed Harmonic differential quadrature (HDQ) where they suggested the trigonometric functions as approximation functions instead of polynomials and obtained good results. Global radius based DQ (RBS-DQ) was later proposed by Shu et al. [50] followed by Eftekhari and Jafari [51] with mixed Finite element Differential Quadrature Method (FEDQ), finite difference differential quadrature method (FDDQ) was proposed by Zhao et al. [52] or modified generalized differential quadrature (MGDQ) by Hsu [53].

Unfortunately none of the above mentioned DQM has been widely used as compared to the one employing Lagrange polynomials as approximating functions, commonly called DQM, because it appeared to be more accurate and simplest for problem solving [54-59] even those including nonuniform geometry [60], laminated plate's problems [61,62] or problems including nonlinearity [34].

### 2.3-Carbon Nanotubes

Since the discovery of CNTs by Iijima [63], this subject has become very attractive for researchers, regarding the number of scientific publications produced about the concern. This situation can be explained by the fact that experiments have revealed their exceptional

high Young's modulus in the range of Terapascal, their low density and their high heat and electricity conductivity [64-66]. It was for example demonstrated that, their excellent mechanical and electrical characteristics make them to be very useful as nanoscale fibres in composite materials. Their cylindrical graphitic structures make them to be mathematically modeled as one dimensional nanosize beams [67-70]. mathematical model takes into account nonlocal effects which means that, the stress in one point of CNTs depends on the all other point's strain of the structure, contrarily to local theory. Once the mechanical, geometrical and mathematical characteristics of such structures were well known, the study of their behavior when subjected to various type of load became important, as the obtained results are very useful for design in industries. Buckling appears as one of the most usually observable behavior of structures in general, and is therefore an interesting field of research. earlier researches on buckling of CNTs include Reddy [71] who revisited the existing theories of beams, namely Euler-Bernoulli, Timoshenko, Reddy, and Levinson beam's theories and rewrote them by using Eringen-nonlocal constitutive relations. After, he employed the variational principle analysis [72] to analytically calculate buckling loads of CNTs considered as nonlocal beams. The effect of nonlocal parameter on the buckling was discussed in details. The nonlocal parameter appeared to decrease the buckling loads. Reddy results will be later confirmed and extended in [73], [74] and [75]. Using the analytical and experimental analysis, Jeng et al. [76] studied the buckling instability of carbon nanotubes probes under nano indentation. They demonstrated that the local buckling is observed for longer nanotubes while shorter one undergo global buckling. Angle of inclination appears also to play a great role in the buckling, as lower inclination angle may create global buckling and higher creates local buckling for nanotubes.

Later, Reza et al. [77] emphasized that the Timoshenko beam theory can capture correctly the small-scale effects on buckling stains on short CNTs for the sheet-type buckling than other existing theories.

Among all the existing theories, Euler –Bernoulli nonlocal theory is mostly used to describe mathematically the CNTs because of its simplicity. This is observable though works of Peddieson et al. [78] where nonlocal differential elasticity approach were used to study the flexural behavior of CNTs. Many methods are currently employed to solve buckling problems of CNTs. These methods include Ritz method [79-83] Finite element method [84] or DQM [85].

## 2.4-Rayleigh -Ritz method

The Rayleigh-Ritz method [86, 87] has been widely used for solving problem in structural mechanics. These problems include vibration/buckling of beams and plates. It is worth to recall that, this method is the powerful technique which can be used for calculating natural frequencies of vibrating beams and plates. Its aim consists on linear combination of mathematical forms of deflection shape which satisfies a kinematic boundary conditions of buckling or vibrating structures.

Its utilization goes back up to more than half of century, as many previous works can demonstrate. In fact, in 1946, Bereuter [88] used Rayleigh-Ritz method for calculating the fundamental frequency of oblique plates, with all edges either simply supported or clamped, with concentrated mass at its center. The chosen trial transverse functions were trigonometric or polynomial functions. Fundamental frequency of clamped plate was calculated, but he was not able to find the trial admissible functions for simply supported oblique plate, this is why he used a finite difference method to solve that case but, unfortunately the obtained results were not accurate, due to the problem of domain discretization. In 1954, Warburton [89] studied the free transverse vibration of the rectangular plate by the use of Rayleigh-Ritz method. All 21 possible boundary conditions formed by free, simply supported and clamped were considered and all vibrating frequencies were calculated and many obtained values were close to those existing in the literature.

Later, characteristic orthogonal function as trial admissible functions of transverse displacement were introduced in the Rayleigh-Ritz approach, for either one dimensional [90, 91] or two dimensional [92-97] structures. The utilization of the above-mentioned method for nanobeams include the works presented by Behara and Chakravarty [98], where The Euler-Bernoulli and Timoshenko beam theories were used. The Rayleigh-Ritz method they used has considered simple and orthonormal polynomials and they observed the good convergence of the obtained results after comparison with those existing in the literature. The small scale effect on the vibrating frequencies and on deflection shapes were discussed.

Recently, Ghannadpour et al. [99] studied the buckling of nonlocal Euler-Bernoulli beams by using the Rayleigh-Ritz method. Four boundary conditions were considered during the analysis and buckling loads calculated, at the different values of nonlocal parameter. Comparisons made here concerning the buckling loads show the convergence of obtained results with previous ones, confirming once more the capacity of this method on solving nanobeams problems.

## 2.5-References

- [1] V.V Bolotin (1963). Nonconservative Problems of the Theory of Elasticity Stability. Pergamon Press , Oxford London
- [2] G. Herrmann (1971). Dynamics and stability of mechanical systems with follower forces. Stanford University, California, California 94305 Washington, D. C. Nasa cr-1782
- [3] H. H. E. Leipholz (1978). Stability of Elastic Structures, Springer Verlag, Wien.
- [4] I. Elishkoff, B. Couch (1987). Application of the symbolic algebra to the instability of the nonconservative system. Journal of Symbolic Computation 4, 391-396
- [5] T. E. Smith, G. Herrmann (1972). Stability of a beam on an elastic foundation subjected to a follower force. Journal of Applied Mechanics 39(2), 628-629
- [6] C. Sundararajan (1976). Stability of columns on elastic foundations subjected to conservative or nonconservative forces. Journal of Sound and Vibration 37, 79–85
- [7] Z. Celep (1980). Stability of a beam on an elastic foundation subjected to a nonconservative load. Journal of Applied Mechanics 47, 111–120
- [8] S. C. Sinha, D. R. Pawlowski (1984). Stability analysis of a tangentially loaded column with a maxwell type viscoelastic foundation. Acta Mechanica . 52, pp. 41–50
- [9] J-O. Kim, K.-S. Lee, J.-W. Lee (2008). Beam stability on an elastic foundation subjected to distributed follower force. Journal of Mechanical Science and Technology 22, 2386-2392
- [10] P. A. Djondjorov, V. M. Vassilev (2008). On the dynamic stability of a cantilever under tangential follower force according to Timoshenko beam theory. Journal of Sound and Vibration 311, 1431–1437
- [11] M. A. De Rosa ,C. Franciosi (1990). The influence of an intermediate support on the stability behaviour of cantilever beams subjected to follower forces. Journal of Sound and Vibration 137(1), 107-115
- [12] B. S. Schwartzman (2007). Large deflections of a cantilever beam subjected to a follower force. Journal of Sound and Vibration 304, 969–973
- [13] B. S. Schwartzman (2009). Direct method for analysis of flexible cantilever beam subjected to two follower forces. International Journal of Non-Linear Mechanics 44, 249-252
- [14] M. Mutyalarao, A. D. Bharathi, B. Nageswara Rao (2014). Equilibrium configurations of cantilever columns under a tip-concentrated subtangential follower force. Canadian Journal of Basic and Applied Sciences. vol. 02(02), 46-63
- [15] S. Z. Imiełowski, R. Z. Bogac (2007). Stability constraints in optimization of cracked columns subjected to compressive follower load. Engineering Transactions. 55(4), 281–292

- [16] H. Ahmadian and H. Azizi (2011). Stability analysis of a nonlinear jointed beam under distributed follower force. *Journal of Vibration and Control* , 17(1) 27–38
- [17] J. Przybylsky (1999). Instability regions for prestressed compound column subjected to a follower force. *Journal of Theoretical and Applied Mechanics* 37(1)
- [18] W. T. Koiter (1996). Unrealistic follower forces. *Journal of Sound and Vibration* 194(14)
- [19] Y. Sugiyama, M. A. Langthjem, B.-J. Ryu (1999). Realistic follower forces. *Journal of Sound and Vibration* 225(4), 779-782
- [20] M. A. Langthjem (2000). Dynamic stability of columns subjected to follower loads: a survey. *Journal of Sound and Vibration* 238(5)
- [21] I. Elishakoff (2005). Controversy associated with the so-called “follower forces”: critical overview. *Applied Mechanics Reviews, ASME* vol 58, 117-152
- [22] N. Willems (1966). Experimental verification of the dynamic stability of a tangentially loaded cantilever column. *Journal of Applied Mechanics*. 35, pp. 460–461
- [23] M. P. Paidoussis (1998) *Fluid-structure interactions slender structures and axial flow* volume 1, London Academic Press
- [24] M. P. Paidoussis, S. J. Price, E. de Langre (2011). *Fluid-Structure Interactions cross-flow-induced instabilities*, Cambridge University Press
- [25] B. S. Kim, (2011). A follower load as a muscle control mechanism to stabilize the lumbar spine. University of Iowa, PhD thesis
- [26] P. A. de Carvalho Pastilha. (2007). Structural optimization for flutter instability problems. *Engenharia Aeroespacial, Universidade Tecnica de Lisboa, Portugal* , Masters thesis
- [27] S. Chae, (2004). Effect of follower forces on aeroelastic stability of flexible Structures. School of Aerospace Engineering Georgia Institute of Technology, PhD thesis
- [28] P. K. Datta, S. Biswas (2011). International aeroelastic behaviour of aerospace structural elements with follower force: A Review. *Journal of Aeronautical and Space Sciences* 12(2), 134–148
- [29] Q. H. Zuo, H. L. Schreyer (1996). Flutter and divergence instability of nonconservative beams and plates. *International Journal of Solids and Structures*, Vol. 33, No. 9, pp. 1355-1367
- [30] J. H. Kim , J. H. Park (1998). On the dynamic stability of rectangular plates subjected to intermediate follower forces. *Journal of Sound and Vibration* 209(5), 882-888
- [31] S. Adali (1982). Stability of a rectangular plate under nonconservative and conservative forces. *International Journal of Solids and Structures* 18 (12), 1043-1052

- [32] G. Jayaramana, A. Struthers (2005). Divergence and flutter instability of elastic especially orthotropic plates subject to follower forces. *Journal of Sound and Vibration* 281, 357–373
- [33] Z-M. Wang, Y-F. Zhou, Y. Wang (2007). Dynamic stability of a non-conservative viscoelastic rectangular plate. *Journal of Sound and Vibration* 307, 250–264
- [34] A. R. M. Teifouet (2013). Nonlinear vibration of 2d viscoelastic plate subjected to tangential follower force. *Engineering Mechanics* 20(1), 59–74
- [35] R. Bellman, J. Casti (1971). Differential quadrature and long-term integration. *Journal of Mathematical Analysis and Applications* 34, 235-238
- [36] R. Bellman, B. G. Kashef, J. Casti (1972). Differential quadrature method: A technique for the rapid solution of nonlinear partial differential equations. *Journal of Computational Physics* 10, 40-52
- [37] W. Chen , T. Zhong (1997). The Study on the nonlinear computations of the DQ and DC. *Numerical Methods for Partial Differential Equations* 13, 57-75
- [38] C. Shu (2000). *Differential quadrature and its application in engineering*. Springer Verlag, London Limited
- [39] Z. Zong , Y. Zhong (2009). *Advanced Differential Quadrature Methods*. Taylor and Francis Group, LLC
- [40] F. Civan , C. M. S liepcevich (1984), Differential quadrature for multi-dimensional problems. *Journal of Mathematical Analysis and Applications* 101, 423-443
- [41]A. Cantoni, A , P. Butler (1976). Eigenvalues and eigenvectors of symmetric centrosymmetric matrices. *Linear Algebra & its Applications*, 13, 275-288
- [42] W. Chen. (1996). *Differential quadrature method and its applications in engineering—applying special matrix product to nonlinear, computations and analysis*. Department of Mechanical Engineering , Shanghai Jiao Tong University, PhD thesis
- [43] H. Du, M. K. Lim , R. M. Lin. (1994). In application of generalized differential quadrature method to structural. *Problems International Journal for Numerical Methods in Engineering*. vol. 37, 1881-1896
- [44] R. E. Bellman, B. G. Kashef, J. Casti (1972). Differential quadrature: A technique for the rapid solution of non-linear partial differential equations. *Journal of Computational Physics* 10, 40–52
- [45] C. W. Bert, M. Malik (1996). Implementing multiple boundary conditions in the DQ solution of higher-order PDE's: Application to free vibration of plates. *International Journal for Numerical Method in Engineering*. 39:1237-1258

- [46] C. Shu, H.A. Du (1997). Generalized approach for implementing general boundary conditions in the GDQ free vibration analysis of plates. *International Journal of Solids and Structures* 34, 837-846
- [47] C. W Bert, M. Malik (1996). Differential quadrature method in computational mechanics: a survey. *Applied Mechanics Reviews of ASME* 49 (1)
- [48] A. Krowiak (2008). Methods based on the differential quadrature in vibration analysis of plates. *Journal of Theoretical and Applied Mechanics* 46, 1, pp. 123-139
- [49] Ö. Civalek, M. Ulker (2004). Free vibration analysis of elastic beams using Harmonic differential quadrature (HDQ). *Mathematical and Computational applications*. Vol. 9 No 2 pp.257-264
- [50] C. Shu, H. Ding, K. S. Yeo (2004). Solution of partial differential equations by a global radial basis function-based differential quadrature method. *Engineering Analysis with Boundary Elements* 28, 1217–1226
- [51] S. A. Eftekhari, A. A. Jafari (2012). Mixed finite element and differential quadrature method for free and forced vibration and buckling analysis of rectangular plates. *Applied Mathematics and Mechanics*. 33(1), 81–98
- [52] C. H. W. Ng, Y. B. Zhao, Y. Xiang and G. W. Wei ( 2009). On the accuracy and stability of a variety of differential quadrature formulations for the vibration analysis of beams. *International Journal of Engineering and Applied Sciences* vol.1, Issue 4, 1-25
- [53] M-H. Hsu (2006). Modified generalized differential quadrature (MGDQ). *Journal of Applied Sciences* 6(7), 1591-1595
- [54] A. M. Kaisy, A. Ramadan, A. Esmaeel, M.Mohamed, M. Nassar (2007). Application of the differential quadrature method to the longitudinal vibration of non-uniform rods. *Engineering Mechanics*, vol. 14, no. 5, p. 303–310
- [55] K. M. Liew, Y.Q. Huang, J. N. Reddy (2003). Vibration analysis of symmetrically laminated plates based on FSDT using the moving least squares differential quadrature method. *Computational Applied Mechanics Engineering* 192, 2203–2222
- [56] K. M. Liew, J.-B. Han and Z. M. Xiao (1996). Differential quadrature method for thick symmetric cross-ply laminates with first-order shear flexibility. *International Journal of Solids and Structures* 33 (18), 2647-2658
- [57] A. Marzani, F. Tornabene, E. Viola (2008). Nonconservative stability problem via generalized differential quadrature method. *Journal of Sound and Vibration* 315, 176-196
- [58] Z-M. Wang, Y-F. Zhou, Y. Wang (2007). Dynamic stability of non-conservative viscoelastic rectangular plate. *Journal of Sound and Vibration* 307, 250-264
- [59] X. Guo, Z-M. Wang, Y. Wang (2011). Dynamic stability of thermoelastic coupling moving plate subjected to follower force using DQM. *Applied Acoustics* 72, 100–107

- [60] Y-F. Zhou, Z-M. Wang (2007). Transverse vibration characteristics of axially moving viscoelastic plate. *Applied Mathematics and Mechanics (English Edition)*, 28 (2), 209–218
- [61] Z-M. Wang, Y-F. Zhou, Y. Wang (2008). Dynamic stability of cracked viscoelastic rectangular plate subjected to tangential follower force. *Journal of Applied Mechanics by ASME* vol. 75 / 061018
- [62] Y-F. Zhou, Z-M. Wang (2008). Vibrations of axially moving viscoelastic plate with parabolically varying thickness. *Journal of Sound and Vibration* 316, 198–210
- [63] S. Iijima (1991). *Nature London* 56, 354
- [64] M. M. J. Treacy, T. W. Ebbesen, G. M. Gibson (1996). Exceptionally high Young's modulus observed for individual carbon nanotubes. *Nature* 381, 6584
- [65] A. Krishnan, E. Dujardin, T. W. Ebbesen, P. N. Yianilos and M. M. J. Treacy (1981). Young's modulus of single-walled nanotubes. *Physical Review B* 58, no 20
- [66] A. Kis, A. Zettl (2008). Nanomechanics of carbon nanotubes. *Philosophy Transactions of Royal Society A* 366, 1591–1611
- [67] A. C. Eringen (1983). On differential equations of nonlocal elasticity and solutions of screw dislocation and surface waves. *Journal of Applied Physics* 54, 4703–4710
- [68] A. C. Eringen. (1972). Nonlocal polar elastic continua. *International Journal of Engineering Sciences* 10 1–16
- [69] A. C. Eringen. (2002). *Nonlocal Continuum Field Theories*. Springer-Verlag, New York
- [70] A. C. Eringen, D. G. B. Edelen. (1972). On nonlocal elasticity. *International Journal of Engineering Sciences*. 10, 233–248
- [71] J. N. Reddy (2007). Nonlocal theories for bending, buckling and vibration of beams. *International Journal of Engineering Science* 45 288–307
- [72] J. N. Reddy (2002). *Energy Principles and Variational Methods in Applied Mechanics*. Second edition. John Wiley & Sons, New York
- [73] M. Aydogdu (2009). A general nonlocal beam theory: Its application to nanobeam bending, buckling and vibration. *Physica E* 41, 1651–1655
- [74] H-T. Thai (2012). A nonlocal beam theory for bending, buckling and vibration of nanobeams. *International Journal of Engineering Science* 52, 56–64
- [75] D. Kumar, C. Heinrich, A. M. Waas (2008). Buckling analysis of carbon nanotubes modeled using nonlocal continuum theories *Journal of Applied Physics* 103, 073521
- [76] Y-R. Jeng, P-C Tsai. (2007). *Applied Physics Letters* 90, 161913

- [77] H-A. Reza, R. Hamid, H. Mirdamadi, H. Khademyzadeh, Warsaw (2012). Buckling analysis of short carbon nanotubes based on a novel Timoshenko beam model. *Journal of Theoretical and Applied Mechanics* 50, 4, pp. 975-986
- [78] J. Peddieson, G.R.Buchanan, R.P McNitt (2003). Application of nonlocal continuum models to nanotechnology. *International Journal of Engineering Sciences* 41:305–12
- [79] S. A. M. Ghannadpour, B.Mohammadi (2010). Buckling analysis of micro- and nano-rods/tubes based on nonlocal Timoshenko beam theory using Chebyshev polynomials. *Advance in Material Resistance* 123–125:619–22
- [81] S. A. M. Ghannadpour, B.Mohammadi (2011). Vibration of nonlocal Euler beams using Chebyshev polynomials. *Key Engineering Materials* 471:1016–21
- [82] C. Polizzotto (2001). Nonlocal elasticity and related variational principles. *International Journal of Solids and Structures* 38, 7359–7380
- [83] S. A. M. Ghannadpour, B. Mohammadi, J. Fazilati. (2013). Bending, buckling and vibration problems of nonlocal Euler beams. *Composite Structures*, 96584-589
- [84] J. K Phadikar, S.C. Pradhan (2010). Variational formulation and finite element analysis for nonlocal elastic nanobeams and nanoplates. *Computer Material Sciences* vol 49, 3, pp 492–499
- [85] S. C. Pradhan, J. K Phadikar (2009). Bending, buckling and vibration analyses of nonhomogeneous nanotubes using GDQ and nonlocal elasticity theory. *Engineering Mechanics – An International Journal* . 33:193
- [86] A. W. Leissa (2005). The historical bases of the Rayleigh and Ritz methods. *Journal of Sound and Vibration* 287 961–978
- [87] S. Ilanko (2009). Comments on the historical bases of the Rayleigh and Ritz methods. *Journal of Sound and Vibration* 319, 731–733
- [88] R. Berbuter (1946). *Theoretische Untersuchungen iiber die Eigenfrequenz Parallelogramftrmiger Platten*, Ecole Polytechnique Federale Publications du Laboratoire de Photdlasticit C No. 3. Edition S. A. Leeman frkres et Cie, Stockerstrasse 64, Zurich
- [89] G. B. Warburton (1954). The vibration of rectangular plates. *Proceedings of the Institution of Mechanical Engineer* 168, 371
- [90] M. Ma, T. McNatt, B. Hays, S. Hunter (2013). Elastic lateral distortional buckling analysis of cantilever I-beams. *Ships and Offshore Structures* 8 (3-4), 261-269
- [91] T-L. Zhu (2011). The vibrations of pre-twisted rotating Timoshenko beams by the Rayleigh–Ritz method. *Computational Mechanics* 47,395–408
- [92] R. B. Bhat (1985). Natural frequencies of rectangular plates using characteristic orthogonal polynomials in Rayleigh-Ritz method. *Journal of Sound and Vibration* 102, 493-499

- [93] M. Dickinson, A. Di-Blasio (1986). On the use of orthogonal polynomials in the Rayleigh-Ritz method for the study of the flexural vibration of plates. *Journal of Sound and Vibration* 108, 51-62
- [94] P. Cupia (1997). Calculation of the natural frequencies of composite plates by the Rayleigh-Ritz method with orthogonal polynomials. *Journal of Sound and Vibration* 201-3 385-387
- [95] E. Carrera, F. A. Fazzolari, L. Demasi. (2011). Vibration Analysis of Anisotropic Simply Supported Plates by Using Variable Kinematic and Rayleigh-Ritz Method. *Journal of Vibration and Acoustics of ASME*,133(6)
- [96] H. Hu, A. Badir, A. Abatan. (2003). Buckling behavior of a graphite/epoxy composite plate under parabolic variation of axial load. *International Journal of Mechanical Sciences* 45 1135 – 1147
- [97] W. L. Li (2004). Vibration analysis of rectangular plates with general elastic boundary support. *Journal of Sound and Vibration* 273, 619–635
- [98] L. Behera, S. Chakraverty (2014). Free vibration of Euler and Timoshenko nanobeams using boundary characteristic orthogonal polynomials. *Applied Nanosciences* 4, 347–358
- [99] S. A. M. Ghannadpour, B. Mohammadi, J. Fazilati (2013). Bending, buckling and vibration problems of nonlocal Euler beams using Ritz method. *Composite Structures* 96, 584-589

## CHAPTER 3 : BASIC CONCEPTS FOR RECTANGULAR PLATES THEORY , VISCOELASTICITY AND DIFFERENTIAL QUADRATURE METHOD

### 3.1-Introduction

The main of the present chapter consists of firstly enlightening the different basic assumptions which are used to derive the equation of vibration of viscoelastic thin rectangular plate subjected to follower and transverse forces. After stating the Kirchhoff theory, displacement field will be derived followed by moments. The theory of viscoelasticity will be explained in details and equation of vibration of viscoelastic plate is derived in terms of transverse displacement. Finally, the theory of differential quadrature used in this thesis will be explained in details, emphasizing on domain discretization and basic formulas of DQM which has helped in solving the polynomial eigenvalue problems obtained in chapters 4, 5 and 6.

### 3.2-Basic definitions

A plate is a structure limited by two parallel planes separated by distance  $h$  and by a closed surface which can be cylindrical or prismatic. The two well-known and most studied are rectangular plate (fig.3.1a) and circular plate. Practically, plate as a basic structure in mechanical and civil engineering industries, and can be observed in real life structures like thin retaining walls, lock gates, aircraft's wings, hull and deck of ship, mattress industries etc. A rectangular plate is considered as thin when its thickness  $h$  is small compared to length and width. When all those three dimensions are on the same order one may talk about thick plate. Taken rather plate's thickness as comparison's element, when the deflection ( $w$ ) is small compared to thickness ( $w \leq 0.2h$ ), the plate is said to undergo small deflection. Bending is the only behavior observed here as shear and uncoupled membrane actions are negligible. Kirchhoff (1824-1887) theory is used in this case for displacements. This is also called Love-Kirchhoff theory or classical plate theory (CTP). When the deflection is greater or equal to thickness ( $w \geq 0.2h$ ) one may use Von Karman (1910) theory for writing the constitutive relations. Reissner-Mindlin plate is also known as most used one, where the first order shear effect is taken into account when using constitutive relations. Also known as Mindlin theory, it's suitable for moderately thick plates [1]. Other existing theories in the literature are Exact theory, where none of the stress is neglected, higher order composite theory, suitable for composite laminated plates, membrane shell theory, for extremely thin plates, where membrane effects are dominant (tents, parachutes, balloon walls,...).

Among all cited, Kirchhoff is the most used theory for plate because of its simplicity . This theory will be used in this thesis for the constitutive relations of rectangular plate.

### 3.3-Basic assumptions

The Kirchhoff theory on the study of the vibration of rectangle plate's vibration has been widely studied. Earlier users include: Warburton [2], Leissa [3, 4] D.G Gorman[5-7], etc. Kinematic suppositions to be taken into account for this model are those in classical plate theory (CPT) and it holds:

- Deflections of the mid-surface (geometric center of the plate) are small compared to the thickness of the plate, and the slope of the deflected plate is small.
- Straight line perpendicular to the midsurface (i.e., transverse normal) before deformation remains straight after deformation : This implies that  $\varepsilon_{zz} = 0$ .
- The transverse normal rotates such that they remain perpendicular to the mid surface after deformation. This implies  $\varepsilon_{xz} = 0$ ,  $\varepsilon_{yz} = 0$ .
- The stress  $\sigma_{zz}$  normal to the midplane is small compared with the other stress components and will be consequently not considered.
- The in-plane plate dimensions are large compared to the thickness.

### 3.4-Constitutive relations and equation of vibration

#### 3.4.1-The displacement and strain

After taking into consideration the assumptions of section (3.3) in the Fig.3.1, showing the displacement of plate, one can use the Chasles law of vectors to determine the plate's displacement field as follows:

$$\vec{U} = u\vec{i} + v\vec{j} + w\vec{k} = \vec{P_0P} = \vec{P_0M} + \vec{MM'} + \vec{M'P} = -z\vec{k} + w\vec{k} + z\vec{n} \quad (3.1)$$

where  $\mathbf{u}$ ,  $\mathbf{v}$  and  $\mathbf{w}$  are displacement components about  $x$ ,  $y$  and  $z$  axis respectively.  $\vec{i}$ ,  $\vec{j}$ ,  $\vec{k}$  are normal vectors of these axis respectively, and  $\vec{n}$  is the normal vector of the deformed surface.  $\vec{n}$  is normal to both  $\vec{e}_1$  and  $\vec{e}_2$ , respectively tangent to deformed lines which are parallels along  $x$  and  $y$  respectively before the deformation.

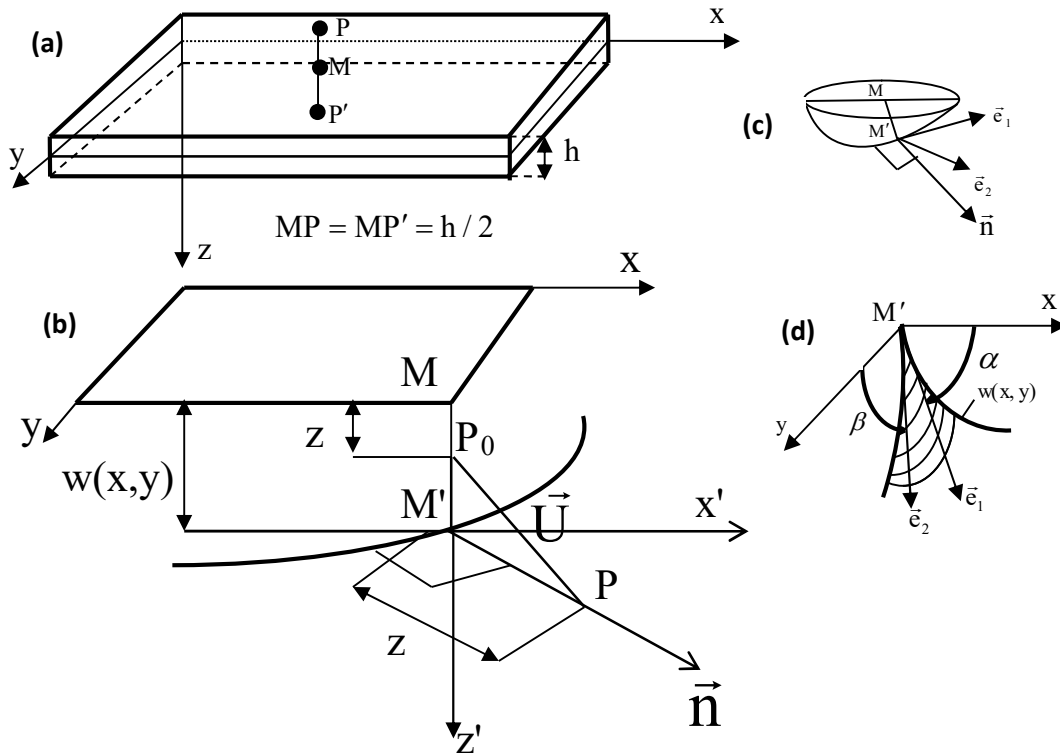


Fig.3.1: Displacement and strain of rectangular plate

Their mathematical expressions are given as follows:

$$\vec{e}_1 = \vec{i} + \frac{\partial w}{\partial x} \vec{k}, \quad \vec{e}_2 = \vec{j} + \frac{\partial w}{\partial y} \vec{k}, \quad \vec{n} = \frac{\vec{e}_1 \wedge \vec{e}_2}{\|\vec{e}_1 \wedge \vec{e}_2\|} \quad (3.2)$$

After the calculation of the cross product in the last term of Eq. (3.2) we finally obtain:

$$\vec{n} = \frac{-\frac{\partial w}{\partial x} \vec{i} - \frac{\partial w}{\partial y} \vec{j} + \vec{k}}{\left[1 + \left(\frac{\partial w}{\partial x}\right)^2 + \left(\frac{\partial w}{\partial y}\right)^2\right]^{1/2}} \approx -\frac{\partial w}{\partial x} \vec{i} - \frac{\partial w}{\partial y} \vec{j} + \vec{k}, \quad (3.3)$$

considering the fact that  $\left[\left(\frac{\partial w}{\partial x}\right)^2 + \left(\frac{\partial w}{\partial y}\right)^2\right] \ll 1$ .

Inserting Eq. (3.3) into Eq. (3.1) we derive the components ( $u, v, w$ ) of the displacement field as follows:

$$u = -z \frac{\partial w}{\partial x}, \quad v = -z \frac{\partial w}{\partial y}, \quad w = w(x, y, t) \quad (3.4)$$

Furthermore, the strain is also derived by applying the formula:

$$\varepsilon_{ij} = \frac{1}{2} \left( \frac{\partial U_i}{\partial x_j} + \frac{\partial U_j}{\partial x_i} \right) \quad (3.5)$$

where  $x$  is a generalized coordinate and  $U$  the generalized displacement.

The formula (3.5) gives the following strain field, after considering Eq. (3.4):

$$\varepsilon_x = -z \frac{\partial^2 w}{\partial x^2}, \quad \varepsilon_y = -z \frac{\partial^2 w}{\partial y^2}, \quad \varepsilon_{xy} = \frac{\gamma_{xy}}{2} = -z \frac{\partial^2 w}{\partial x \partial y} \quad (3.6)$$

### 3.4.2-Stress, resultant and stress couples

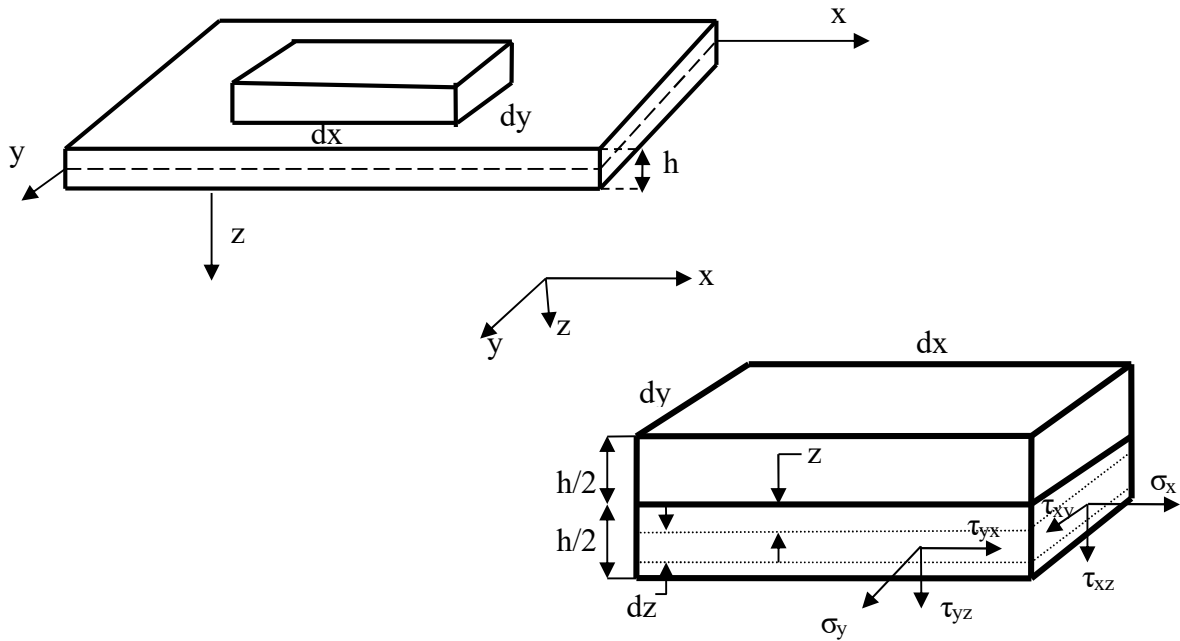


Fig. 3.2: Stress repartition on the plate's slice

In terms of strains, the stress components are given by the following expressions:

$$\varepsilon_x = \frac{\sigma_x}{E} - \nu \frac{\sigma_y}{E}, \quad \varepsilon_y = \frac{\sigma_y}{E} - \nu \frac{\sigma_x}{E}, \quad \varepsilon_{xy} = \gamma_{xy}/2 = \tau_{xy}/2G \quad (3.7)$$

where  $G = \frac{E}{2(1+\nu)}$ ,  $E$  the Young's modulus and  $\nu$  the Poisson's coefficient.

Substituting Eq. (3.6) into Eq. (3.7) we get the stress expressions as follow:

$$\sigma_x = \frac{-E}{1-\nu^2} z \left( \frac{\partial^2 w}{\partial x^2} + \nu \frac{\partial^2 w}{\partial y^2} \right), \quad \sigma_y = \frac{-E}{1-\nu^2} z \left( \frac{\partial^2 w}{\partial y^2} + \nu \frac{\partial^2 w}{\partial x^2} \right), \quad \tau_{xy} = \frac{-E}{1+\nu} z \frac{\partial^2 w}{\partial x \partial y} \quad (3.8)$$

### 3.4.3-Moments and shear forces:

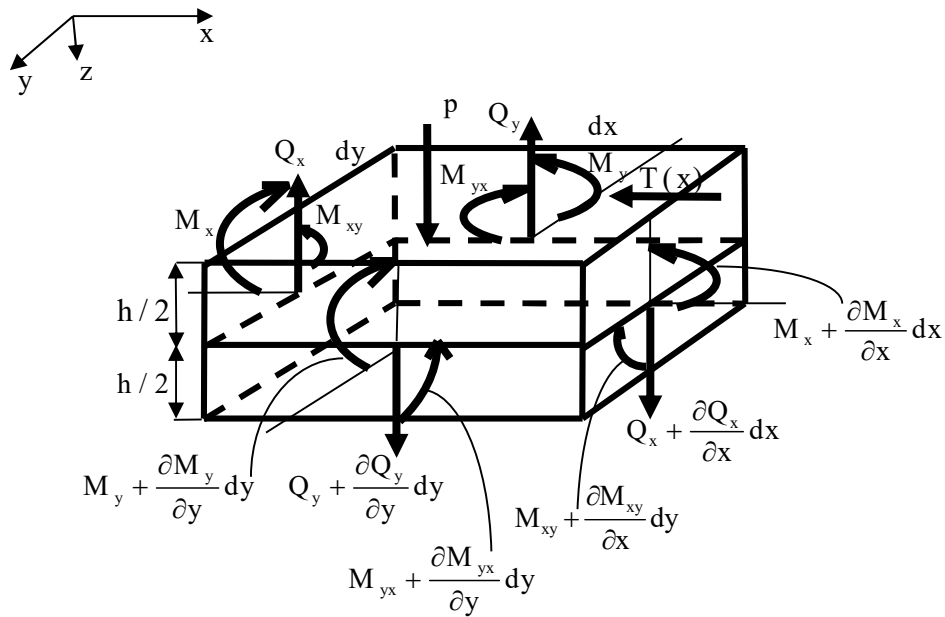


Fig. 3.3: Moments and shear forces on a rectangular plate's slice

The application of the third law of Newton on Fig.3.3 gives the equilibrium equations in terms of bending moments  $M_x$ ,  $M_y$  and twisting moment  $M_{xy}=M_{yx}$ .

The forces summation about  $z$  axis gives:

$$\frac{\partial Q_x}{\partial x} dx dy + \frac{\partial Q_y}{\partial y} dx dy - p dx dy - \rho h \frac{\partial^2 w}{\partial t^2} dx dy = 0 \quad (3.9)$$

From where we get:

$$\frac{\partial Q_x}{\partial x} + \frac{\partial Q_y}{\partial y} - p - \rho h \frac{\partial^2 w}{\partial t^2} = 0 \quad (3.10)$$

Similarly, The moment summation about  $X$  and  $y$  axis respectively gives:

$$\frac{\partial M_x}{\partial x} + \frac{\partial M_{xy}}{\partial y} - Q_x - T_x \frac{\partial w}{\partial x} = 0 \quad (3.11)$$

and

$$\frac{\partial M_y}{\partial x} + \frac{\partial M_{xy}}{\partial y} - Q_y = 0 \quad (3.12)$$

Combining Eqs.(3.10), (3.11) and (3.12) we came out with the d'Alembert Eq.(3.13) representing the moment equilibrium equation of vibration of elastic thin plate subjected to in distributed force  $T(x)$  and transversal force  $p$ .

$$\frac{\partial^2 M_x}{\partial x^2} + 2 \frac{\partial^2 M_{xy}}{\partial x \partial y} + \frac{\partial^2 M_y}{\partial y^2} - T(x) \frac{\partial^2 w}{\partial x^2} - p - \rho h \frac{\partial^2 w}{\partial t^2} = 0 \quad (3.13)$$

3.5-Equation of Viscoelastic rectangular thin plate subjected to follower force  $T(x)$  and transversal force  $p$ .

### 3.5.1-The viscoelasticity

Plate-like structures, may experience both viscous and elastic phenomena. For example like wood-made plates, concrete-made plates, high temperature-made plates, biological tissues-made plates can face such behavior. This behavior is called viscoelasticity [8-11]. In opposition with elasticity, viscoelastic materials may take more time to recover after being deformed. Mathematically one says the stress-strain relation involves a time. During a creep, strain of such materials continues to increase under constant load and ultimately approaches an asymptote (Fig 3.4a). For stress relaxation, their stress required to maintain a constant strain decrease as time involve (Fig 3.4b). Hysteresis phenomenon is present for viscoelastic materials: This is, loading and unloading curves do not coincide but form a slope (Fig 3.4c).

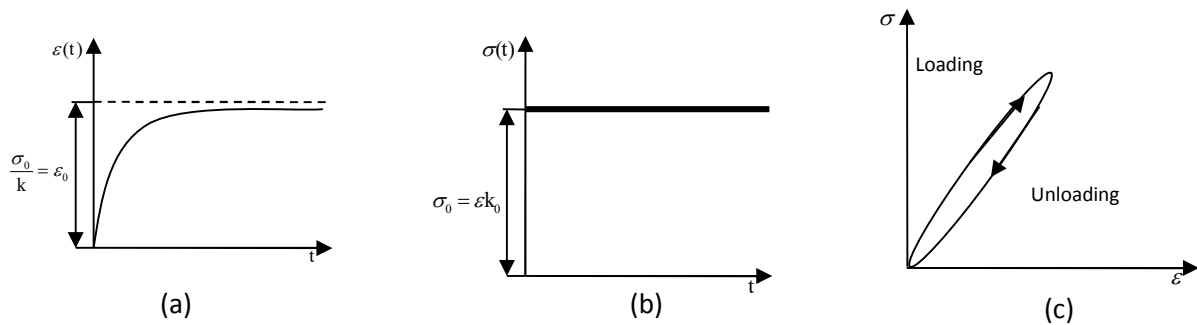


Fig. 3.4: Creep response (a), relaxation response (b), hysteresis loop (c) of viscoelastic solid materials

Many viscoelasticity models exist, characterizing the mathematical relationship between stress and strain. These include Maxwell model (Fig. 3.5b), suitable for fluids, Kelvin-Voigt model for solids (Fig 3.5a). Maxwell and Kelvin-Voigt stand for basic models and can be used to build another models such as solid standard model (Fig 3.5c). Boltzmann model is also applied sometimes and uses integral equation to express stress-strain relationship.

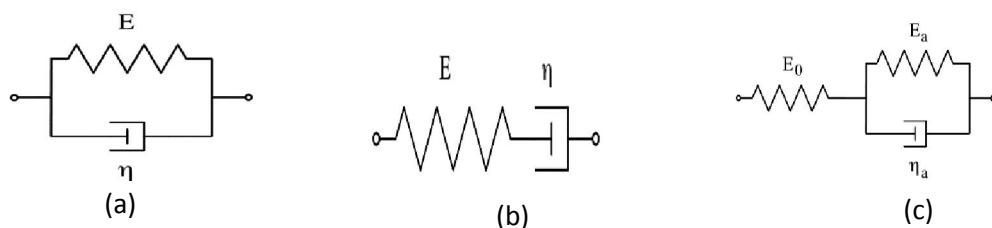


Fig. 3. 5: Viscoelastic models: Kelvin-Voigt (a), Maxwell (b), Solid standard (c) [12]

### 3.5.2-The viscoelastic Equation

Generally, the 3D constitutive stress-strain viscoelastic relation is given by:

$$\begin{cases} \mathbf{P}_d \mathbf{s}_{ij} = \mathbf{Q}_d \mathbf{e}_{ij} \\ \mathbf{P}_s \sigma_{ii} = \mathbf{Q}_s \varepsilon_{ii} \end{cases} \quad (3.14)$$

where  $\mathbf{s}_{ij}$  and  $\mathbf{e}_{ij}$  stand for deviatoric tensor of stress and strain respectively while  $\sigma_{ii}$  and  $\varepsilon_{ii}$  are respectively spherical tensor of stress and strain.

$$s_{ij} = \sigma_{ij} - \frac{1}{3} \text{trace}(\sigma) \delta_{ij}, \quad e_{ij} = \varepsilon_{ij} - \frac{1}{3} \text{trace}(\varepsilon) \delta_{ij}, \quad \sigma_{ii} = \frac{1}{3} \sigma_{kk} \delta_{ij}, \quad \varepsilon_{ii} = \frac{1}{3} \varepsilon_{kk} \delta_{ij} \quad (3.15)$$

The operators:

$$\mathbf{P}_d = \sum_{k=0}^l \mathbf{p}'_k \frac{d^k}{dt^k}, \quad \mathbf{Q}_d = \sum_{k=0}^r \mathbf{q}'_k \frac{d^k}{dt^k}, \quad \mathbf{P}_s = \sum_{k=0}^l \mathbf{p}''_k \frac{d^k}{dt^k}, \quad \mathbf{Q}_s = \sum_{k=0}^{r_1} \mathbf{q}''_k \frac{d^k}{dt^k}, \quad \mathbf{p}'_k, \mathbf{q}'_k, \mathbf{p}''_k, \mathbf{q}''_k \text{ depend}$$

on materials properties.

In Laplace domain, Eq. (3.14) is written as:

$$\begin{cases} \bar{\mathbf{P}}_d \bar{\mathbf{s}}_{ij} = \bar{\mathbf{Q}}_d \bar{\mathbf{e}}_{ij} \\ \bar{\mathbf{P}}_s \bar{\sigma}_{ii} = \bar{\mathbf{Q}}_s \bar{\varepsilon}_{ii} \end{cases} \quad (3.16)$$

Following viscoelastic law, for plane stress problem, strain stress constitutive relationship in the Laplace domain is written as [13]:

$$\begin{cases} \bar{\mathbf{P}}_0 \bar{\sigma}_x = \bar{\mathbf{Q}}_0 \bar{\varepsilon}_x + \bar{\mathbf{Q}}_1 \bar{\varepsilon}_y \\ \bar{\mathbf{P}}_0 \bar{\sigma}_y = \bar{\mathbf{Q}}_0 \bar{\varepsilon}_y + \bar{\mathbf{Q}}_1 \bar{\varepsilon}_x \\ \bar{\mathbf{P}}_d \bar{\tau}_{xy} = \bar{\mathbf{Q}}_d \bar{\varepsilon}_{xy} \end{cases} \quad (3.17)$$

Where

$$\begin{cases} \bar{\mathbf{P}}_0 = \bar{\mathbf{P}}_d (\bar{\mathbf{P}}_d \bar{\mathbf{Q}}_s + 2\bar{\mathbf{Q}}_d \bar{\mathbf{P}}_s) \\ \bar{\mathbf{Q}}_0 = \bar{\mathbf{Q}}_d (2\bar{\mathbf{P}}_d \bar{\mathbf{Q}}_s + \bar{\mathbf{Q}}_d \bar{\mathbf{P}}_s) \\ \bar{\mathbf{Q}}_1 = \bar{\mathbf{Q}}_d (\bar{\mathbf{P}}_d \bar{\mathbf{Q}}_s - \bar{\mathbf{Q}}_d \bar{\mathbf{P}}_s) \end{cases} \quad (3.18)$$

With  $\bar{\sigma}_x, \bar{\sigma}_y, \bar{\tau}_{xy}, \bar{\varepsilon}_x, \bar{\varepsilon}_y, \bar{\varepsilon}_{xy}$  the Laplace transformations of  $\sigma_x, \sigma_y, \tau_{xy}, \varepsilon_x, \varepsilon_y, \varepsilon_{xy}$

respectively and  $\bar{\mathbf{P}}_d, \bar{\mathbf{P}}_0, \bar{\mathbf{Q}}_d, \bar{\mathbf{Q}}_0, \bar{\mathbf{Q}}_1$  respectively Laplace transformations for

$\mathbf{P}_d, \mathbf{P}_0, \mathbf{Q}_d, \mathbf{Q}_0, \mathbf{Q}_1$ .

Recalling the expressions linking the moments to the stresses:

$$M_x = \int_{-b/2}^{b/2} z \sigma_x dz, \quad M_y = \int_{-b/2}^{b/2} z \sigma_y dz, \quad M_{xy} = M_{yx} = \int_{-b/2}^{b/2} z \tau_{xy} dz \quad (3.19)$$

we apply viscoelastic operator to the moment expressions, and take into account Eq.(3.8) and (3.17), then end up with:

$$\begin{cases} \bar{P}_0(\bar{M}_x) = - \int_{-b/2}^{b/2} z^2 \left[ \bar{Q}_0 \frac{\partial^2 \bar{w}}{\partial x^2} + \bar{Q}_1 \frac{\partial^2 \bar{w}}{\partial y^2} \right] dz \\ \bar{P}_0(\bar{M}_y) = - \int_{-b/2}^{b/2} z^2 \left[ \bar{Q}_1 \frac{\partial^2 \bar{w}}{\partial x^2} + \bar{Q}_0 \frac{\partial^2 \bar{w}}{\partial y^2} \right] dz \\ \bar{P}_d(\bar{M}_{xy}) = \bar{P}_d(\bar{M}_{yx}) = - \int_{-b/2}^{b/2} z^2 \bar{Q}_d \frac{\partial^2 \bar{w}}{\partial x \partial y} dz \end{cases} \quad (3.20)$$

Applying the product of the Laplace transformation of viscoelastic operators  $\bar{P}_0$  and  $\bar{P}_d$  to the Laplace transformation of Eq. (3.13), we have:

$$\bar{P}_0 \bar{P}_d \left( \frac{\partial^2 \bar{M}_x}{\partial x^2} \right) + 2 \bar{P}_0 \bar{P}_d \left( \frac{\partial^2 \bar{M}_{xy}}{\partial x \partial y} \right) + \bar{P}_0 \bar{P}_d \left( \frac{\partial^2 \bar{M}_y}{\partial y^2} \right) - \bar{P}_0 \bar{P}_d \bar{T}(x) \frac{\partial^2 \bar{w}}{\partial x^2} + \bar{P}_0 \bar{P}_d \bar{p} - \bar{P}_0 \bar{P}_d \rho h \frac{\partial^2 \bar{w}}{\partial t^2} = 0 \quad (3.21)$$

where the bar on each variable is its Laplace transformation.

Considering the continuity of partial derivative, Eq. (3.21) becomes

$$\bar{P}_d \left( \frac{\partial^2 [\bar{P}_0(\bar{M}_x)]}{\partial x^2} \right) + 2 \bar{P}_0 \left( \frac{\partial^2 [\bar{P}_d(\bar{M}_{xy})]}{\partial x \partial y} \right) + \bar{P}_d \left( \frac{\partial^2 [\bar{P}_0(\bar{M}_y)]}{\partial y^2} \right) - \bar{P}_0 \bar{P}_d \left[ \bar{p} + \bar{T}(x) \frac{\partial^2 \bar{w}}{\partial x^2} - \rho h \frac{\partial^2 \bar{w}}{\partial t^2} \right] = 0 \quad (3.22)$$

Considering that the present plate obeys the Kelvin-Voigt law of viscoelasticity, stress-strain relation is derived as [14] :

$$s_{ij} = 2G e_{ij} + 2\eta \dot{e}_{ij}, \quad \sigma_{ii} = 3K \varepsilon_{ii} \quad (3.23)$$

From where one can find by taking inverse Laplace transformation of Eq.(3.16)

$$\begin{cases} \bar{P}_d = 1, & \bar{Q}_d = 2\eta \frac{\partial}{\partial t} \\ \bar{P}_s = 1, & \bar{Q}_s = 3K \end{cases} \quad (3.24)$$

In Eq. (3.24),  $K$ ,  $\eta$ ,  $G$  are bulk modulus, viscoelastic coefficient and shear modulus, respectively. They can be expressed as  $K = E/3(1-2\nu)$  and  $G = E/(1+2\nu)$  in terms of  $E$  and  $\nu$ .

After taking Eq.(3.20) into account in Eq.(3.22) and carry out the inverse Laplace transformation, we derive the equation of viscoelastic nonconservative plate when subjected to follower force  $T(x)$  and transversal force  $p$  as:

$$\frac{h^3}{12} \left( A_3 + A_4 \frac{\partial}{\partial t} + A_5 \frac{\partial^2}{\partial t^2} \right) \nabla^4 w + \left( A_1 + A_2 \frac{\partial}{\partial t} \right) \left( p + T(x) \frac{\partial^2 w}{\partial x^2} + \rho h \frac{\partial^2 w}{\partial t^2} \right) = 0 \quad (3.25)$$

where

$$A_1 = 3K + 4G, \quad A_2 = 4\eta, \quad A_3 = 4G(3K + G), \quad A_4 = \eta(8G + 12K), \quad A_5 = 4\eta^2$$

$$\nabla^4 w = \frac{\partial^4 w}{\partial x^4} + 2 \frac{\partial^4 w}{\partial x^2 \partial y^2} + \frac{\partial^4 w}{\partial y^4}. \quad (3.26)$$

The solution of Eq. (3.25) associated to the considered boundary conditions will be given in chapter 4 chapter 5 and chapter 6 in details.

### 3.6-Differential quadrature method

#### 3.6.1-The form of weighting coefficients

DQ method involves approximating the partial derivatives of the function  $W(X, Y)$  at a sample point  $(X_i, Y_j)$  by the weighted sum of the function  $W_{i,j}$  values [15]. Let the number of sample points denoted by  $N$  in  $X$  direction and  $M$  in  $Y$  direction. The  $r^{\text{th}}$  order partial derivative with respect to  $X$ ,  $s^{\text{th}}$  order partial derivative with respect to  $Y$  and the  $(r+s)^{\text{th}}$  order mixed partial derivative of  $W(X, Y)$  with respect to both  $X$  and  $Y$  are discretely expressed at the point  $(X_i, Y_j)$  as:

$$\frac{\partial^r W(X_i, Y_j)}{\partial X^r} = \sum_{k=1}^N A_{ik}^{(r)} W_{kj}, \quad \frac{\partial^s W(X_i, Y_j)}{\partial Y^s} = \sum_{l=1}^M B_{jl}^{(s)} W_{il}, \quad \frac{\partial^{r+s} W(X_i, Y_j)}{\partial X^r \partial Y^s} = \sum_{k=1}^N A_{ik}^{(r)} \sum_{l=1}^M B_{jl}^{(s)} W_{kl} \quad (3.27)$$

where  $i = 1, 2, \dots, N$ ,  $k = 1, 2, \dots, N-1$ ,  $j = 1, 2, \dots, M$  and  $l = 1, 2, \dots, M-1$ . For  $r = s = 1$  the coefficients  $A_{ik}^{(r)}$  and  $B_{jl}^{(s)}$  are defined as [16]:

$$A_{ik}^{(1)} = \begin{cases} \prod_{\mu=1, \mu \neq i}^N \frac{X_i - X_\mu}{(X_i - X_k) \prod_{\mu=1, \mu \neq k}^N (X_k - X_\mu)} & \text{for } i, k = 1, 2, \dots, N, i \neq k \\ \sum_{\mu=1, \mu \neq i}^N \frac{1}{X_i - X_\mu} & \text{for } i = 1, 2, \dots, N, i = k \end{cases} \quad (3.28)$$

$$B_{jl}^{(1)} = \begin{cases} \prod_{\mu=1, \mu \neq j}^M \frac{Y_j - Y_\mu}{(Y_j - Y_1) \prod_{\mu=1, \mu \neq 1}^M (Y_1 - Y_\mu)} & \text{for } j, l = 1, 2, \dots, M, j \neq 1 \\ \sum_{\mu=1, \mu \neq j}^M \frac{1}{Y_j - Y_\mu} & \text{for } j = 1, 2, \dots, M, j = 1 \end{cases} \quad (329)$$

For  $r = 2, 3, \dots, N - 1$  and  $s = 2, 3, \dots, M - 1$

$$A_{ik}^{(r)} = \begin{cases} r \left( A_{ii}^{(r-1)} A_{ik}^{(1)} - \frac{A_{ik}^{(r-1)}}{X_i - X_k} \right) & \text{for } i, k = 1, 2, \dots, N, i \neq k \\ - \sum_{\mu=1, \mu \neq i}^N A_{i\mu}^{(r)} & \text{for } i = 1, 2, \dots, N, i = k \end{cases} \quad (3.30)$$

$$B_{jl}^{(s)} = \begin{cases} s \left( B_{jj}^{(s-1)} B_{jl}^{(1)} - \frac{B_{jl}^{(s-1)}}{Y_j - Y_l} \right) & \text{for } j, l = 1, 2, \dots, M, j \neq 1 \\ - \sum_{\mu=1, \mu \neq j}^M B_{j\mu}^{(s)} & \text{for } j = 1, 2, \dots, M, j = 1 \end{cases} \quad (3.31)$$

### 3.6.2-The choice of discrete points: The $\delta$ -technics

$X_i$  and  $Y_j$  are discrete points which can be taken either uniform, non-uniform, or the mixed depending on the problem to be solved. Among the non-uniform discrete point forms, Gaubatto-Chebyshev [17] is the most used, because it generates very accurate weighting coefficients. For some problems, the  $\delta$  point may be mixed to uniform or non-uniform discrete points. This  $\delta$ -technique was proposed by Jang, Bert and Striz [18] and its aim consists on eliminating the difficulties in implementing two conditions at a single boundary point. The Dirichlet condition ( $w=0$ ) is applied at the boundary point itself, and derivative condition at its adjacent point which is at a distance  $\delta$  from the boundary point (Figure 3.6). This technics is suitable for Simply supported and Clamped boundary conditions, as they have each one Dirichlet condition and one involving derivative. One should notice that, although this technics has been suitable to solve many problems and in finding eigenfrequencies, it appears to be questionable as the derivative boundary condition is not computed at the right place. The choice of  $\delta$  becomes then very important and its value determines the success or fail of obtaining accurate results. In fact, that value must be very

small ( $\delta \leq 10^{-4}$ ). This technique is used in this thesis to implement CSCS boundary conditions.

### 3.6.3-Treatment of boundary conditions

#### 3.6.3a-Modification of weighting coefficient matrices

This treatment is used in problems where  $\delta$  technics is not used in the discrete points of the discretized domain. Here, for one edge, just Dirichlet boundary is implemented in the physical domain. The derivative boundary is implemented inside the coefficient matrices.

This approach is based on the definition of differential quadrature method, where

$$\frac{\partial^n W(X_i, Y_j)}{\partial X^n} = \frac{\partial}{\partial X} \left[ \frac{\partial^{n-1} W(X_i, Y_j)}{\partial X^{n-1}} \right] \quad (3.32)$$

Since

$$\frac{\partial^r W(X_i, Y_j)}{\partial X^r} = \sum_{k=1}^N A_{ik}^{(r)} W_{kj} = [A^{(r)}] W_{jk} \quad (3.33)$$

Then

$$\frac{\partial^n W(X_i, Y_j)}{\partial X^n} = [A^{(1)}][A^{(n-1)}] W_{jk} = [A^{(n-1)}][A^{(1)}] W_{jk} \quad (3.34)$$

Taking for example  $n=4$ , and supposing that the considered edge is clamped, the first derivative boundary weighting coefficient matrices will be modified and becomes  $[\tilde{A}^{(1)}]$ . This new matrix will be used to compute the second, third and fourth derivative coefficient matrix as in [19]:

$$[\tilde{A}^{(2)}] = [A^{(1)}][\tilde{A}^{(1)}], [\tilde{A}^{(3)}] = [A^{(1)}][\tilde{A}^{(3)}], [\tilde{A}^{(4)}] = [A^{(1)}][\tilde{A}^{(3)}] \quad (3.35)$$

All the weighting coefficients will then be modified through this process which consist to zero some elements of matrices. This technics is very simple to realise for simply supported and clamped edges, as they boundary conditions are homogeneous. We used it in this thesis for implementing boundary conditions of completely simply supported plate (SSSS) [15].

3.6.3b- Coupling boundary conditions with general Equation (CBCGE=general approach)

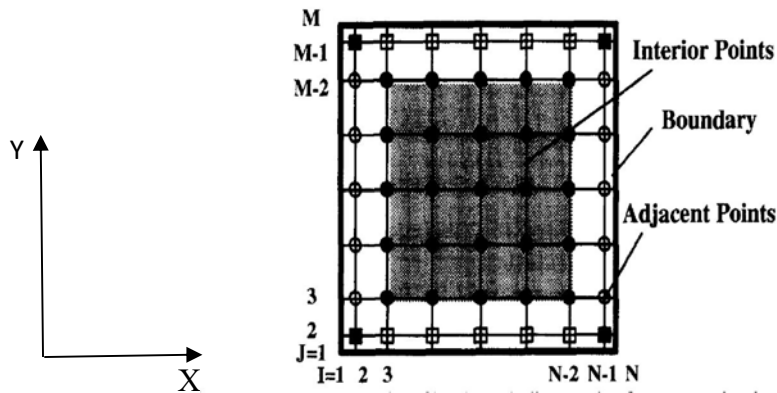


Fig. 3.6: Differential quadrature domain discretization for rectangular plate [20]

For plate containing non homogeneous boundary conditions the modification of weighting coefficients matrix is no more usable. To overcome that drawback, CBCGE (coupling boundary condition with general equation) is used. Here, the whole domain of plate is divided into two (Fig. 3.6). The Boundary domain and the working domain. The boundary points include the border points and their adjacent while the rest constitutes the working points. This implies that the displacement field of plate is split up in  $W_q$  (working domain) and  $W_b$  (boundary domain).

### 3.7-References

- [1] P. G. Ciarley (1997). Mathematical Elastic Theory of Plates. Vol II: North-Holland
- [2] G. B. Warburton (1954). The Vibration of Rectangular Plates. Proceedings of the Institution of Mechanical Engineer 168: 371
- [3] A. W. Leissa (1973). Free vibration of rectangular plates. Journal of Sound and Vibration 31:251-93
- [4] A. W. Leissa (1969). Vibration of Plates, NASA, SP-160, Washington DC
- [5] G. J. Gorman (1981). An analytical solution for the free vibration analysis of rectangular plates resting on symmetrically distributed point supports. Journal of Sound and Vibration 79(4), 561-574

- [6] G. J. Gorman (1978). Free vibration analysis of the completely free rectangular plate by the method of superposition. *Journal of Sound and Vibration* 57(3), 437-447
- [7] D. J. Gorman (1984). An exact analytical approach to the free vibration analysis of rectangular plates with mixed boundary conditions. *Journal of Sound and Vibration* 93(2), 235-247
- [8] J. Soukup, J. Volek (2007). Thin rectangular viscoelastic orthotropic plate under transverse impuls loading. *Applied and Computational Mechanics* 657-666
- [9] S. M. Schmalholz, Y.Y. Podladchikov (2001). Viscoelastic Folding: Maxwell versus Kelvin Rheology. *Geophysical Research Letters* Vol.28, 9, 1835-1838
- [10] F. Moraveca, N. Letzelter (2007). On the modeling of the linear viscoelastic behaviour of biological materials using Comsol Multiphysics. *Applied and Computational Mechanics* 1, 175-184
- [11] G. Zhang (2005). Evaluating the viscoelastic properties of biological tissues in a new way. *Journal of Musculoskelet Neuronal Interaction* (1):85-90
- [12] D. C. Hammerand (1999). PhD thesis, Geometrically-linear and nonlinear analysis of viscoelastic composites using the finite element method, Faculty of Virginia Polytechnics Institute and State University
- [13] W. Flugge (1975). *Viscoelasticity*. Springer, Berlin
- [14] T. Q. Yang (2004). *Viscoelasticity Theory and Applications*. Science Press, Beijing
- [15] C. W. Bert, M. Malik, (1996). Implementing multiple boundary conditions in the DQ solution of higher-order PDE's: Application to free vibration of plates. *International Journal for Numerical Method in Engineering* 39:1237-1258
- [16] Y-Q. Tang, L-Q. Chen (2011). Nonlinear free transverse vibration of in-plane moving plate: without and with internal resonances. *Journal of Sound and Vibration* 330:110–26
- [17] Z-M. Wang, Y-F Zhou, Y. Wang (2007). Dynamic stability of non-conservative viscoelastic rectangular plate. *Journal of Sound and Vibration* 307:250-264
- [18] S. K. Jang, C. W. Bert, A. G. Striz (1989). Application of differential quadrature to static analysis of structural components. *International Journal for Numerical Methods in Engineering* 28, 561–577
- [19] C. Shu, *Differential quadrature and its application in Engineering*, Springer, 2000
- [20] C. Shu, H.A. Du (1997). Generalized approach for implementing general boundary conditions in the GDQ free vibration analysis of plates. *International Journal of Solids and Structures* 34, 837-846

CHAPTER 4 - PAPER 1:

NONCONSERVATIVE STABILITY OF VISCOELASTIC RECTANGULAR PLATES WITH FREE EDGES UNDER UNIFORMLY DISTRIBUTED FOLLOWER FORCE. Published in International Journal of Mechanical Sciences



# Nonconservative stability of viscoelastic rectangular plates with free edges under uniformly distributed follower force



Mouafo Teifouet Armand Robinson, Sarp Adali\*

Discipline of Mechanical Engineering, University of KwaZulu-Natal, Durban, South Africa

## ARTICLE INFO

### Article history:

Received 6 April 2015

Received in revised form

4 October 2015

Accepted 30 December 2015

Available online 7 January 2016

### Keywords:

Dynamic stability

Viscoelastic plate

Uniformly distributed follower force

Nonconservative stability

Differential quadrature method

## ABSTRACT

Dynamic stability of viscoelastic rectangular plates under a uniformly distributed tangential follower load is studied. Two sets of boundary conditions are considered, namely, clamped in one boundary and free in other boundaries (CFFF) and two opposite edges simply supported and other two edges free (SFSF). By considering the Kelvin–Voigt model of viscoelasticity, the equation of motion of the plate is derived. The differential quadrature method is employed to obtain the numerical solution and it is verified against known results in the literature. Numerical results are given for the real and imaginary parts of the eigenfrequencies to investigate the divergence and flutter instabilities. It is observed that the type of stability differs for CFFF and SFSF plates indicating the strong influence of the boundary conditions on the dynamic stability of viscoelastic plates. In particular it is found that CFFF plates undergo flutter instability and SFSF plates divergence instability. One consequence is that SFSF plates become unstable at a load less than the load for CFFF plates as the effects of viscoelasticity as well as the aspect ratio are found to be minor for SFSF plates.

© 2016 Elsevier Ltd. All rights reserved.

## 1. Introduction

The dynamic stability of systems such as beams, plates, shells, pipes conveying fluid and rockets subject to follower forces has been studied extensively. Plate structures are of importance in diverse fields of technology like aeronautics, automotive design and offshore structures, and as a result substantial work has been performed on their stability under nonconservative loads. It has been observed by Herrmann [1] that the load parameter has a great effect on the stability of an elastic system subjected to a nonconservative force. By considering a cantilever plate subjected to biaxial subtangential loading, Farshad [2] studied the effect of load parameter on dynamic stability. Influence of aspect ratio on the stability of a plate subjected to conservative and non-conservative forces was studied by Adali [3]. Various effects on dynamic stability of rectangular plates have been investigated in Leipholz and Pfent [4], Kumar and Srivasta [5], Higuchi and Dowell [6], Zuo and Schreyer [7], Kumar et al. [8], Kim and Park [9], Kim and Kim [10] and in Jayaraman and Struthers [11].

More recently dynamic stability of viscoelastic structures has been the focus of a number of publications. Stability of viscoelastic columns under follower forces has been studied by Langthjem and Sugiyama [12], Darabseh and Genin [13] and Zhuo and Fen [14]. The

corresponding work for viscoelastic plates is given in Eshmatov [15] for follower forces, in Wang et al. [16], Wang and Zhou [17] for uniformly tangential and in Robinson and Adali [18] for triangularly distributed tangential follower forces. Robinson [19] took non-linearity and tangential follower forces into account for simply supported plates, and Wang et al. [20] the effect of piezoelectric layers for viscoelastic plates with a combination of simple and clamped supports. Despite the increasing attention on the stability of viscoelastic plates subject to follower forces, the boundary conditions which appeared in the literature so far include only the clamped and simply supported cases [16,17,19,20]. It is noted that the main difference in the nonconservative stability of viscoelastic columns and plates is that the formulations for the two-dimensional structures lead to governing equations expressed in the complex domain leading to complex eigenvalue problems.

A rectangular plate may experience divergence or flutter instability depending on the boundary conditions and quite often plates with free boundaries are employed in practice. In the present study, the stability of rectangular viscoelastic plates subject to a uniformly distributed tangential follower force and free boundary conditions is studied using the Kelvin–Voigt model of viscoelastic behavior. In particular dynamic stability of viscoelastic plates with CFFF and SFSF boundary conditions is established where C, F and S stand for clamped, free and simply supported boundary conditions, respectively. Free boundary conditions are experienced in many engineering applications indicating the importance of studying the dynamic stability for these cases. In the present

\* Corresponding author. Tel.: +27 312603203; fax: +27 312603217.

E-mail address: [adali@ukzn.ac.za](mailto:adali@ukzn.ac.za) (S. Adali).

study, differential quadrature method [19,21] is employed to solve the governing equation which is expressed in the complex domain using Laplace transformation. Previously the differential quadrature method was applied to nonconservative stability in Marzani et al. [22].

In Section 2, the equations governing the vibrations of non-conservatively loaded viscoelastic plates are established using Laplace transformation following the approach implemented in Wang et al. [16], Wang and Zhou [17] and Wang et al. [23]. In Section 3 the differential quadrature method is implemented to discretize the equation of motion and the boundary conditions. This is followed by the verification of results in Section 4 and numerical results in Section 5. Numerical results are given to investigate the divergence and flutter instabilities for CFFF and SFSF plates by way of plotting the real and imaginary parts of the eigenvalues with respect to the follower load. The effects of the aspect ratio and viscoelastic constant on stability are also studied. Finally, Section 6 is devoted to concluding remarks.

## 2. Equation of motion for viscoelastic plate

We consider a thin rectangular plate of dimensions  $a \times b$  and thickness  $h$  with Young's modulus of  $E$ , Poisson's ratio  $\nu$  and density  $\rho$ . The Cartesian coordinate system  $x, y, z$  which has its origin at mid-thickness is shown in Fig. 1. Using the Kirchhoff plate theory, the displacements  $u, v, w$  along  $x, y$  and  $z$  directions, respectively, are given by

$$u = -z\psi_x, \quad v = -z\psi_y, \quad w = w(x, y, t) \quad (1)$$

where the angles of rotation  $\psi_x$  and  $\psi_y$  are related to the transverse displacement  $w$  through the relations

$$\psi_x = \frac{\partial w}{\partial x}, \quad \psi_y = \frac{\partial w}{\partial y} \quad (2)$$

The linear strain–displacement relations are given by

$$\epsilon_x = -z \frac{\partial^2 w}{\partial x^2}, \quad \epsilon_y = -z \frac{\partial^2 w}{\partial y^2}, \quad \epsilon_{xy} = \frac{\gamma_{xy}}{2} = -z \frac{\partial^2 w}{\partial x \partial y} \quad (3)$$

where  $\epsilon_x$  and  $\epsilon_y$  are the normal strain components, and  $\gamma_{xy}$  is the shear strain component.

In the present study the plate material is taken as viscoelastic of the Kelvin–Voigt type. The constitutive equations for this case can be written as in Refs. [16–18, 20].

$$s_{ij} = 2G \mathbf{e}_{ij} + 2 \eta \dot{\mathbf{e}}_{ij} \quad (4a)$$

$$\sigma_{ii} = 3K \epsilon_{ii} \quad (4b)$$

where  $K, \eta, G$  are bulk modulus, viscoelastic coefficient and shear modulus, respectively. They can be expressed as  $K = E/3(1-2\nu)$  and  $G = E/(1+2\nu)$  in terms of  $E$  and  $\nu$ . The quantities  $s_{ij}$  and  $\mathbf{e}_{ij}$  are, respectively, the deviatoric tensors of stress and strain while  $\mathbf{s}_{ii}$  and  $\sigma_{ii}$  stand for the spherical tensors of strain and stress. The bending moments  $M_x, M_y$  and twisting moments  $M_{xy}, M_{yx}$  are given by:

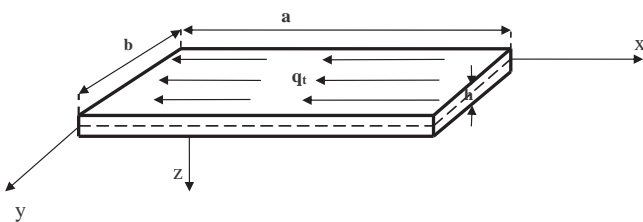


Fig. 1. Viscoelastic plate subject to distributed tangential follower force  $q_t$ .

$$M_x = \int_{-h/2}^{h/2} z \sigma_x dz, \quad M_y = \int_{-h/2}^{h/2} z \sigma_y dz \quad (5a)$$

$$M_{xy} = \int_{-h/2}^{h/2} z \sigma_{xy} dz, \quad M_{yx} = \int_{-h/2}^{h/2} z \sigma_{yx} dz \quad (5b)$$

where  $\sigma_x$  and  $\sigma_y$  are the normal stress components,  $\sigma_{xy}$  and  $\sigma_{yx}$  are the shear stress components. The plate is subject to a uniformly distributed tangential follower force  $q_t$  as shown in Fig. 1. The equation governing the vibrations of the plate under the distributed follower force can be written as

$$\frac{\partial^2 M_x}{\partial x^2} + 2 \frac{\partial^2 M_{xy}}{\partial x \partial y} + \frac{\partial^2 M_y}{\partial y^2} - q_t(a-x) \frac{\partial^2 w}{\partial x^2} - \rho h \frac{\partial^2 w}{\partial t^2} = 0 \quad (6)$$

Following the methodology employed in [16] and [17], Laplace transformations of Eqs. (4)–(6) are performed. Carrying out the inverse Laplace transformations of the resulting equations [24], the differential equation governing the vibration of the non-conservative viscoelastic rectangular plate is obtained as

$$\frac{h^3}{12} \left( A_3 + A_4 \frac{\partial}{\partial t} + A_5 \frac{\partial^2}{\partial t^2} \right) \nabla^4 w + q_t(a-x) \left( A_1 + A_2 \frac{\partial}{\partial t} \right) \frac{\partial^2 w}{\partial x^2} + \left( A_1 + A_2 \frac{\partial}{\partial t} \right) \frac{\partial^2 w}{\partial t^2} = 0 \quad (7)$$

where

$$A_1 = 3K + 4G, \quad A_2 = 4\eta, \quad A_3 = 4G(3K + G), \quad A_4 = 4\eta(2G + 3K), \quad A_5 = 4\eta^2 \quad (8)$$

and

$$\nabla^4 w = \frac{\partial^4 w}{\partial x^4} + 2 \frac{\partial^4 w}{\partial x^2 \partial y^2} + \frac{\partial^4 w}{\partial y^4} \quad (9)$$

Introducing the dimensionless variables

$$X = \frac{x}{a}, \quad Y = \frac{y}{b}, \quad \bar{w} = \frac{w}{h}, \quad \lambda = \frac{a}{b} \quad (10a)$$

$$q = \frac{12q_t a^3(1-\nu^2)}{Eh^3}, \quad \tau = \frac{th}{a^2} \sqrt{\frac{E}{12\rho(1-\nu^2)}}, \quad H = \frac{\eta h}{a^2 E} \sqrt{\frac{E}{12\rho(1-\nu^2)}} \quad (10b)$$

the governing Eq. (7) can be rewritten as

$$\left( 1 + c_1 \frac{\partial}{\partial \tau} + c_2 \frac{\partial^2}{\partial \tau^2} \right) \nabla^4 \bar{w} + q(1-X) \left( 1 + c_3 \frac{\partial}{\partial \tau} \right) \frac{\partial^2 \bar{w}}{\partial X^2} + \left( 1 + c_3 \frac{\partial}{\partial \tau} \right) \frac{\partial^2 \bar{w}}{\partial \tau^2} = 0 \quad (11)$$

where  $\tau$  is dimensionless time,  $H$  is dimensionless delay time of the material, and

$$c_1 = \frac{4(2-\nu)(1+\nu)}{3} H, \quad c_2 = \frac{4(1-2\nu)(1+\nu)^2}{3} H^2, \quad c_3 = \frac{4(1-2\nu)(1+\nu)}{3(1-\nu)} H \quad (12)$$

are real constants which depend on the delay time  $H$ , and

$$\nabla^4 \bar{w} = \frac{\partial^4 \bar{w}}{\partial X^4} + 2\lambda^2 \frac{\partial^4 \bar{w}}{\partial X^2 \partial Y^2} + \lambda^4 \frac{\partial^4 \bar{w}}{\partial Y^4} \quad (13)$$

The solution of Eq. (11) is expressed in the form

$$\bar{w}(X, Y, \tau) = W(X, Y) \exp(j\omega\tau) \quad (14)$$

where  $j = \sqrt{-1}$  and  $\omega$  is the dimensionless frequency which is in general a complex number. Substituting Eq. (14) into Eq. (11), one obtains the differential equation

$$\left( 1 + c_1 j\omega + c_2 j^2 \omega^2 \right) \nabla^4 W + q(1-X) \left( 1 + c_3 j\omega \right) \frac{\partial^2 W}{\partial X^2} + \left( 1 + c_3 j\omega \right) j^2 \omega^2 = 0 \quad (15)$$

in terms of the space variables  $X$  and  $Y$ . The boundary conditions considered in the present study are given next.

CSSS refers to the plate with one edge clamped and other three edges simply supported. This case is considered for verification purposes. For this case the boundary conditions are given by

$$W(0, Y) = \frac{\partial W}{\partial X} \Big|_{X=0} = 0, \quad W(1, Y) = \frac{\partial^2 W}{\partial X^2} \Big|_{X=1} = 0 \quad \text{for } 0 \leq Y \leq 1 \quad (16a)$$

$$W(X, 0) = \frac{\partial^2 W}{\partial Y^2} \Big|_{Y=0} = 0, \quad W(X, 1) = \frac{\partial^2 W}{\partial Y^2} \Big|_{Y=1} = 0 \quad \text{for } 0 \leq X \leq 1 \quad (16b)$$

CFFF refers to the plate with one edge clamped and other three edges free. For this case the boundary conditions are given by

$$W(0, Y) = \frac{\partial W}{\partial X} \Big|_{X=0} = 0, \quad \frac{\partial^2 W}{\partial X^2} + \nu \lambda^2 \frac{\partial^2 W}{\partial Y^2} \Big|_{X=1} = 0, \quad \frac{\partial^3 W}{\partial X^3} + (2-\nu)\lambda^2 \frac{\partial^3 W}{\partial X \partial Y^2} \Big|_{X=1} = 0 \quad \text{for } 0 \leq Y \leq 1 \quad (17a)$$

$$\lambda^2 \frac{\partial^2 W}{\partial Y^2} + \nu \frac{\partial^2 W}{\partial X^2} \Big|_{Y=0,1} = 0, \quad \lambda^2 \frac{\partial^3 W}{\partial Y^3} + (2-\nu) \frac{\partial^3 W}{\partial X^2 \partial Y} \Big|_{Y=0,1} = 0 \quad \text{for } 0 \leq X \leq 1 \quad (17b)$$

$$\frac{\partial^2 W}{\partial X \partial Y} \Big|_{X=1, Y=0} = 0, \quad \frac{\partial^2 W}{\partial X \partial Y} \Big|_{X=1, Y=1} = 0 \quad (17c)$$

SFSF refers to the plate with opposite edges simply supported and free. For this case the boundary conditions are given by

$$W(0, Y) = W(1, Y) = 0, \quad \frac{\partial^2 W}{\partial X^2} \Big|_{X=0,1} = 0 \quad \text{for } 0 \leq Y \leq 1 \quad (18a)$$

$$\lambda^2 \frac{\partial^2 W}{\partial Y^2} + \nu \frac{\partial^2 W}{\partial X^2} \Big|_{Y=0,1} = 0, \quad \lambda^2 \frac{\partial^3 W}{\partial Y^3} + (2-\nu) \frac{\partial^3 W}{\partial X^2 \partial Y} \Big|_{Y=0,1} = 0 \quad \text{for } 0 \leq X \leq 1 \quad (18b)$$

### 3. Differential quadrature method

Although a number of numerical schemes can be used to solve the differential Eq. (15) subject to the boundary conditions (16)–(18), the differential quadrature scheme is one of the most accurate methods. Essentially a partial derivative of the function  $W(X, Y)$  at a sample point  $(X_i, Y_j)$  is considered as a weighted linear sum of the function  $W(X_i, Y_j) \equiv W_{ij}$  (Bert and Malik [25]). It is noted that using differential quadrature free corners can be taken into account easily. Let  $N$  and  $M$  be the total number of discrete points along  $X$  and  $Y$  directions, respectively. Considering the 2D rectangular plate defined on the domain  $0 \leq X, Y \leq 1$ ,  $r$ th order partial derivative of  $W(X, Y)$  with respect to  $X$ ,  $s$ th order partial derivative of  $W(X, Y)$  with respect to  $Y$  and  $(r+s)$ th order mixed partial derivative of  $W(X, Y)$  with respect to  $X$  and  $Y$  at a given point  $(X_i, Y_j)$  are expressed as (Bert and Malik [25]):

$$\frac{\partial^r W(X_i, Y_j)}{\partial X^r} = \sum_{k=1}^N A_{ik}^{(r)} W_{kj} \quad \text{for } i = 1, 2, \dots, N, \quad j = 1, 2, \dots, M \quad (19)$$

$$\frac{\partial^s W(X_i, Y_j)}{\partial Y^s} = \sum_{k=1}^M B_{jk}^{(s)} W_{ki} \quad \text{for } i = 1, 2, \dots, N, \quad j = 1, 2, \dots, M \quad (20)$$

$$\frac{\partial^{r+s} W(X_i, Y_j)}{\partial X^r \partial Y^s} = \sum_{k=1}^N A_{ik}^{(r)} \sum_{l=1}^M B_{jl}^{(s)} W_{kl} \quad (21)$$

where  $A_{ik}^{(r)}$  and  $B_{jl}^{(s)}$  are the weighting coefficients as defined in [26] given by

$$A_{ik}^{(1)} = \begin{cases} \prod_{\mu=1, \mu \neq i}^N \frac{X_i - X_\mu}{(X_i - X_k) \prod_{\mu=1, \mu \neq k}^N (X_k - X_\mu)} & \text{for } i, k = 1, 2, \dots, N, i \neq k \\ \sum_{\mu=1, \mu \neq i}^N \frac{1}{X_i - X_\mu} & \text{for } i = 1, 2, \dots, N, i = k \end{cases} \quad (22)$$

$$B_{jl}^{(1)} = \begin{cases} \prod_{\mu=1, \mu \neq j}^M \frac{Y_j - Y_\mu}{(Y_j - Y_l) \prod_{\mu=1, \mu \neq l}^M (Y_l - Y_\mu)} & \text{for } j, l = 1, 2, \dots, M, j \neq l \\ \sum_{\mu=1, \mu \neq j}^M \frac{1}{Y_j - Y_\mu} & \text{for } j = 1, 2, \dots, M, j = l \end{cases} \quad (23)$$

for  $r = s = 1$  and

$$A_{ik}^{(r)} = \begin{cases} r \left( A_{ii}^{(r-1)} A_{ik}^{(1)} - \frac{A_{ik}^{(r-1)}}{X_i - X_k} \right) & \text{for } k = 1, 2, \dots, N, i \neq k \\ - \sum_{\mu=1, \mu \neq i}^N A_{i\mu}^{(r)} & \text{for } i = 1, 2, \dots, N, i = k \end{cases} \quad (24)$$

$$B_{jl}^{(s)} = \begin{cases} s \left( B_{jj}^{(s-1)} B_{jl}^{(1)} - \frac{B_{jl}^{(s-1)}}{Y_j - Y_l} \right) & \text{for } l = 1, 2, \dots, M, j \neq l \\ - \sum_{\mu=1, \mu \neq j}^M B_{j\mu}^{(s)} & \text{for } j = 1, 2, \dots, M, j = l \end{cases} \quad (25)$$

for  $r = 2, 3, \dots, N-1$  and  $s = 2, 3, \dots, M-1$ . The distribution of the grid points is specified based on the approach developed in [26] and we use the Coupling Boundary Conditions with General Equation (CBCGE) technique to implement the boundary conditions [27]. Accordingly, the form of the grid points for CFFF plate is given by

$$X_i = 3\xi_i^2 - 2\xi_i^3, \quad Y_j = 3\chi_j^2 - 2\chi_j^3 \quad (26)$$

where

$$\xi_i = \frac{1}{2} \left[ 1 - \cos \left( \frac{i-1}{N-1} \pi \right) \right] \quad \text{for } i = 1, 2, \dots, N \quad (27a)$$

$$\chi_j = \frac{1}{2} \left[ 1 - \cos \left( \frac{j-1}{M-1} \pi \right) \right] \quad \text{for } j = 1, 2, \dots, M \quad (27b)$$

The forms of the grid points for CSSS and SFSF plates are taken as

$$X_i = \frac{1}{2} \left[ 1 - \cos \left( \frac{i-1}{N-1} \pi \right) \right] \quad \text{for } i = 1, 2, \dots, N \quad (28a)$$

$$Y_j = \frac{1}{2} \left[ 1 - \cos \left( \frac{j-1}{M-1} \pi \right) \right] \quad \text{for } j = 1, 2, \dots, M \quad (28b)$$

With the above considerations, Eq. (11) is transformed into the following discretized form:

$$c_{1j^3} W_{ij} \omega^3 + S_{ij} \omega^2 + T_{ij} \omega + U_{ij} + q(1-X) \sum_{i=1}^N A_{ik}^{(2)} W_{kj} = 0 \quad (29)$$

where

$$S_{ij} = c_2 j^2 \left( \sum_{k=1}^N A_{ik}^{(4)} W_{kj} + 2\lambda^2 \sum_{l=1}^M B_{jl}^{(2)} \sum_{k=1}^N A_{ik}^{(2)} W_{kl} + \lambda^4 \sum_{l=1}^M B_{jl}^{(4)} W_{il} \right) + j^2 W_{ij}$$

$$T_{ij} = c_3 j \left( \sum_{k=1}^N A_{ik}^{(4)} W_{kj} + 2\lambda^2 \sum_{l=1}^M B_{jl}^{(2)} \sum_{k=1}^N A_{ik}^{(2)} W_{kl} + \lambda^4 \sum_{l=1}^M B_{jl}^{(4)} W_{il} \right) + q(1-X) \sum_{k=1}^N A_{ik}^{(2)} W_{kj}$$

$$U_{ij} = \sum_{k=1}^N A_{ik}^{(4)} W_{kj} + 2\lambda^2 \sum_{l=1}^M B_{jl}^{(2)} \sum_{k=1}^N A_{ik}^{(2)} W_{kl} + \lambda^4 \sum_{l=1}^M B_{jl}^{(4)} W_{il}$$

The discretized form of boundary conditions (16) are given by

$$W_{ij} = W_{Nj} = W_{i,1} = W_{i,M} = 0 \quad \text{for } i = 1, 2, \dots, N \quad \text{and } j = 1, 2, \dots, M \quad (30a)$$

$$\sum_{k=1}^N A_{ik}^{(2)} W_{kj} = 0 \quad \text{for } i = 1 \quad \text{and } j = 1, 2, \dots, M \quad (30b)$$

$$\sum_{l=1}^M B_{jl}^{(2)} W_{il} = 0 \quad \text{for } i = 1, 2, \dots, N \quad \text{and } j = 1, M \quad (30c)$$

The discretized form of boundary conditions (17) is given next. For  $X = 0$  and  $X = 1$

$$W_{1j} = 0 \quad \text{for } j = 1, 2, \dots, M \quad (31a)$$

$$\sum_{k=1}^N A_{1k}^{(1)} W_{kj} = 0 \quad \text{for } j = 2, 3, \dots, M-1 \quad (31b)$$

$$\sum_{k=1}^N A_{Nk}^{(2)} W_{kj} + \nu \lambda^2 \sum_{l=1}^M B_{jl}^{(2)} W_{Nl} = 0 \quad \text{for } j = 2, 3, \dots, M-1 \quad (31c)$$

$$\sum_{k=1}^N A_{Nk}^{(3)} W_{kj} + (2-\nu)\lambda^2 \sum_{k=1}^N \sum_{l=1}^M A_{Nk}^{(1)} B_{jl}^{(2)} W_{kl} = 0 \quad \text{for } j = 2, 3, \dots, M-1 \quad (31d)$$

For  $Y = 0$  and  $Y = 1$

$$\lambda^2 \sum_{l=1}^M B_{1l}^{(2)} W_{il} + \nu \sum_{k=1}^N A_{ik}^{(2)} W_{kM} = 0 \quad \text{for } i = 2, 3, \dots, N-1 \quad (32a)$$

$$\lambda^2 \sum_{l=1}^M B_{1l}^{(3)} W_{il} + (2-\nu) \sum_{k=1}^N \sum_{l=1}^M A_{ik}^{(2)} B_{1l}^{(1)} W_{kl} = 0 \quad \text{for } i = 3, 4, \dots, N-2 \quad (32b)$$

$$\lambda^2 \sum_{l=1}^M B_{Ml}^{(2)} W_{il} + \nu \sum_{k=1}^N A_{ik}^{(2)} W_{kM} = 0 \quad \text{for } i = 2, 3, \dots, N-1 \quad (32c)$$

$$\lambda^2 \sum_{l=1}^M B_{Ml}^{(3)} W_{il} + (2-\nu) \sum_{k=1}^N \sum_{l=1}^M A_{ik}^{(2)} B_{Ml}^{(1)} W_{kl} = 0 \quad \text{for } i = 3, 4, \dots, N-2 \quad (32d)$$

At two free corners

$$\sum_{k=1}^N \sum_{l=1}^M A_{ik}^{(1)} B_{jl}^{(1)} W_{kl} = 0 \quad \text{for } i = N, \quad j = 1, M \quad (33)$$

The discretized form of boundary conditions (18) is given next. For  $X = 0$  and  $X = 1$

$$W_{1j} = 0 \quad \text{for } j = 1, 2, \dots, M \quad (34a)$$

$$\sum_{k=1}^N A_{1k}^{(1)} W_{kj} = 0 \quad \text{for } j = 2, 3, \dots, M-1 \quad (34b)$$

$$W_{Nj} = 0 \quad \text{for } j = 1, 2, \dots, M \quad (34c)$$

**Table 1**

Comparison of frequencies of CFFF and SFSF elastic plates with existing results for aspect ratios  $\lambda = 1.0$  and  $\lambda = 1.5$ .

$\lambda$	BC	$\omega_1$		$\omega_2$		$\omega_3$	
		Present	[28]	Present	[28]	Present	[28]
1.0	CFFF	3.485	3.492	8.604	8.525	21.586	21.429
	SFSF	9.631	9.631	16.135	16.135	36.726	36.726
1.5	CFFF	3.481	3.477	11.748	11.676	21.630	21.618
	SFSF	9.554	9.558	21.618	21.619	38.726	38.721

**Table 2**

Comparison of frequencies of CFFF and SFSF elastic plates with existing results for aspect ratios  $\lambda = 0.5$  and  $\lambda = 2.0$ .

$\lambda$	BC	$\omega_1$		$\omega_2$		$\omega_3$	
		Present	[29]	Present	[29]	Present	[29]
0.5	CFFF	3.496	3.508	5.383	5.372	10.241	10.260
	SFSF	9.736	9.870	11.685	11.660	17.685	17.660
2.0	CFFF	3.480	3.508	14.999	14.930	22.082	21.610
	SFSF	9.539	9.870	27.548	27.520	38.521	39.480

**Table 3**

Comparison of frequencies of CSSS elastic plates with existing results for the aspect ratios  $\lambda = 1.0$ ,  $\lambda = 1.5$  and  $\lambda = 2.0$  with  $H = 0$ ,  $q = 0$ .

$\lambda$	$\omega_1$		$\omega_2$		$\omega_3$	
	Present	[17]	Present	[17]	Present	[17]
0.5	17.33	–	23.64	–	35.05	–
1.0	23.64	23.64	51.67	–	58.60	58.65
1.5	35.05	35.05	69.87	69.91	100.18	–
2.0	51.67	51.67	86.13	86.13	140.84	140.84

**Table 4**

Comparison of flutter loads  $q$  of CSSS viscoelastic plates with existing results for the aspect ratios  $\lambda = 1.0$ ,  $\lambda = 1.5$  and  $\lambda = 2.0$  with  $H = 0$ .

$\lambda = 1.0$	$\lambda = 1.5$		$\lambda = 2.0$		
	Present	[17]	Present	[17]	Present
141.0	142.5	181.1	181.0	236.0	234.0

$$\sum_{k=1}^N A_{Nk}^{(2)} W_{kj} = 0 \quad \text{for } j = 2, 3, \dots, M-1 \quad (34d)$$

For  $Y = 0$  and  $Y = 1$

$$\lambda^2 \sum_{l=1}^M B_{1l}^{(2)} W_{il} + \nu \sum_{k=1}^N A_{ik}^{(2)} W_{kM} = 0 \quad \text{for } i = 2, 3, \dots, N-1 \quad (35a)$$

$$\lambda^2 \sum_{l=1}^M B_{1l}^{(3)} W_{il} + (2-\nu) \sum_{k=1}^N \sum_{l=1}^M A_{ik}^{(2)} B_{1l}^{(1)} W_{kl} = 0 \quad \text{for } i = 3, 4, \dots, N-2 \quad (35b)$$

$$\lambda^2 \sum_{l=1}^M B_{Ml}^{(2)} W_{il} + \nu \sum_{k=1}^N A_{ik}^{(2)} W_{kM} = 0 \quad \text{for } i = 2, 3, \dots, N-1 \quad (35c)$$

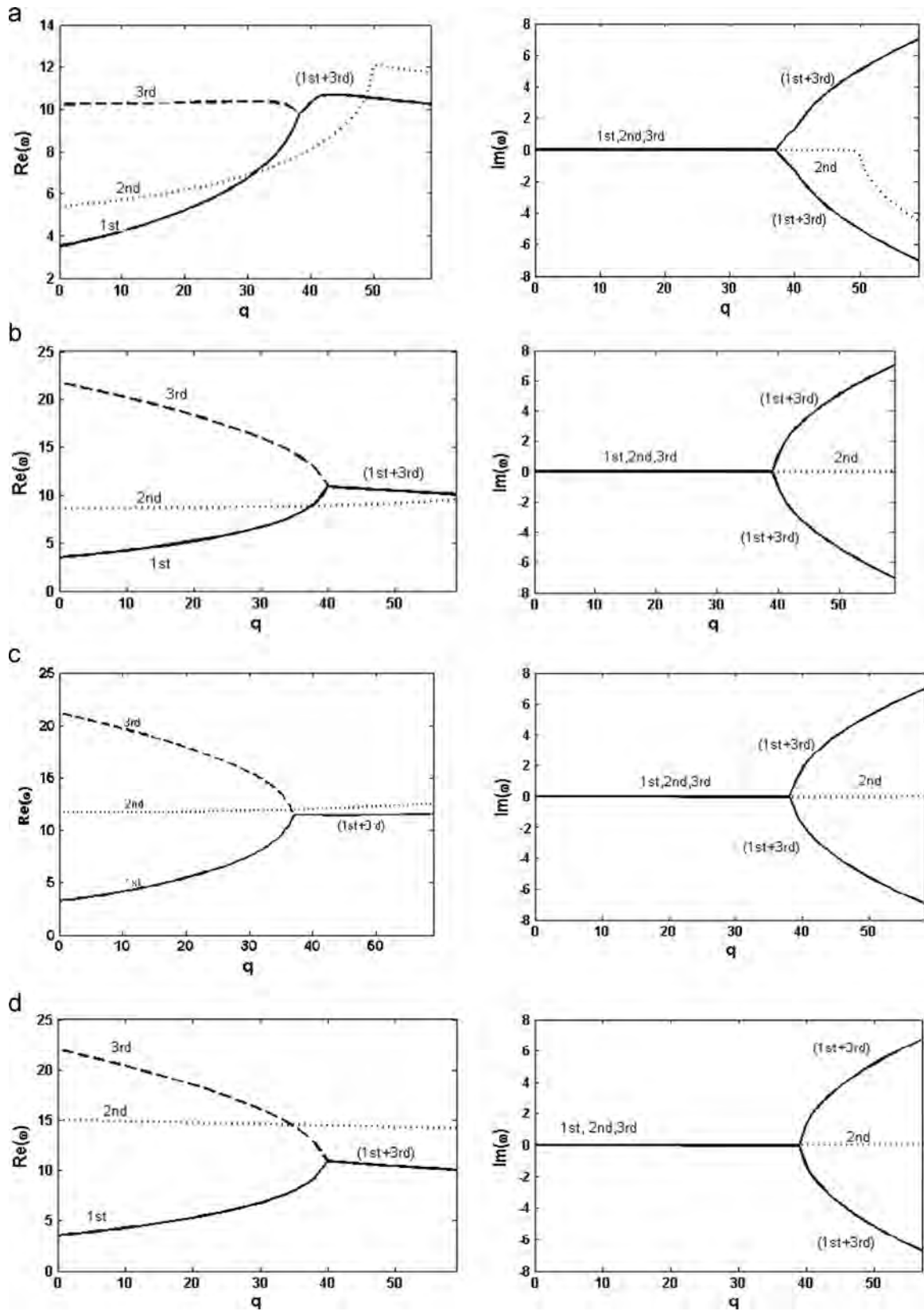


Fig. 2. Real and imaginary components of first three frequencies of CFFF plate plotted against  $q$  with  $H = 10^{-5}$  for (a)  $\lambda = 0.5$ , (b)  $\lambda = 1.0$ , (c)  $\lambda = 1.5$ , (d)  $\lambda = 2.0$ .

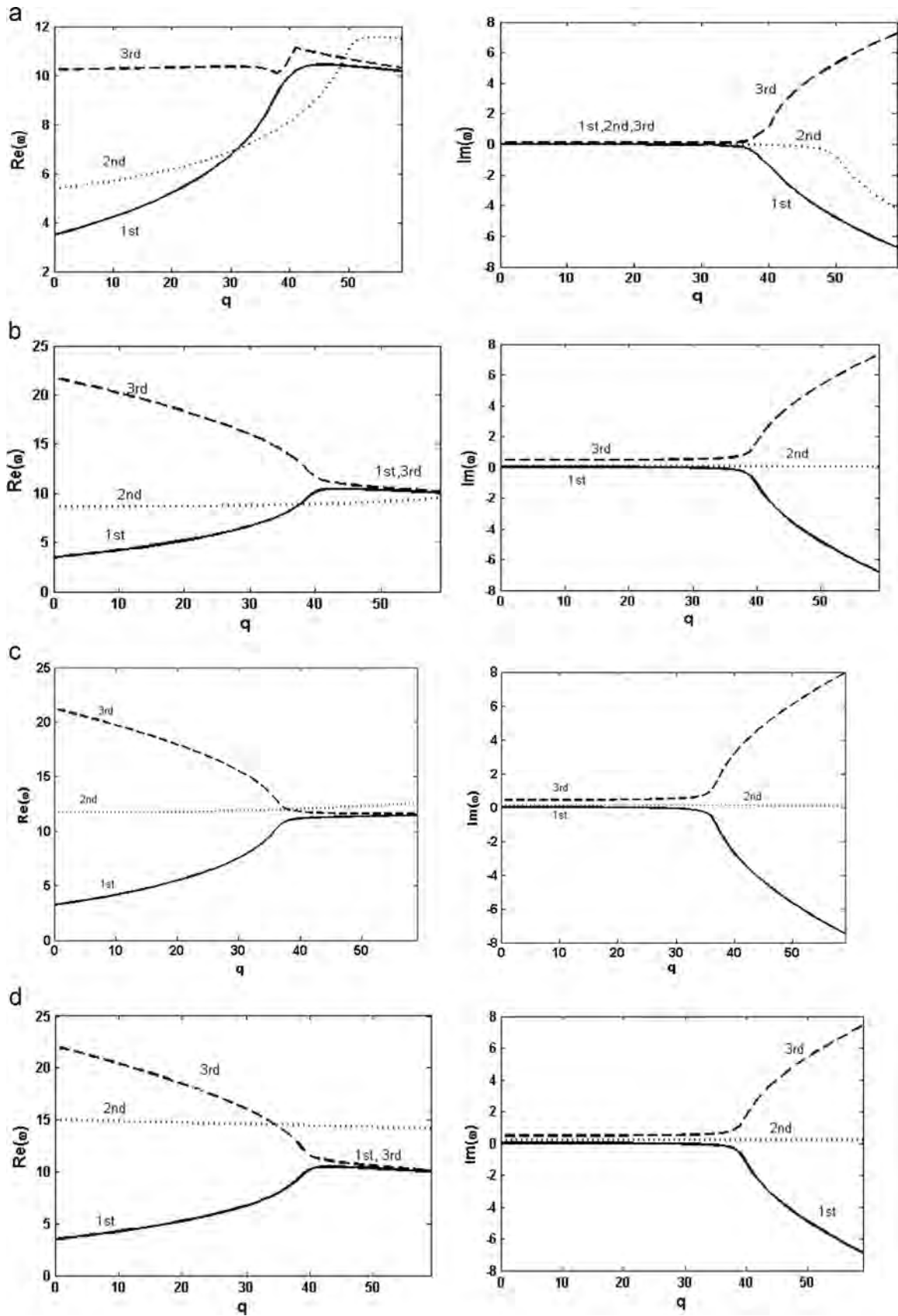


Fig. 3. Real and imaginary components of first three frequencies of CFFF plate plotted against  $q$  with  $H = 10^{-3}$  for (a)  $\lambda = 0.5$ , (b)  $\lambda = 1.0$ , (c)  $\lambda = 1.5$ , (d)  $\lambda = 2.0$ .

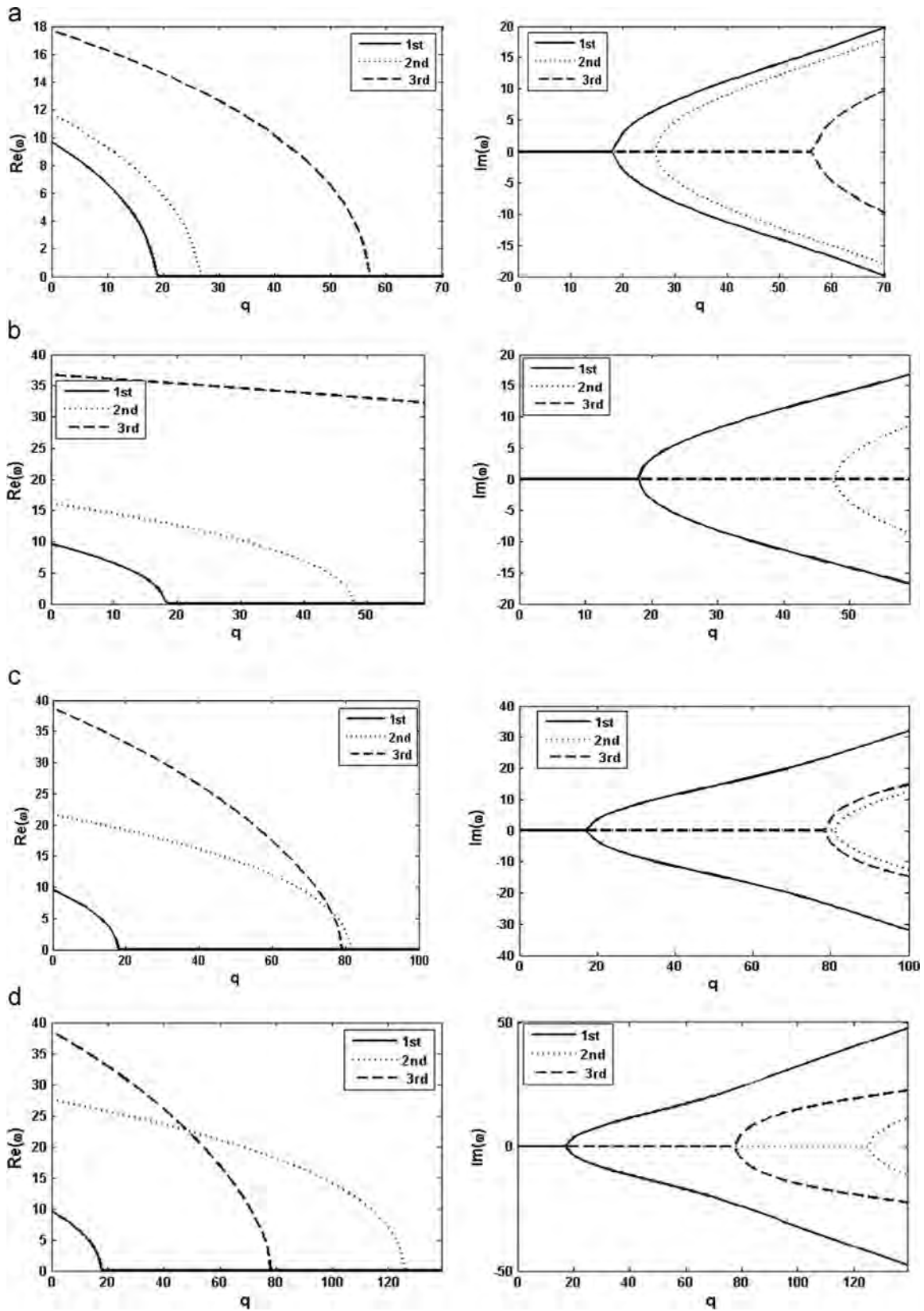


Fig. 4. Real and imaginary components of first three frequencies of SFSF plate.

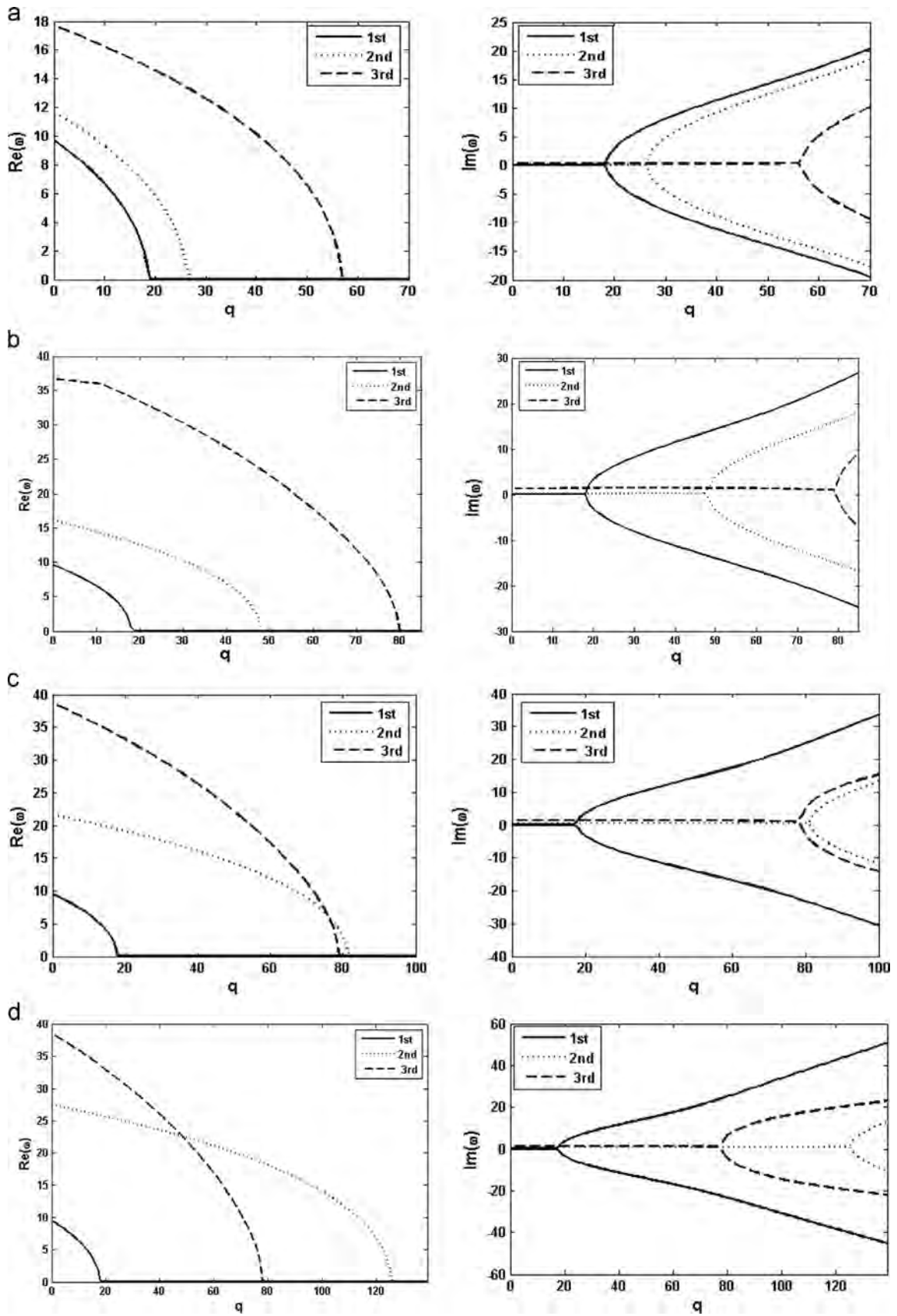


Fig. 5. Real and imaginary components of first three frequencies of SFSF plate plotted against  $q$  with  $H = 10^{-3}$  for (a)  $\lambda = 0.5$ , (b)  $\lambda = 1.0$ , (c)  $\lambda = 1.5$ , (d)  $\lambda = 2.0$ .

$$\lambda^2 \sum_{l=1}^M B_{Ml}^{(3)} W_{il} + (2-\nu) \sum_{k=1}^N \sum_{l=1}^M A_{ik}^{(2)} B_{Ml}^{(1)} W_{kl} = 0 \quad \text{for } i = 3, 4, \dots, N-2 \quad (35d)$$

The discretized Eq. (29) with the boundary conditions (30)–(35) can be rearranged and written in the following form:

$$\{\omega^3[\mathbf{C}_3] + \omega^2[\mathbf{C}_2] + \omega[\mathbf{C}_1] + [\mathbf{C}_0]\} \{W_{ij}\} = \{0\} \quad (36)$$

where  $[\mathbf{C}_0]$ ,  $[\mathbf{C}_1]$ ,  $[\mathbf{C}_2]$  and  $[\mathbf{C}_3]$  are  $(N-4) \times (M-4)$  by  $(N-4) \times (M-4)$  matrices [27] and depend on dimensionless parameters such as delay time  $H$ , dimensionless follower load  $q$ , and the aspect ratio  $\lambda$ . This equation may be viewed as the generalized eigenvalue problem describing the vibration of the plate. It is noted that Eq. (36) is equivalent to (29) where the expressions for the corresponding matrices are given explicitly.

#### 4. Verification

To check the accuracy of the DQ method, first three eigenfrequencies of freely vibrating ( $q_f = 0$ ) elastic plate ( $H = 0$ ) are compared with the exact results of [28] in Table 1 and with [29] in Table 2 for CFFF and SFSF boundary conditions.

The corresponding results for CSSS boundary conditions are given in Table 3 where the comparisons are made with the results of Ref. [17]. Numerical values obtained by DQ method match very closely with the results available in the literature.

Next the results for a viscoelastic plate subject to a distributed tangential load and CSSS boundary conditions are compared with those given in Wang and Zhou [17]. The results are shown in Table 4 and it is observed that the present results obtained by DQ are in good agreement with those obtained by a power series approach in Wang and Zhou [17].

#### 5. Numerical results and discussion

Next the viscoelastic plate subject to a distributed tangential force is studied. Results for CFFF boundary conditions are given in Fig. 2 for various aspect ratios with  $H = 10^{-5}$ . Fig. 2 shows the real and the imaginary parts of the frequency plotted against the tangential load  $q$  for the aspect ratios  $\lambda = 0.5$ ,  $\lambda = 1.0$ ,  $\lambda = 1.5$  and  $\lambda = 2.0$ . It is observed that the real part of the first vibration mode increases with the load while the third vibration mode decreases until they form a single mode without leading to divergence instability. Thus, there exists a threshold value  $q_f$  of the load above which the first and third modes have the same values. Imaginary part of the frequency is zero when the load is below the threshold value indicating that the vibration of the plate is less affected by the presence of viscoelastic damping. When the threshold value is exceeded, flutter instability occurs [9]. Imaginary part of the frequency exhibits negative value for  $q \geq q_f$  leading to the exponential growth of the deflection.

Corresponding results for  $H = 10^{-3}$  are given in Fig. 3. When the delay-time  $H$  (damping) becomes large corresponding to a plate with a large viscoelastic coefficient, there is more dissipation in the system. Results indicate that the plate become unstable not by divergence instability, but through the single mode flutter instability resulting from the negative imaginary part of the eigenvalue of the first mode. The imaginary parts of the second and third modes remain positive as opposed to being zero which was the case for  $H = 10^{-5}$  (Fig. 2).

Results for SFSF boundary conditions are given in Fig. 4 for aspect ratios  $\lambda = 0.5$ ,  $\lambda = 1.0$ ,  $\lambda = 1.5$  and  $\lambda = 2.0$  with  $H = 10^{-5}$ . The real parts of the first three modes decrease with increasing  $q$  until they become zero which contrasts with CFFF plates where

$q > 0$  until flutter instability occurs. Imaginary part of the frequency is zero up to  $q_{cr}$  (divergence load) which is less than the corresponding value for CFFF plates indicating that SFSF plates are less affected by the presence of viscoelastic damping. When the load exceeds  $q_{cr}$ , the real part of the mode is still zero while there appears two branches in the imaginary part; a positive branch which increases with the load and a negative branch which decreases and is responsible for the growth of the deflection. This behavior indicates the beginning of divergence instability of the plate. Corresponding results for SFSF plates are given in Fig. 5 for  $H = 10^{-3}$  which indicates that viscoelastic coefficient  $H$  does not affect the divergence stability for SFSF plates. Another difference as compared to Fig. 4 for  $H = 10^{-5}$  is that the imaginary part of the third mode remains positive for  $\lambda = 1.0$ ,  $\lambda = 1.5$  and  $\lambda = 2.0$  (Fig. 5b–d).

plotted against  $q$  with  $H = 10^{-5}$  for (a)  $\lambda = 0.5$ , (b)  $\lambda = 1.0$ , (c)  $\lambda = 1.5$ , (d)  $\lambda = 2.0$ .

#### 6. Conclusions

Dynamic stability of a viscoelastic plate subject to a distributed tangential follower load is studied. Two cases of boundary conditions are considered, namely, clamped-free (CFFF) and simply supported-free (SFSF). The viscoelastic constitutive relation is taken as Kelvin–Voigt type and the equation of motion is derived by using Laplace transformation. The numerical solution of the problem is obtained by differential quadrature method which is employed to transform the continuous formulation into a discrete set of algebraic equations. The solution method is verified by using the available results in the literature.

In the case of CFFF plates the instability occurs by flutter and not by divergence as the real part of the first vibration mode increases with increasing load and forms a single mode with the third vibration mode without leading to divergence instability. When a threshold value is exceeded, the imaginary part of the first frequency becomes negative, leading to the exponential growth of the vibrations. An interesting result is the observation that the stability behavior of CFFF plates differs from that of the SFSF plates in which case the instability occurs by divergence as the real parts of the first three modes decrease with increasing  $q$  until they become zero. For SFSF plates,  $q_{cr}$  (divergence load) is less than the critical flutter load of CFFF plates as the viscoelastic damping is not as effective for SFSF plates. As such the boundary conditions strongly influence the stability of the plate. Viscoelastic coefficient was found to have little effect on the divergence instability of SFSF plates. It was also observed that the aspect ratio has little effect on the flutter load of CFFF plates as well as on the divergence load of SFSF plates.

#### Acknowledgment

The research reported in this paper was supported by research grants from the University of KwaZulu–Natal (UKZN) and from National Research Foundation (NRF) of South Africa under the grant reference number IFR150209113856. The authors gratefully acknowledge the support provided by UKZN and NRF.

#### References

- [1] Hermann G. Stability of equilibrium of elastic systems subjected to non-conservative forces. *Appl Mech Rev* 1967;20:103–8.
- [2] Farshad M. Stability of cantilever plate subjected to biaxial subtangential loading. *J Sound Vib* 1978;58:555–61.

- [3] Adali S. The stability of rectangular plate under nonconservative and conservative forces. *Int J Solids Struct* 1982;18:1043–52.
- [4] Leipholz HHE, Pfent P. Application of extended equation of Galerkin to stability problems of rectangular plates with free edges and subjected to uniformly distributed follower forces. *Comput Methods Appl Mech Eng* 1983;37:341–65.
- [5] Kumar A, Srivasta AK. Stability of thin rectangular elastic plates under a follower force. *Mech Res Commun* 1986;13:165–8.
- [6] Higuchi K, Dowell EH. Dynamic stability of a completely free plate subjected to a controlled non-conservative follower force. *J Sound Vib* 1989;132(1):115–28.
- [7] Zuo QH, Schreyer HL. Flutter and divergence instability of nonconservative beams and plates. *Int J Solids Struct* 1995;33:1355–67.
- [8] Kumar LR, Datta PK, Prabhakara DL. Dynamic instability characteristics of laminated composite plates subjected to partial follower edge load with damping. *Int J Mech Sci* 2003;45(9):1429–48.
- [9] Kim JH, Park JH. On the dynamic stability of rectangular plates subjected to intermediate follower forces. *J Sound Vib* 1998;5:882–8.
- [10] Kim JH, Kim HS. A study on the dynamic stability of plates under follower load. *Comput Struct* 2000;74:351–63.
- [11] Jayaraman G, Strusthers A. Divergence and flutter instability of elastic specially orthotropic plates subjected to follower forces. *J Sound Vib* 2005;281:351–73.
- [12] Langthjem MA, Sugiyama Y. Dynamic stability of viscoelastic beam under follower forces. *J Sound Vib* 2000;238:809–51.
- [13] Darabseh TT, Genin J. Dynamic stability of viscoelastic columns loaded by follower force. *J Mech Eng Sci* 2004;218:1091–101.
- [14] Zhuo RH, Fen SZ. Dynamic stability of viscoelastic beam under follower force. *ASCE J Eng Mech* 2005;22:26–30.
- [15] Eshmatov B Kh. Nonlinear vibrations and dynamic stability of viscoelastic orthotropic rectangular plates. *J Sound Vib* 2007;300:709–26.
- [16] Wang Z-M, Zhou Y-F, Wang Y. Dynamic stability of non-conservative viscoelastic rectangular plate. *J Sound Vib* 2007;307:250–64.
- [17] Wang Z-M, Zhou Y-F. Exact solutions for stability of viscoelastic rectangular plate subjected to tangential follower force. *Arch Appl Mech* 2014;84:1081–9.
- [18] Robinson MTA, Adali, S. Dynamic stability of viscoelastic rectangular plates subjected to triangular tangential follower loads [in preparation].
- [19] Robinson MTA. Nonlinear vibration of 2D viscoelastic plate subjected to tangential follower force. *Eng Mech* 2013;20(1):59–74.
- [20] Wang Y, Wang Z, Zu L. Stability of viscoelastic rectangular plate with a piezoelectric layer subjected to follower force. *Arch Appl Mech* 2013;83:495–507.
- [21] Civalek Ö. Application of differential quadrature (DQ) and harmonic differential quadrature (HDQ) for buckling analysis of thin isotropic plates and elastic columns. *Eng Struct* 2004;26(2):171–86.
- [22] Marzani A, Tornabene F, Viola E. Nonconservative stability problem via generalized differential quadrature method. *J Sound Vib* 2008;315:176–96.
- [23] Wang Z-M, Wang Y, Guo X. Dynamic stability of linearly varying thickness viscoelastic plate with crack and subjected to tangential follower forces. *Appl Acoust* 2009;70:845–56.
- [24] Flügge W. *Viscoelasticity*. Berlin: Springer; 1975.
- [25] Bert CW, Malik M. Implementing multiple boundary conditions in the DQ solution of higher-order PDE's: application to free vibration of plates. *Int J Numer Meth Eng* 1996;39:1237–58.
- [26] Tang Y-Q, Chen L-Q. Nonlinear free transverse vibration of in-plane moving plate: without and with internal resonances. *J Sound Vib* 2011;330:110–26.
- [27] Shu C, Du HA. Generalized approach for implementing general boundary conditions in the GDQ free vibration analysis of plates. *Int J Solids Struct* 1997;34:837–46.
- [28] Leissa AW. Free vibration of rectangular plates. *J Sound Vib* 1973;31:251–93.
- [29] Leissa AW. *Vibration of Plates*, NASA, SP-160, Washington DC; 1969.

**CHAPTER 5-PAPER 2:**  
**NONCONSERVATIVE STABILITY OF VISCOELASTIC RECTANGULAR  
PLATES SUBJECTED TO TRIANGULARLY DISTRIBUTED TANGENTIAL  
FOLLOWER LOADS. Submitted to *journal of Theoretical and Applied  
Mechanics.***

# NONCONSERVATIVE STABILITY OF VISCOELASTIC PLATES SUBJECT TO TRIANGULARLY DISTRIBUTED FOLLOWER LOADS

MOUAFO TEIFOUET ARMAND ROBINSON<sup>1,2</sup>, SARP ADALI<sup>1</sup>

<sup>1</sup> *Discipline of Mechanical Engineering, University of KwaZulu-Natal, Durban 4041, South Africa*

<sup>2</sup> *Department of Physics, University of Dschang, Cameroon*

Emails: [adali@ukzn.ac.za](mailto:adali@ukzn.ac.za), [armandmouafo@yahoo.fr](mailto:armandmouafo@yahoo.fr)

## Abstract

Divergence and flutter instabilities of viscoelastic rectangular plates under triangularly distributed tangential follower loads are studied. Two sets of boundary conditions are considered, namely, simply supported plates and plates with a combination of clamped and simply supported edges. The constitutive relations for the viscoelastic plates are of Kelvin-Voigt type with the effect of viscoelasticity on stability studied numerically. The method of solution is differential quadrature which is employed to discretize the equation of motion and the boundary conditions leading to a generalized eigenvalue problem. After verifying the method of solution, numerical results are given for the real and imaginary parts of the eigenfrequencies to investigate flutter and divergence characteristics and dynamic stability of the plates with respect to various problem parameters.

*Keywords:* viscoelastic plates, dynamic stability, triangularly distributed follower load

## 1. Introduction

Dynamic stability of elastic structures subject to nonconservative loads is of practical importance in such fields as aerospace, mechanical, and civil engineering. As a result the subject has been studied extensively to quantify the behaviour of beams, plates and shells under follower forces. These forces can be concentrated, uniformly distributed or triangularly distributed depending on the specific application. They act in the tangential direction and are not derivable from a potential due to their nonconservative nature as presented in works by Kumar and Srivasta (1986), Przybylski (1999), Gajewski (2000), Krilov (2013).

Early work on the nonconservative instability under uniformly distributed follower loads mostly involved one dimensional elastic structures, namely, columns (Sugiyama and Kawagoe, 1975; Leipholz, 1975; Chen and Ku, 1991). Stability of columns under triangularly distributed

loads has been studied by Leipholz and Bhalla (1977), Sugiyama and Mladenov (1983) and Ryu *et al.* (2000). More recent studies on nonconservative loading include columns subject to uniformly distributed follower loads by Kim (2010), Kim *et al.* (2008) and Kazemi-Lari *et al.* (2013) and to triangularly distributed follower loads by Kim (2011). Studies on nonconservative stability of two-dimensional structures mostly involved rectangular plates under follower loads (Culkowski and Reismann, 1977; Farshad, 1978; Adali, 1982) and under uniformly distributed tangential loads (Leipholz, 1978; Leipholz and Pfenndt, 1982, 1983; Wang and Ji, 1992).

Recent work on the stability of elastic plates under nonconservative loads includes works by Zuo and Shreyer (1996), Kim and Park (1998), Kim and Kim (2000), and Jayaraman and Struthers (2005). Dynamic stability of functionally graded plates under uniformly distributed axial loads has been studied by Ruan *et al.* (2012) and shells by Toriki *et al.* (2014a, b). These studies neglected the effect of viscoelasticity on the stability of the columns and plates.

Dynamic stability of one-dimensional viscoelastic structures has been the subject of the works by Marzani and Potapov (1999), Langthjem and Sugiyama (2000), Darabseh and Genin (2004), Zhuo and Fen (2005), Ilyasov and Ilyasova (2006), and Elfelsoufi and Azrar (2006). Recently the dynamic stability of viscoelastic plates has been studied for a number of cases (Ilyasov and Aköz, 2000; Wang *et al.*, 2007, 2009, 2013; Zhou and Wang, 2014; Robinson and Adali, 2016). Vibrations of a simply supported plate with nonlinear strain-displacement relations and subject to a uniformly distributed tangential force were studied by Robinson (2013). Dynamic stability of viscoelastic shells has been studied by Ilyasov (2010).

Although the dynamic stability under triangularly distributed tangential forces have been studied in the case of columns (see Leipholz and Bhalla, 1977; Sugiyama and Mladenov, 1983; Ryu *et al.*, 2000; Kim, 2011), dynamic stability of plates, and in particular, viscoelastic plates under this type of loading does not seem to be studied so far.

Present work extends the results of Robinson and Adali (2016) which studied the nonconservative stability of the viscoelastic plates with free edges and under uniformly distributed follower loads, to the case of plates with simply supported and simply supported-clamped plates and subject to triangularly distributed follower loads. Comparisons are given for the uniformly and triangularly distributed follower loads. The stability problem is solved for the simply supported plates and for plates with a combination of simple and clamped supports by differential quadrature method. Divergence and flutter loads are determined and the effect of viscoelasticity and the boundary conditions on dynamic stability is investigated. The method of solution is verified against the known results in the literature.

## 2. Viscoelastic plate subject to triangularly distributed load

We consider a rectangular plate of uniform thickness  $h$  having dimensions  $a \times b$  in the  $x$  and  $y$  directions, respectively. It is subject to a non-uniform tangential follower force  $q_t = q_0 x/a$ . The material of the plate is viscoelastic which is expressed by the Kelvin-Voigt constitutive relations given by

$$\mathbf{s}_{ij} = 2G \mathbf{e}_{ij} + 2\eta \dot{\mathbf{e}}_{ij} \quad (2.1)$$

$$\sigma_{ii} = 3K \varepsilon_{ii} \quad (2.2)$$

where  $\mathbf{s}_{ij}$  and  $\mathbf{e}_{ij}$  are deviatoric tensor of stress and strain, respectively, and  $\sigma_{ii}$  and  $\varepsilon_{ii}$  are the spherical tensor of stress and strain with  $\eta$  denoting the viscoelastic coefficient. Bulk modulus  $K$  and shear modulus  $G$  can be expressed in terms of the Young's modulus  $E$  and Poisson's ratio  $\nu$  as  $K = E/3(1-2\nu)$  and  $G = E/(1+2\nu)$ . The equation of vibration of the viscoelastic plate subject to a triangular follower load is first obtained in the Laplace domain (see Wang *et al.*, 2007; Zhou and Wang, 2014). By inverse Laplace transformation, the governing equation can be expressed in the time domain as

$$\frac{h^3}{12} \left( A_3 + A_4 \frac{\partial}{\partial t} + A_5 \frac{\partial^2}{\partial t^2} \right) \nabla^4 w + \left( A_1 + A_2 \frac{\partial}{\partial t} \right) \left( \frac{q_0(a-x)^2}{2} \frac{\partial^2 w}{\partial x^2} + \rho h \frac{\partial^2 w}{\partial t^2} \right) = 0 \quad (2.3)$$

where  $\rho$  is the density of the plate and

$$A_1 = 3K + 4G, \quad A_2 = 3K + 4G, \quad A_3 = 4\eta \quad (2.4a)$$

$$A_4 = 4G(3K + G), \quad A_5 = \eta(8G + 12K), \quad A_6 = 4\eta^2 \quad (2.4b)$$

$$\nabla^4 w = \frac{\partial^4 w}{\partial x^4} + 2 \frac{\partial^4 w}{\partial x^2 \partial y^2} + \frac{\partial^4 w}{\partial y^4} \quad (2.5)$$

After introducing the dimensionless coefficients

$$X = \frac{x}{a}, \quad Y = \frac{y}{b}, \quad \bar{w} = \frac{w}{h}, \quad \lambda = \frac{a}{b} \quad (2.6a)$$

$$q = \frac{6q_0 a^4 (1-\nu^2)}{Eh^3}, \quad \tau = \frac{th}{a^2} \sqrt{\frac{E}{12\rho(1-\nu^2)}}, \quad H = \frac{\eta h}{a^2} \sqrt{\frac{1}{12\rho(1-\nu^2)E}} \quad (2.6b)$$

the non-dimensional equation of motion is obtained as

$$\left( 1 + g_1 \frac{\partial}{\partial \tau} + g_2 \frac{\partial^2}{\partial \tau^2} \right) \nabla^4 \bar{w} + \left( 1 + g_3 \frac{\partial}{\partial \tau} \right) \left( q(1-X)^2 \frac{\partial^2 \bar{w}}{\partial X^2} + \frac{\partial^2 \bar{w}}{\partial \tau^2} \right) = 0 \quad (2.7)$$

where

$$g_2 = \frac{4(1-2\nu)(1+\nu)^2}{3} H^2, \quad g_3 = \frac{4(1-2\nu)(1+\nu)}{3(1-\nu)} H \quad (2.8)$$

$$\nabla^4 \bar{w} = \frac{\partial^4 \bar{w}}{\partial X^4} + 2\lambda^2 \frac{\partial^4 \bar{w}}{\partial X^2 \partial Y^2} + \lambda^4 \frac{\partial^4 \bar{w}}{\partial Y^4} \quad (2.9)$$

In equations (2.8), (2.9),  $H$  is the dimensionless delay time of the material and  $\tau$  is dimensionless time defined in Eq. (2.6b). Let

$$\bar{w}(X, Y, \tau) = W(X, Y) e^{j\omega\tau} \quad (2.10)$$

where  $j = \sqrt{-1}$  and  $\omega$  the dimensionless vibration frequency. Substitution of equation (2.10) into equation (2.7) yields the differential equation

$$\left(1 + g_1 j\omega + g_2 j^2 \omega^2\right) \nabla^4 W + (1 + g_3 j\omega) \left( q(1-X)^2 \frac{\partial^2 W}{\partial X^2} + j^2 \omega^2 \right) = 0 \quad (2.11)$$

in terms of the space variables  $X$  and  $Y$ . The boundary conditions considered in the present work are the simply supported plates (SSSS) and plates with two opposite edges clamped and two others simply supported (CSCS). SSSS boundary conditions are given by

$$\bar{w}(X, Y, \tau) = \frac{\partial^2 \bar{w}}{\partial X^2} \Big|_{X=0} = 0 \quad \text{for } 0 \leq Y \leq 1 \quad (2.12a)$$

$$\bar{w}(X, Y, \tau) = \frac{\partial^2 \bar{w}}{\partial Y^2} \Big|_{Y=0,1} = 0 \quad \text{for } 0 \leq X \leq 1 \quad (2.12b)$$

CSCS boundary conditions are given by

$$\bar{w}(X, Y, \tau) = \frac{\partial \bar{w}}{\partial X} \Big|_{X=0} = 0 \quad \text{for } 0 \leq Y \leq 1 \quad (2.13a)$$

$$\bar{w}(X, Y, \tau) = \frac{\partial^2 \bar{w}}{\partial Y^2} \Big|_{Y=0,1} = 0 \quad \text{for } 0 \leq X \leq 1 \quad (2.13b)$$

### 3. Differential quadrature (DQ) method

DQ method involves approximating the partial derivatives of the function  $W(X, Y)$  at a sample point  $(X_i, Y_j)$  by the weighted sum of the function  $W_{ij}$  values (see Bert and Malik, 1996; Krowiak, 2008). Let the number of sample points denoted by  $N$  in  $X$  direction and  $M$  in  $Y$  direction. The  $r^{th}$  order partial derivative with respect to  $X$ ,  $s^{th}$  order partial derivative with respect to  $Y$  and the  $(r+s)^{th}$  order mixed partial derivative of  $W(X, Y)$  with respect to both  $X$  and  $Y$  are discretely expressed at the point  $(X_i, Y_j)$  as:

$$\begin{aligned} \frac{\partial^r W(X_i, Y_j)}{\partial X^r} &= \sum_{k=1}^N A_{ik}^{(r)} W_{kj}, & \frac{\partial^s W(X_i, Y_j)}{\partial Y^s} &= \sum_{l=1}^M B_{jl}^{(s)} W_{il} \\ \frac{\partial^{r+s} W(X_i, Y_j)}{\partial X^r \partial Y^s} &= \sum_{k=1}^N A_{ik}^{(r)} \sum_{l=1}^M B_{jl}^{(s)} W_{kl} \end{aligned} \quad (3.1)$$

where  $i = 1, 2, \dots, N$ ,  $k = 1, 2, \dots, N-1$ ,  $j = 1, 2, \dots, M$  and  $l = 1, 2, \dots, M-1$ .

For  $r = s = 1$  the coefficients  $A_{ik}^{(r)}$  and  $B_{jl}^{(s)}$  are defined as

$$A_{ik}^{(1)} = \begin{cases} \prod_{\mu=1, \mu \neq i}^N \frac{X_i - X_\mu}{(X_i - X_k) \prod_{\mu=1, \mu \neq k}^N (X_k - X_\mu)} & \text{for } i, k = 1, 2, \dots, N \ (i \neq k) \\ \sum_{\mu=1, \mu \neq k}^N \frac{1}{X_i - X_\mu} & \text{for } i = 1, 2, \dots, N \ (i = k) \end{cases} \quad (3.2)$$

$$B_{jl}^{(1)} = \begin{cases} \prod_{\mu=1, \mu \neq j}^M \frac{Y_j - Y_\mu}{(Y_j - Y_l) \prod_{\mu=1, \mu \neq l}^M (Y_l - Y_\mu)} & \text{for } j, l = 1, 2, \dots, M \ (j \neq l) \\ \sum_{\mu=1, \mu \neq j}^M \frac{1}{Y_j - Y_\mu} & \text{for } j = 1, 2, \dots, M \ (j = l) \end{cases} \quad (3.3)$$

For  $r = 2, 3, \dots, N-1$  and  $s = 2, 3, \dots, M-1$

$$A_{ik}^{(r)} = \begin{cases} r \left( A_{ii}^{(r-1)} A_{ik}^{(1)} - \frac{A_{ik}^{(r-1)}}{X_i - X_k} \right) & \text{for } i, k = 1, 2, \dots, N \ (i \neq k) \\ - \sum_{\mu=1, \mu \neq i}^N A_{i\mu}^{(r)} & \text{for } i = 1, 2, \dots, N \ (i = k) \end{cases} \quad (3.4)$$

$$B_{jl}^{(s)} = \begin{cases} s \left( B_{jj}^{(s-1)} B_{jl}^{(1)} - \frac{B_{jl}^{(s-1)}}{Y_j - Y_l} \right) & \text{for } j, l = 1, 2, \dots, M \ (j \neq l) \\ - \sum_{\mu=1, \mu \neq j}^M B_{j\mu}^{(s)} & \text{for } j = 1, 2, \dots, M \ (j = l) \end{cases} \quad (3.5)$$

The distribution of the grid points are taken as non-uniform and for the simply supported plate, the grid points are specified as

$$X_1 = 0, \quad X_N = 1, \quad X_i = \frac{1}{2} \left[ 1 + \cos \left( \frac{2i-3}{2N-4} \pi \right) \right] \quad \text{for } i = 2, 3, \dots, N-1 \quad (3.6)$$

$$Y_1 = 0, \quad Y_M = 1, \quad Y_j = \frac{1}{2} \left[ 1 - \cos \left( \frac{2j-3}{2N-4} \pi \right) \right] \quad \text{for } j = 2, 3, \dots, M-1 \quad (3.7)$$

For the plate with two opposite edges simply supported and other two edges clamped, the  $\delta$  method combined with the weighted coefficient method is adopted. Thus the grid points for CSCS plate are given by

$$X_1 = 0, \quad X_2 = \delta, \quad X_{N-1} = 1 - \delta, \quad X_N = 1, \quad X_i = \frac{1}{2} \left[ 1 - \cos \left( \frac{i-2}{N-3} \pi \right) \right] \quad \text{for } i = 3, 4, \dots, N-2 \quad (3.8)$$

$$Y_1 = 0, \quad Y_M = 1, \quad Y_j = \frac{1}{2} \left[ 1 - \cos \left( \frac{2j-3}{2N-4} \pi \right) \right] \quad \text{for } j = 2, 3, \dots, M-1 \quad (3.9)$$

where  $\delta \ll 1$ . Using equation (3.1), the discretized form of the differential equation (2.11) can be expressed as

$$c_1 j^3 W_{ij} \omega^3 + (c_2 S_{ij} + W_{ij}) j^2 \omega^2 + \left( c_3 S_{ij} + c_1 q (1-X)^2 \sum_{k=1}^N A_{ik}^{(2)} W_{kj} \right) j \omega + q (1-X)^2 \sum_{k=1}^N A_{ik}^{(2)} W_{kj} = 0 \quad (3.10)$$

where

$$S_{ij} = \sum_{k=1}^N A_{ik}^{(4)} W_{kj} + 2\lambda^2 \sum_{l=1}^M B_{jl}^{(2)} \sum_{k=1}^N A_{ik}^{(2)} W_{kl} + \lambda^4 \sum_{l=1}^M B_{jl}^{(4)} W_{il} \quad (3.11)$$

$$c_1 = \frac{4(1-2\nu)(1+\nu)}{3(1-\nu)} H, \quad c_2 = \frac{4(1-2\nu)(1+\nu)^2}{3} H^2, \quad c_3 = \frac{4(1-2\nu)(1+\nu)}{3} H \quad (3.12)$$

The discretized form of boundary conditions (2.12) are given by

$$W_{1j} = W_{Nj} = W_{i1} = W_{iM} = 0 \quad \text{for } i = 1, 2, \dots, N \text{ and } j = 1, 2, \dots, M \quad (3.13a)$$

$$\sum_{k=1}^N A_{ik}^{(2)} W_{kj} = 0 \quad \text{for } i = 1, N \text{ and } j = 1, 2, \dots, M \quad (3.13b)$$

$$\sum_{l=1}^M B_{jl}^{(2)} W_{il} = 0 \quad \text{for } i = 1, 2, \dots, N \quad \text{and } j = 1, M \quad (3.13c)$$

The corresponding equations for the boundary conditions (2.13) are:

$$W_{1j} = W_{Nj} = W_{i1} = W_{iM} = 0 \quad \text{for } i = 1, 2, \dots, N \quad \text{and } j = 1, 2, \dots, M \quad (3.14a)$$

$$\sum_{k=1}^N A_{ik}^{(1)} W_{kj} = 0 \quad \text{for } i = 2, N-1 \quad \text{and } j = 2, 3, \dots, M-2 \quad (3.14b)$$

$$\sum_{l=1}^M B_{jl}^{(2)} W_{il} = 0 \quad \text{for } i = 1, 2, \dots, N \quad \text{and } j = 1, M \quad (3.14c)$$

#### 4 . Numerical results and discussion

Results for the viscoelastic plate subject to triangularly distributed tangential force are given in comparison to the results for a viscoelastic plate subject to uniformly distributed tangential force which was studied in Wang *et al.* (2007) and Zhou and Wang (2014). Results for SSSS and CSCS boundary conditions are given in Table 1 for  $H = 10^{-5}$  (nondimensional viscoelasticity coefficient). Table 1 shows that the flutter load, denoted by  $q_f$ , is higher in the case of the load having triangular distribution as expected. In Table 1,  $q_{d1}$  and  $q_{d2}$  denote the divergence loads of the 1<sup>st</sup> and 2<sup>nd</sup> modes, respectively.

Figs. 1-3 show the real and the imaginary parts of the first three frequencies plotted against the load  $q$  for uniformly and triangularly distributed tangential loads for SSSS plates with  $H = 10^{-5}$  and  $\lambda = 1$ ,  $\lambda = 1.5$  and  $\lambda = 2$ , respectively. The corresponding results for the imaginary part of the frequencies for  $H = 10^{-3}$  are given in Figs. 4-5. It is noted that the results given in Figs. 1-5 for the uniformly distributed tangential load are the same as the ones given in Wang *et al.* (2007). As such they provide the verification of the method of solution outlined in section 3.

Comparisons of the loads with uniform and triangular distributions indicate that the results are qualitatively similar, but the magnitudes of the follower load causing divergence or flutter instability differ considerably. Comparisons between Figs. 1a, 2a, 3a ( $H = 10^{-5}$ ) and Figs. 4a, 4b and 5 ( $H = 10^{-3}$ ) indicate that the imaginary parts of the frequencies remain positive for  $H = 10^{-3}$  up to the flutter load. The corresponding results for CSCS plates with  $H = 10^{-5}$  are given in Figs. 6-8 with  $\lambda = 1$ ,  $\lambda = 1.5$  and  $\lambda = 2$ , respectively. The results for the uniformly distributed tangential loads are also shown in the figures which verify the results of

Wang et al. (2007). In this case it is observed that the real parts of the vibration modes behave differently as compared to SSSS plates shown in Figs. 1-3. For the case  $\lambda = 1$  (Fig. 6a) the real parts of the first and the third modes join to form a single mode. For  $\lambda = 1.5$  and  $\lambda = 2$ , the first and the second modes join as shown in Figs. 7a and 8a, respectively. Thus, in the case of CSCS boundary conditions, there exists a threshold value  $q$  above which the first mode can join the second or third mode to form a single mode and this value depends on the aspect ratio. Moreover, it is observed that for the aspect ratios of  $\lambda = 1.5$  and  $\lambda = 2$ , the plate does not show divergence instability and loses stability by flutter.

Table 1. Comparison of flutter loads  $q$  of viscoelastic plates with  $H = 10^{-5}$  for various aspect ratios.

Aspect ratio $\lambda$	Boundary conditions	Uniformly distributed load Wang <i>et al.</i> (2007)	Triangularly distributed load
1.0	SSSS	$q_{d1} = 67.5$ $q_{d2} = 132.1$	$q_{d1} = 95.1$ $q_{d2} = 225.1$
	CSCS	$q_{d1} = 143.5$ $q_f = 168.0$	$q_f = 226.0$
1.5	SSSS	$q_{d1} = 136.8$ $q_{d2} = 224.7$	$q_{d1} = 174.0$ $q_{d2} = 329.0$
	CSCS	$q_f = 202.8$	$q_f = 270.0$
2.0	SSSS	$q_{d1} = 224.8$ $q_{d2} = 340.5$	$q_{d1} = 273.04$ $q_{d2} = 453.2$
	CSCS	$q_f = 251.5$	$q_f = 333.0$

For CSCS boundary conditions with  $H = 10^{-3}$ , the results are given in Figs. 9-11. For this value of  $H = 10^{-3}$ , the real parts of the frequencies do not form a single mode and the imaginary parts remain positive until the threshold values are exceeded and the flutter instability occurs as shown in Figs. 9b, 10b and 11b. Imaginary parts of the frequencies exhibit negative values for  $q \geq q_f$  leading to the exponential growth of the deflection.

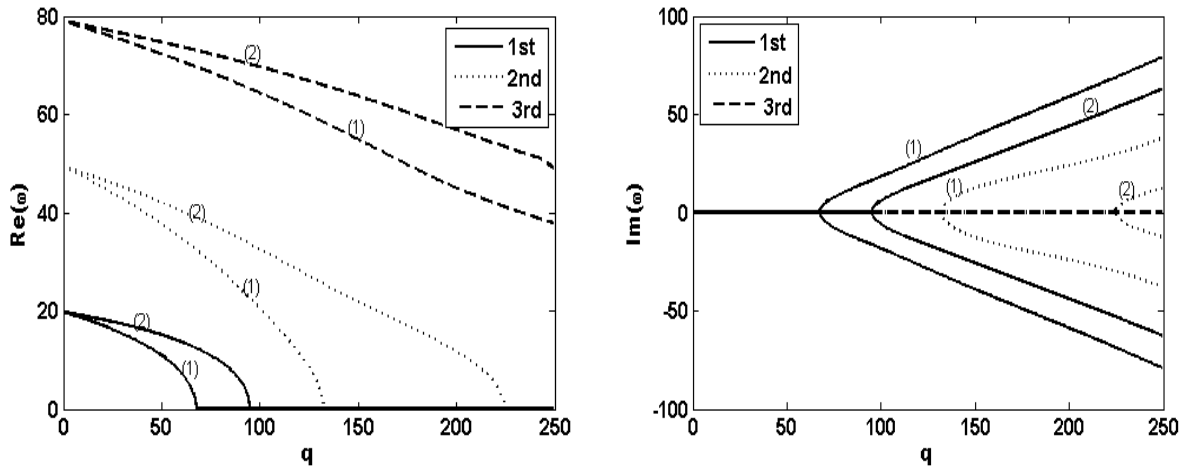


Fig. 1. First three frequencies of SSSS plate vs follower force for  $\lambda = 1$ ,  $H = 10^{-5}$ ,  
 (1) Uniformly distributed load, (2) Triangularly distributed load

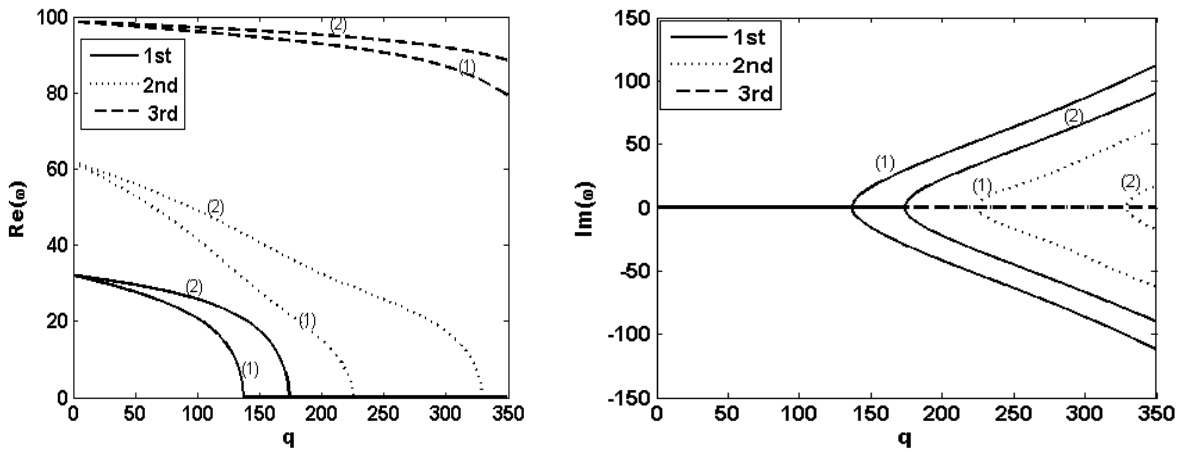


Fig. 2. First three frequencies of SSSS plate vs follower force for  $\lambda = 1.5$ ,  $H = 10^{-5}$ ,  
 (1) Uniformly distributed load, (2) Triangularly distributed load

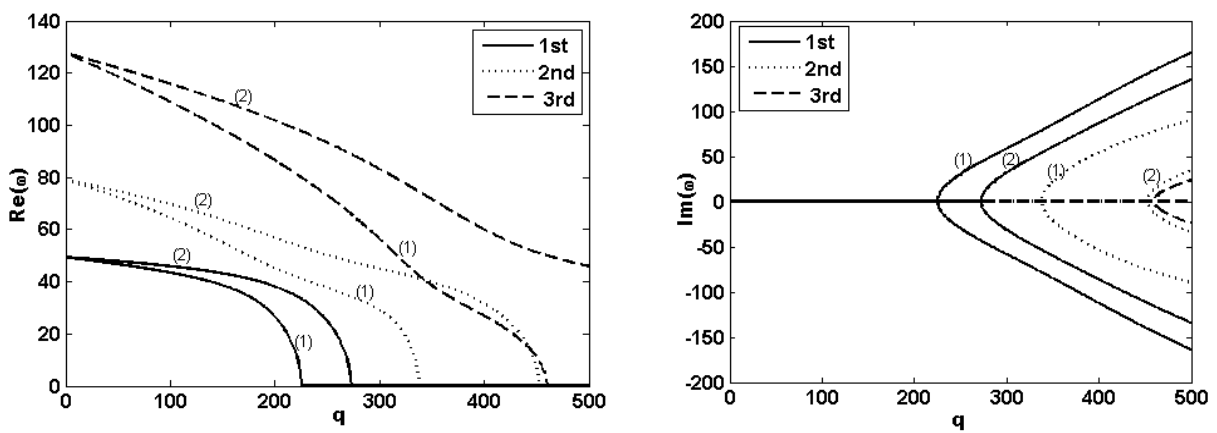


Fig. 3. First three frequencies of SSSS plate vs follower force for  $\lambda = 2$ ,  $H = 10^{-5}$ ,  
 (1) Uniformly distributed load, (2) Triangularly distributed load

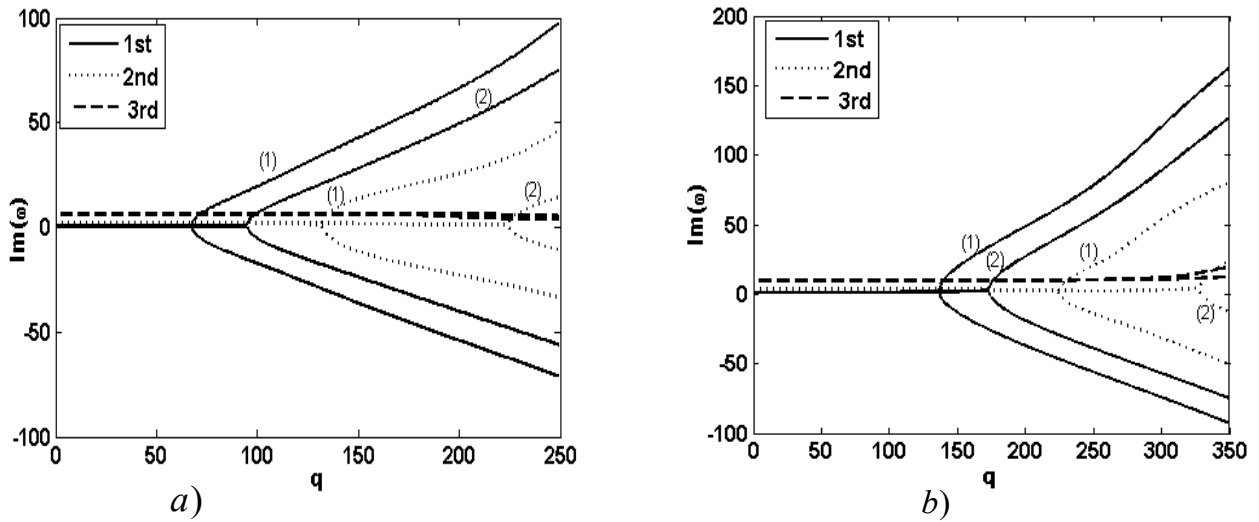


Fig. 4. Imaginary parts of frequencies of SSSS plate vs follower force for a)  $\lambda = 1$  and b)  $\lambda = 1.5$ ,  $H = 10^{-3}$ , (1) Uniformly distributed load, (2) Triangularly distributed load

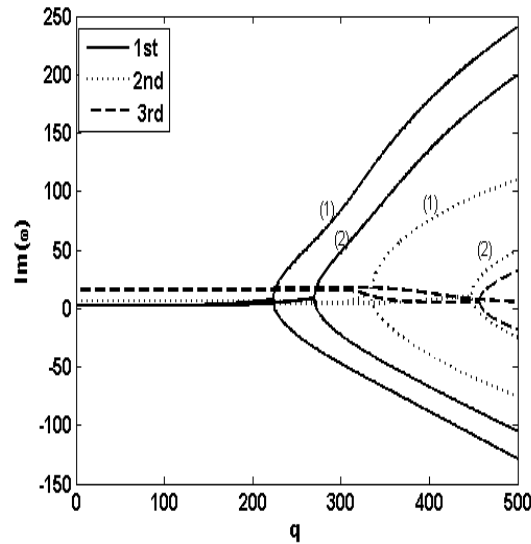


Fig. 5. Imaginary part of frequency of SSSS plate vs follower force for  $\lambda = 2$ ,  $H = 10^{-3}$ , (1) Uniformly distributed load, (2) Triangularly distributed load.

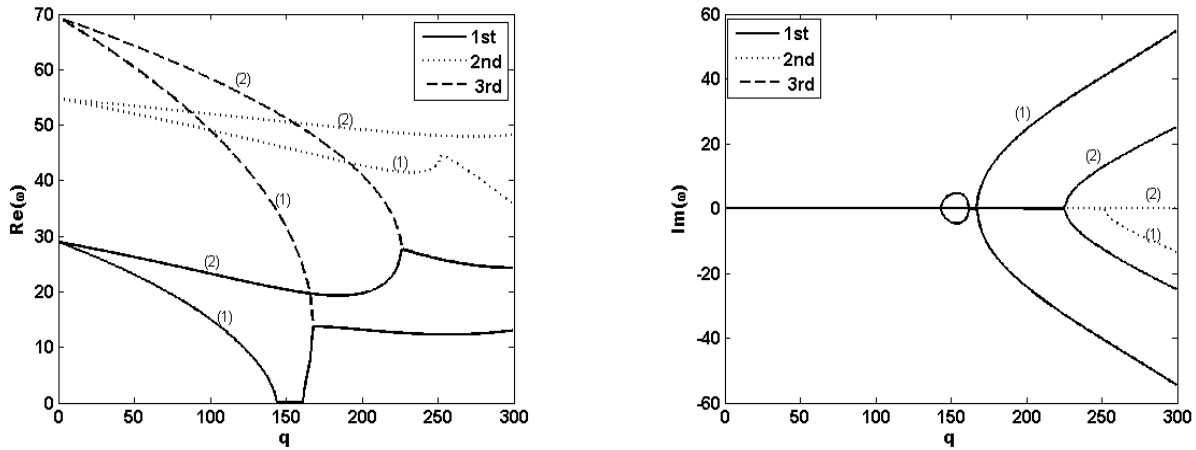


Fig. 6. First three frequencies of CSCS plate vs follower force for  $\lambda = 1$ ,  $H = 10^{-5}$ ; (1) Uniformly distributed load, (2) Triangularly distributed load

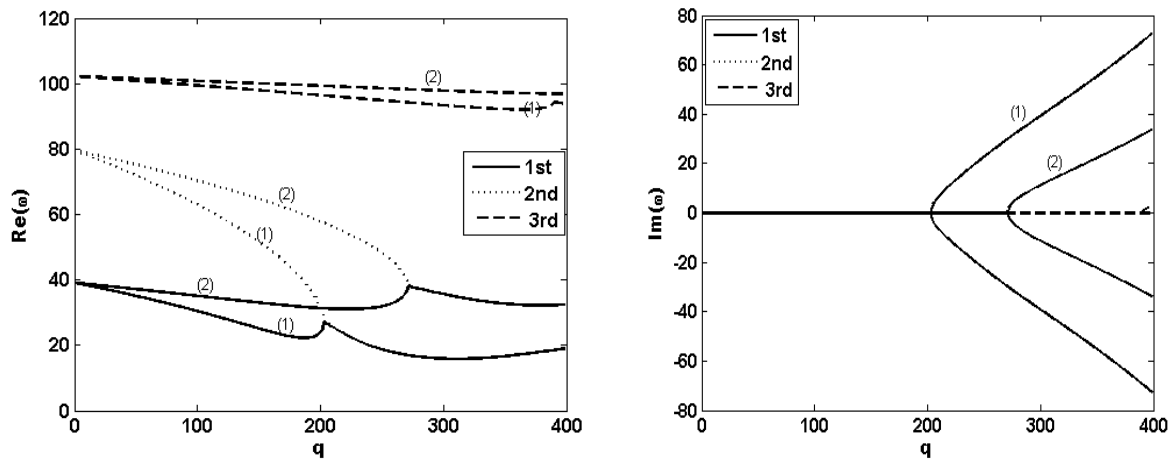


Fig. 7. First three frequencies of CSCS plate vs follower force for  $\lambda = 1.5$ ,  $H = 10^{-5}$ , (1) Uniformly distributed load, (2) Triangularly distributed load

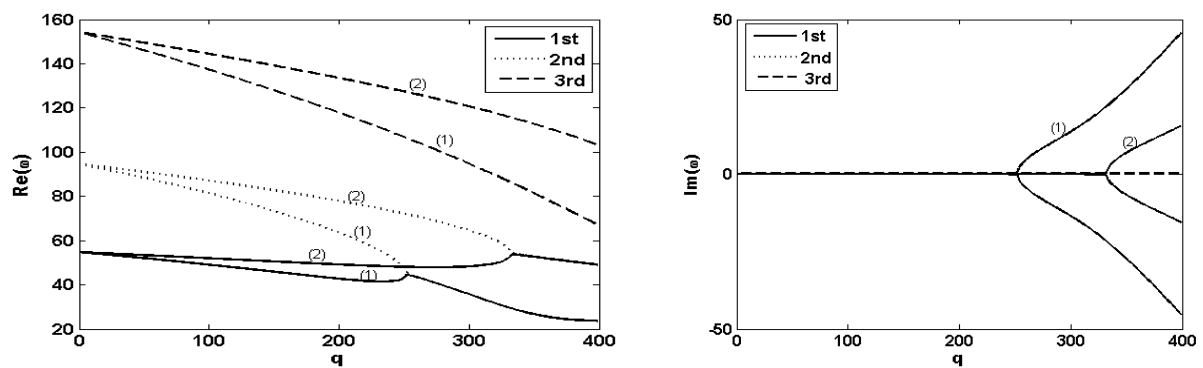


Fig. 8. First three frequencies of CSCS plate vs follower force for  $\lambda = 2$ ,  $H = 10^{-5}$ , (1) Uniformly distributed load, (2) Triangularly distributed load

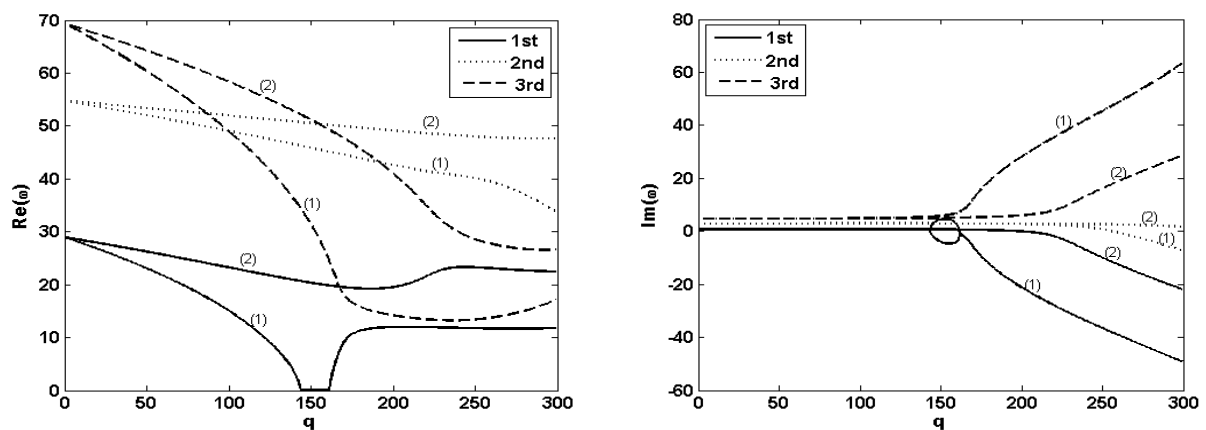


Fig. 9. First three frequencies of CSCS plate vs follower force for  $\lambda = 1$ ,  $H = 10^{-3}$ , (1) Uniformly distributed load, (2) Triangularly distributed load

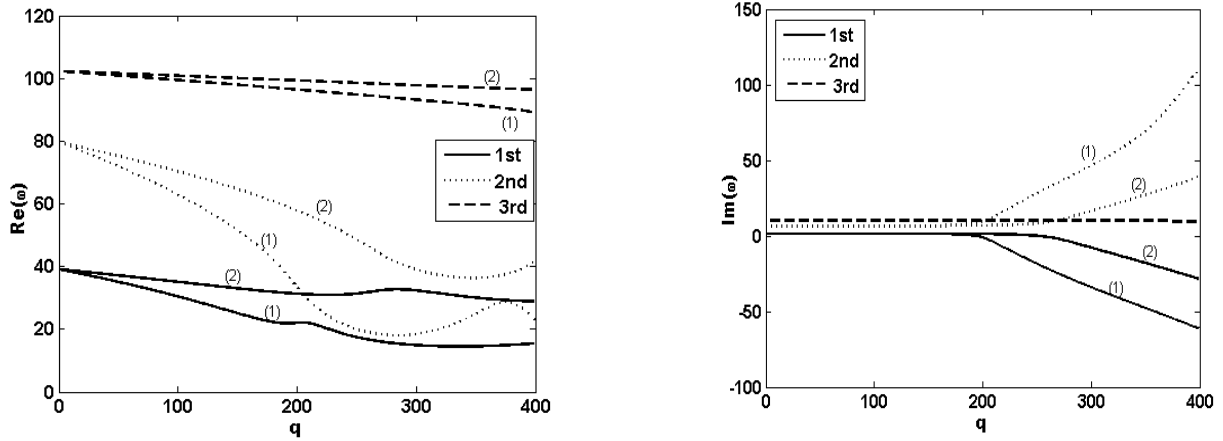


Fig. 10. First three frequencies of CSCS plate vs follower force for  $\lambda = 1.5$ ,  $H = 10^{-3}$ , (1) Uniformly distributed load, (2) Triangularly distributed load

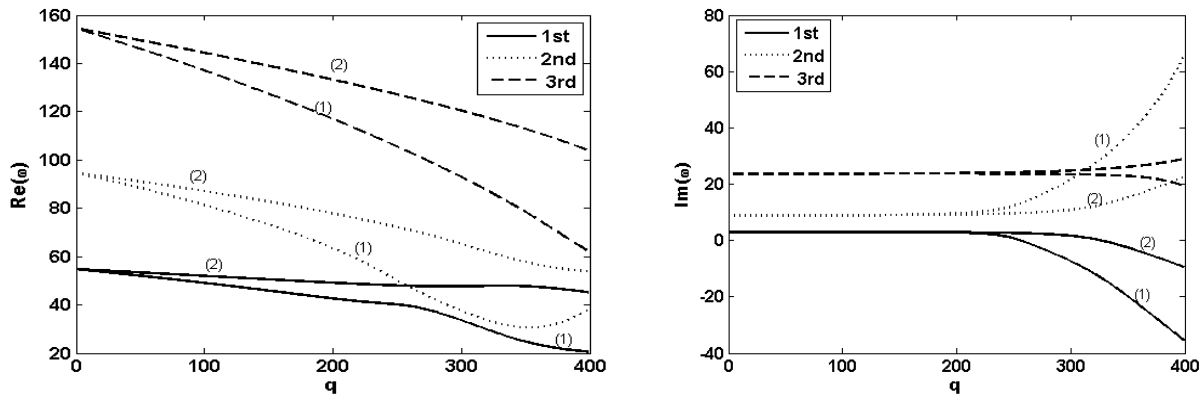


Fig. 11. First three frequencies of CSCS plate vs follower force for  $\lambda = 2$ ,  $H = 10^{-3}$ , (1) Uniformly distributed load, (2) Triangularly distributed load

## 5. Conclusions

Differential quadrature method is employed to study the dynamic stability of rectangular viscoelastic plates subject to triangularly distributed tangential follower loads. Kelvin-Voigt viscoelastic model is taken as the constitutive equation of the plate. Two boundary conditions are investigated, namely, simple supports and a combination of simple and fixed supports. The solution is verified against previous results obtained for SSSS and CSCS viscoelastic plates subject to uniformly distributed tangential loads by Wang *et al.* (2007).

Numerical results are given to study the effects of the aspect ratio and degree of viscoelasticity on the real and imaginary parts of the frequencies. The effect of uniformly and triangularly distributed follower loads on dynamic stability is compared numerically. It is observed that in the case of CSCS plates, the flutter instability occurs before the divergence instability for higher aspect ratios. In the case of SSSS plates the degree of viscoelasticity does not affect the divergence

load, but this effect is more pronounced for CSCS plates. At higher levels of viscoelasticity (higher values of  $H$ ) the imaginary parts of the complex frequencies become positive rather than zero for low values of the follower load.

### Acknowledgment

The research reported in this paper was supported by research grants from the University of KwaZulu-Natal (UKZN) and from National Research Foundation (NRF) of South Africa. The authors gratefully acknowledge the support provided by UKZN and NRF.

### References

1. ADALI S., 1982, Stability of a rectangular plate under nonconservative and conservative forces, *International Journal of Solids and Structures*, **18**, 1043–1052
2. BERT C.W., MALIK M., 1996, Implementing multiple boundary conditions in the DQ solution of higher-order PDE's: Application to free vibration of plates, *International Journal of Numerical Methods in Engineering*, **39**, 1237-1258
3. CHEN L.-W., KU D.-M., 1991, Stability analysis of a Timoshenko beam subjected to distributed follower forces using finite elements, *Computers & Structures*, **41**, 813-819
4. CULKOWSKI P.M., REISMANN H., 1977, Plate buckling due to follower edge forces, *ASME Journal of Applied Mechanics*, **99**, 768–769
5. DARABSEH T.T., GENIN J., 2004, Dynamic stability of viscoelastic columns loaded by a follower force, *Journal of Mechanical Engineering Science*, **218**, 1091–1101
6. ELFELSOUFI Z., AZRAR L., 2006, Integral equation formulation and analysis of the dynamic stability of damped beams subjected to subtangential follower forces, *Journal of Sound and Vibration*, **296**, 690-713
7. FARSHAD M., 1978, Stability of cantilever plates subjected to biaxial subtangential loading, *Journal of Sound and Vibration*, **58**, 555–561
8. GAJEWSKI A., 2000, Vibrations and stability of a non-conservatively compressed prismatic column under nonlinear creep conditions, *Journal of Theoretical and Applied Mechanics*, **38**, 259-270
9. ILYASOV M.H., 2010, Parametric vibrations and stability of viscoelastic shells, *Mechanics of Time-Dependent Materials*, **14**, 153–171
10. ILYASOV M.H., AKÖZ Y.A., 2000, The vibration and dynamic stability of viscoelastic plates, *International Journal of Engineering Science*, **38**, 695–714
11. ILYASOV M.H., ILYASOVA N.M., 2006, Flutter of viscoelastic strips, *Mechanics of Time-Dependent Materials*, **10**, 201-213
12. JAYARAMAN G., STRUTHERS A., 2005, Divergence and flutter instability of elastic specially orthotropic plates subject to follower forces, *Journal of Sound and Vibration*, **281**, 357–373
13. KAZEMI-LARI M.A., GHAVANLOO E., FAZELZADEH S.A., 2013, Structural instability of carbon nanotubes embedded in viscoelastic medium and subjected to distributed tangential load, *Journal of Mechanical Science and Technology*, **27**, 2085-2091
14. KIM J.H., KIM H.S., 2000, A study on the dynamic stability of plates under a follower load, *Computers & Structures*, **74**, 351–363
15. KIM J.H., PARK J.H., 1998, On the dynamic stability of rectangular plates subjected to intermediate follower forces, *Journal of Sound and Vibration*, **209**, 882–888

16. KIM J.-O., LEE K.-S., LEE J.-W., 2008, Beam stability on an elastic foundation subjected to distributed follower force, *Journal of Mechanical Science and Technology*, **22**, 2386-2392
17. KIM N.I., 2010, Dynamic stability behavior of damped laminated beam subjected to uniformly distributed subtangential forces, *Composite Structures*, **92**, 2768–2780
18. KIM N.I., 2011, Divergence and flutter instability of damped laminated beams subjected to a triangular distribution of nonconservative forces, *Advances in Structural Engineering*, **14**, 1075–1091
19. KIRILLOV O.N., 2013, *Nonconservative Stability Problems of Modern Physics*, Walter de Gruyter GmbH, Berlin/Boston
20. KROWIAK A., 2008, Methods based on the differential quadrature in vibration analysis of plates, *Journal of Theoretical and Applied Mechanics*, **46**, 123-139
21. KUMAR A., SRIVASTA A.K., 1986, Stability of thin rectangular elastic plates under a follower force, *Mechanics Research Communications*, **13**, 165-168
22. LANGTHJEM M.A., SUGIYAMA Y., 2000, Dynamic stability of viscoelastic beam under follower forces, *Journal of Sound and Vibration*, **238**, 809-851
23. LEIPHOLZ, H.H.E., 1975, An extremum principle for the buckling problem of the clamped-clamped rod subjected to tangential follower forces, *Mechanics Research Communications*, **2**, 119-123
24. LEIPHOLZ H.H.E., 1978, Stability of a rectangular simply supported plate subjected to nonincreasing tangential follower forces, *ASME Journal of Applied Mechanics*, **45**, 223–224
25. LEIPHOLZ H.H.E., BHALLA K., 1977, On the solution of the stability problem of elastic rods subjected to triangularly distributed tangential follower forces, *Ingenieur-Archiv*, **46**, 115-124
26. LEIPHOLZ, H.H.E., PFENDT F., 1982, On the stability of rectangular completely supported plates with uncoupled boundary conditions subjected to uniformly distributed follower forces, *Computer Methods in Applied Mechanics Engineering*, **30**, 19–52
27. LEIPHOLZ H.H.E., PFENDT F., 1983, Application of extended equations of Galerkin to stability problems of rectangular plates with free edges and subjected to uniformly distributed follower forces, *Computer Methods in Applied Mechanics and Engineering*, **37**, 341–365
28. MARZANI A., POTAPOV V.D., 1999, On the stability of a nonlinear viscoelastic rod subjected to a longitudinal force in the form of a random stationary process, *Mechanics of Time-Dependent Materials*, **2**, 335–349
30. PRZYBYLSKI J., 1999, Instability regions of a prestressed compound column subjected to a follower force, *Journal of Theoretical and Applied Mechanics*, **37**, 148-162
31. ROBINSON M.T.A., 2013, Nonlinear vibration of 2D viscoelastic plate subjected to tangential follower force, *Engineering Mechanics*, **20**, 59–74
32. ROBINSON M.T.A., ADALI S., 2016, Nonconservative stability of viscoelastic rectangular plates with free edges under uniformly distributed follower force, *International Journal of Mechanical Sciences*, **107**, 150-159
33. RUAN M., WANG Z.-M., WANG Y., 2012, Dynamic stability of functionally graded materials skew plates subjected to uniformly distributed tangential follower forces, *Journal of Vibration and Control*, **18**, 913-923
34. RYU B.J., SUGIYAMA Y., YIM K.B., LEE G.S., 2000, Dynamic stability of an elastically restrained column subjected to triangularly distributed subtangential forces, *Computers & Structures*, **76**, 611-619

35. SUGIYAMA Y., KAWAGOE H., 1975, Vibration and stability of elastic columns under the combined action of uniformly distributed vertical and tangential forces, *Journal of Sound and Vibration*, **38**, 341-355
36. SUGIYAMA Y., MLADENOV K.A., 1983, Vibration and stability of elastic columns subjected to triangularly distributed sub-tangential forces, *Journal of Sound and Vibration*, **88**, 447-457
37. TORKI M.E., KAZEMI M.T., HADDADPOUR H., MAHMOUDKHANI S., 2014a, Dynamic stability of cantilevered functionally graded cylindrical shells under axial follower forces, *Thin-Walled Structures*, **79**, 138-146
38. TORKI M.E., KAZEMI M.T., REDDY J.N., HADDADPOUD H., MAHMOUDKHANI S., 2014b, Dynamic stability of functionally graded cantilever cylindrical shells under distributed axial follower forces, *Journal of Sound and Vibration*, **333**, 801-817
39. WANG Z.M., JI Y.Z., 1992, The dynamic stability of rectangular plates under the action of tangential follower force, *Journal of Vibration Engineering*, **5**, 78-83
40. WANG Z.M., ZHOU Y.-F., WANG Y., 2007, Dynamic stability of non-conservative viscoelastic rectangular plate, *Journal of Sound and Vibration*, **307**, 250-264
41. WANG Z., WANG Y., GUO X., 2009, Dynamic stability of linearly varying thickness viscoelastic rectangular plate with crack and subjected to tangential follower force, *Applied Acoustics*, **70**, 845-856
42. WANG Y., WANG Z., ZU L., 2013, Stability of viscoelastic rectangular plate with a piezoelectric layer subjected to follower force, *Archive of Applied Mechanics*, **83**, 495-507
43. ZHOU Y.-F., WANG Z.-M., 2014, Exact solutions for the stability of viscoelastic rectangular plate subjected to tangential follower force, *Archive of Applied Mechanics*, **84**, 1081-1089
44. ZHUO R.H., FEN S.Z., 2005, Dynamic stability of viscoelastic beam under follower force, *ASCE Journal of Engineering Mechanics*, **22**, 26-30
45. ZUO Q.H., SHREYER H.L., 1996, Flutter and divergence instability of nonconservative beams and plates, *International Journal of Solids and Structures*, **33**, 1355-1367

CHAPTER 6-PAPER 3:  
DYNAMIC STABILITY OF VISCOELASTIC PLATES UNDER AXIAL  
FLOW BY DIFFERENTIAL QUADRATURE METHOD. Accepted to be  
published in Engineering Computations .



**Dynamic Stability of Viscoelastic Plates under Axial Flow by  
Differential Quadrature Method**

Journal:	<i>Engineering Computations</i>
Manuscript ID	Draft
Manuscript Type:	Research Article
Keywords:	Dynamic stability, Viscoelastic plate, Differential quadrature method, Flutter, Critical flow velocity

SCHOLARONE™  
Manuscripts

Review

# Dynamic Stability of Viscoelastic Plates under Axial Flow by Differential Quadrature Method

## Part 1

### Abstract

**Purpose** – Cantilever plates subject to axial flow can lose stability by flutter and properties such as viscoelasticity and laminar friction affect dynamic stability. The purpose of the present study is to investigate the dynamic stability of viscoelastic cantilever plates subject to axial flow by using the differential quadrature method.

**Design/methodology/approach** – Equation of motion of the viscoelastic plate is derived by implementing Kelvin-Voigt model of viscoelasticity and applying inverse Laplace transformation. The differential quadrature method is employed to discretize the equation of motion and the boundary conditions leading to a generalized eigenvalue problem. The solution is verified using the existing results in the literature and numerical results are given for critical flow velocities.

**Findings** – It is observed that higher aspect ratios lead to imaginary part of third frequency becoming negative and causing single-mode flutter instability. It was found that flutter instability does not occur at low aspect ratios. Moreover the friction coefficient is found to affect the magnitude of critical flow velocity, however, its effect on the stability behaviour is minor.

**Originality/value** – The effects of various problem parameters on the dynamic stability of a viscoelastic plate subject to axial flow were established. It was shown that laminar friction coefficient of the flowing fluid increases the critical fluid velocity and higher aspect ratios lead to single-mode flutter instability. The effect of increasing damping of viscoelastic material on the flutter instability was quantified and it was found that increasing viscoelasticity can lead to divergence instability.

**Keywords** Dynamic stability, Viscoelastic plate, Differential quadrature method, Flutter, Critical flow velocity.

**Paper type** Research paper

### 1. Introduction

Elastic plates subject to axial flow may lose stability when the flow velocity exceeds a critical value. The mode of dynamic instability is flutter and the flutter amplitude grows as the flow velocity increases (Lemaitre *et al.*, 2005). This kind of instability can be typically observed in a flag flapping in the wind which was first studied by Taneda (1968) who made an experimental study of the phenomenon. Datta and Gottenberg (1975) studied flutter of a strip and predicted the critical flow velocity by modelling the strip as a cantilever beam and employing slender wing theory to evaluate the aerodynamic loads. Other studies of one-dimensional plates in axial flow include Doaré *et al.* (2011), Favier *et al.* (2015) and Yadykin *et al.* (2001). A widely studied area is the flutter instability of flags and the recent work on the subject include Connell and Yue (2007), Pang *et al.* (2010), Eloy *et al.* (2012), Virot *et al.* (2013) and Chen *et al.* (2014a, b).

The subject has applications in a number of fields such as aerospace engineering involving wing flutter (Tang and Dowell, 2004), paper industry (Watanabe *et al.*, 2002a, b), and medical fields (palatal snoring) (Baliant and Lucey, 2005; Huang, 1995a). More recently there has been extensive research on energy harvesting from aeroelastic flutters using piezoelectric materials (Allen and Smits, 2001; Bryant and Garcia, 2011; Perez *et al.*, 2015; Tang *et al.*, 2009a; Wang and Ko, 2010). The subject of loss of stability of beams and plates by flutter has been studied in a number of books (Païdoussis, 2004; Axisa and Antunes, 2007; Amabili, 2008).

The present paper studies the fluid-induced vibrations and dynamic stability of cantilevered viscoelastic plates under axial flow and investigates the effect of viscoelasticity and other problem parameters on the aeroelastic stability. Loss of stability of elastic plates in axial flow has been the subject of a number of studies (Eloy *et al.*, 2007, 2008; Howell *et al.*, 2009; Huang, 1995b; Huang and Zhang, 2013; Tang and Païdoussis, 2007; Tang *et al.*, 2009b; Yamaguchi *et al.*, 2000a, b; Zhao *et al.*, 2012) in which the critical flow velocity for plate flutter has been determined based on dynamic stability analysis and various parameters affecting the stability has been studied. Fluid-structure interactions have been studied numerically by Rossi and Oñate (2010).

Most of the studies on the subject involved elastic plates and the corresponding studies on viscoelastic structures have been few even though there are several applications of viscoelastic materials. A recent work on the subject is the study of flutter stability of a flag of fractional viscoelastic material (Chen *et al.*, 2014b). Flutter of one dimensional viscoelastic strips has been studied in (Potapov, 1995, 2004; Kiiko, 1996; Ilyasov and Ilyasova, 2006; Pokazeyev, 2008; Kiiko and Pokazeev, 2013) and the flutter of simply supported viscoelastic plates in (Khudayarov, 2005). Stability of elastic and viscoelastic plates in supersonic flow was studied by Vadim and Potapov (1995), Khudayarov (2010), and Merrett and Hilton (2010). Recent works on the dynamic stability of viscoelastic plates under distributed follower loads include Robinson (2013), Robinson and Adali (2016) and

Robinson and Adali (under review). In most studies the effect of the coefficient of friction of the flowing fluid has been neglected. The present study provides a systematic study of the effects and interaction of the friction coefficient, aspect ratio and viscoelastic damping coefficient on the dynamic stability of a viscoelastic plate under axial flow.

The numerical solution is obtained by differential quadrature method which has been used in several studies to solve engineering problems due to its accuracy and efficiency (Cheng *et al.*, 2015; De Rosa and Lippiello, 2016; Forouzesh and Jafari, 2015; Korkmaz and Dağ, 2013; Kumar *et al.*, 2013, Mittal *et al.*, 2013). Further engineering applications of differential quadrature method can be found in the book by Shu (2000). Present study employs differential the quadrature method to investigate the dynamic stability behaviour of a viscoelastic plate in axial flow and determines the effect of problem parameters on flutter instability. First the differential equation governing the dynamic stability of a rectangular viscoelastic plate subjected to a uniform air flow is derived via inverse Laplace transformation. The plate is specified as a cantilevered plate with the constitutive equation described by Kelvin-Voigt model. The numerical solution of the problem is obtained by differential quadrature (DQ) method which is implemented to discretize the equation of motion and the boundary conditions. This discretization leads to a generalized eigenvalue problem with complex eigenvalues. The effects of aspect ratio, delay time, and frictional coefficient on flutter instability are studied and the real and complex eigenvalues are plotted with respect to flow velocity.

## 2. Governing equation

We consider a thin rectangular plate of dimensions  $a \times b$  and thickness  $h$  with Young's modulus  $E$ , Poisson's ratio  $\nu$  and density  $\rho$ . The Cartesian coordinate system  $x, y, z$  which has its origin at mid-thickness is shown in Figure 1 and  $(x, y, z)$  indicates the location of a point of the undeformed plate.

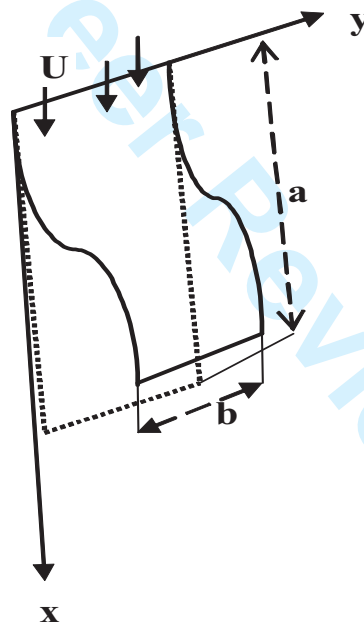


**Figure 1.**  
Geometry of the cantilever plate in axial flow

Using the Kirchhoff plate theory, the displacements  $u, v, w$  along  $x, y$  and  $z$  directions, respectively, are given by

$$u = -z\psi_x, \quad v = -z\psi_y, \quad w = w(x, y, t) \quad (1)$$

where the angles of rotation  $\psi_x$  and  $\psi_y$  are related to  $w$  through the relations

$$\psi_x = \frac{\partial w}{\partial x}, \quad \psi_y = \frac{\partial w}{\partial y} \quad (2)$$

The linear strain-displacement relations are given by

$$\varepsilon_x = -z \frac{\partial^2 w}{\partial x^2}, \quad \varepsilon_y = -z \frac{\partial^2 w}{\partial y^2}, \quad \varepsilon_{xy} = \frac{\gamma_{xy}}{2} = -z \frac{\partial^2 w}{\partial x \partial y} \quad (3)$$

The plate is defined as viscoelastic of the Kelvin-Voigt type and the constitutive equations can be written as follows (Wang *et al.*, 2007)

$$\mathbf{s}_{ij} = 2G \mathbf{e}_{ij} + 2\eta \dot{\mathbf{e}}_{ij}, \quad \sigma_{ii} = 3K \varepsilon_{ii} \quad (4)$$

where  $K$ ,  $\eta$ ,  $G$  are bulk elastic modulus, viscoelastic coefficient and shear elastic modulus, respectively. They can be expressed as  $K = E/3(1-2\nu)$  and  $G = E/2(1+\nu)$  in terms of  $E$  and  $\nu$ . The quantities  $\mathbf{s}_{ij}$  and  $\mathbf{e}_{ij}$  are, respectively, the deviatoric tensors of stress and strain while  $\mathbf{s}_{ii}$  and  $\sigma_{ii}$  stand for the spherical tensors of strain and stress. The bending moments  $M_x$ ,  $M_y$  and twisting moments  $M_{xy}$ ,  $M_{yx}$  are given by

$$M_x = \int_{-h/2}^{h/2} z \sigma_x dz, \quad M_y = \int_{-h/2}^{h/2} z \sigma_y dz \quad (5a)$$

$$M_{xy} = \int_{-h/2}^{h/2} z \tau_{xy} dz, \quad M_{yx} = \int_{-h/2}^{h/2} z \tau_{yx} dz \quad (5b)$$

The plate is subject to an axial fluid flow in the  $x$  direction. When the fluid is incompressible with a uniform velocity  $U$ , the plate is subjected to a force per unit area  $p(x)$  as well as the tension  $T(x)$ . The fluid force  $p(x)$  can be derived through the unsteady potential flow model (Lemaitre *et al.*, 2005) and is given by

$$p = m_a \frac{\partial^2 w}{\partial t^2} + 2m_a U \frac{\partial^2 w}{\partial t \partial x} + m_a U^2 \frac{\partial^2 w}{\partial x^2} \quad (6)$$

where the first term is the inertia force independent of the flow velocity  $U$ , the second term is a Coriolis type force proportional to  $U$ , and the last term stands for a stiffness force proportional to  $U^2$ . All three terms are scaled by the added mass  $m_a$  due to the presence of the fluid. In the following, we focus our attention in a hanging configuration. In this case the local tension  $T(x)$  which takes into account the effects of friction due to the axial flow along the two sides of the plate is given by (Datta and Gottenberg, 1975):

$$T(x) = mg(a-x) + f \rho_f U^{3/2} \nu_f^{1/2} (a^{1/2} - x^{1/2}) \quad (7)$$

where  $\nu_f$  is the viscosity of fluid,  $f$  is the laminar friction coefficient,  $g$  is the constant of gravity,  $m$  is the mass of the plate per unit area and  $\rho_f$  is the density of the fluid.

Equilibrium equation of the non-conservative rectangular plate can be expressed as follows:

$$\frac{\partial^2 M_x}{\partial x^2} + 2 \frac{\partial^2 M_{xy}}{\partial x \partial y} + \frac{\partial^2 M_y}{\partial y^2} - p + \frac{\partial}{\partial x} \left( T \frac{\partial w}{\partial x} \right) - m \frac{\partial^2 w}{\partial t^2} = 0 \quad (8)$$

By making use of the scheme described in (Wang *et al.*, 2007), that is, combining first the Laplace transformation of Equations (4), (6), (7) and (8), and next carrying out the Laplace inverse transformation of the resulting equation, a differential equation governing the vibration of the non-conservative viscoelastic rectangular plate can be obtained as

$$\frac{h^3}{12} \left( A_3 + A_4 \frac{\partial}{\partial t} + A_5 \frac{\partial^2}{\partial t^2} \right) \nabla^4 w - \left( A_1 + A_2 \frac{\partial}{\partial t} \right) \left[ \frac{\partial}{\partial x} \left( T \frac{\partial w}{\partial x} \right) + L(w) \right] = 0 \quad (9)$$

where  $\nabla^4 w = \frac{\partial^4 w}{\partial x^4} + 2 \frac{\partial^4 w}{\partial x^2 \partial x^2} + \frac{\partial^4 w}{\partial y^4}$  and

$$L(w) = m_a U^2 \frac{\partial^2 w}{\partial x^2} + 2m_a U \frac{\partial^2 w}{\partial x \partial t} + (m + m_a) \frac{\partial^2 w}{\partial t^2} \quad (10)$$

$$A_1 = 3K + 4G, \quad A_2 = 4\eta, \quad A_3 = 3G(6K + 2G), \quad A_4 = 4\eta(2G + 3K), \quad A_5 = 4\eta^2 \quad (11)$$

Introducing the dimensionless variables

$$a_1 = \frac{a}{d}, \quad X = \frac{x}{a}, \quad Y = \frac{y}{b}, \quad \bar{w} = \frac{w}{h}, \quad \lambda = \frac{a}{b}$$

$$k = \frac{f \rho_f v_f^{1/2}}{mgd^2} \left( \frac{D}{m} \right)^{3/4}, \quad V = \left( \frac{m_a}{D} \right)^{1/2} U d, \quad \beta = \frac{m_a}{m + m_a} \quad (12)$$

$$\tau = \frac{t}{d^2} \sqrt{\frac{D}{m + m_a}}, \quad H = \frac{\eta}{d^2 E} \sqrt{\frac{D}{m + m_a}}$$

where  $d = \left( \frac{D}{mg} \right)^{1/3}$ ,  $D = Eh^3/12(1-\nu^2)$  is the bending stiffness, the governing equation (9) can be written as

$$\left( 1 + c_1 \frac{\partial}{\partial \tau} + c_2 \frac{\partial^2}{\partial \tau^2} \right) \nabla^4 \bar{w} - \left( 1 + c_3 \frac{\partial}{\partial \tau} \right) \frac{\partial}{\partial X} \left( T_{nd} \frac{\partial \bar{w}}{\partial X} + L_{nd}(\bar{w}) \right) = 0 \quad (13)$$

where  $\tau$  is dimensionless time,  $H$  is dimensionless delay time of the material, and

$$c_1 = \frac{4(2-\nu)(1+\nu)}{3} H, \quad c_2 = \frac{4(1-2\nu)(1+\nu)^2}{3} H^2, \quad c_3 = \frac{4(1-2\nu)(1+\nu)}{3(1-\nu)} H \quad (14)$$

$$T_{nd}(x) = a_1 - X + kV^{3/2} (a_1^{1/2} - X^{1/2}), \quad L_{nd}(\bar{w}) = V^2 \frac{\partial^2 \bar{w}}{\partial X^2} + 2\beta^{1/2} V \frac{\partial^2 \bar{w}}{\partial X \partial \tau} + \frac{\partial^2 \bar{w}}{\partial \tau^2} \quad (15)$$

$$\nabla^4 \bar{w} = \frac{\partial^4 \bar{w}}{\partial X^4} + 2\lambda^2 \frac{\partial^4 \bar{w}}{\partial X^2 \partial Y^2} + \lambda^4 \frac{\partial^4 \bar{w}}{\partial Y^4} \quad (16)$$

Equation (13) is the dimensionless form of the differential Eq. (9) which governs the vibrations of the viscoelastic rectangular plate subject to an axial flow. The solution of equation (13) is taken in the form  $\bar{w}(X, Y, \tau) = W(X, Y) \exp(\sqrt{-1} \omega \tau)$  where  $\omega$  is the dimensionless complex frequency.

The boundary conditions for the CFFF plate (one edge clamped and others free) are expressed as follows:

$$\bar{w}(0, Y) = \frac{\partial \bar{w}}{\partial X} \Big|_{X=0} = 0, \quad \frac{\partial^2 \bar{w}}{\partial X^2} + \nu \lambda^2 \frac{\partial^2 \bar{w}}{\partial Y^2} \Big|_{X=1} = 0, \quad \frac{\partial^3 \bar{w}}{\partial X^3} + (2-\nu) \lambda^2 \frac{\partial^3 \bar{w}}{\partial X \partial Y^2} \Big|_{X=1} = 0 \quad \text{for } 0 \leq Y \leq 1 \quad (17a)$$

$$\lambda^2 \frac{\partial^2 \bar{w}}{\partial Y^2} + \nu \frac{\partial^2 \bar{w}}{\partial X^2} \Big|_{Y=0,1} = 0, \quad \lambda^2 \frac{\partial^3 \bar{w}}{\partial Y^3} + (2-\nu) \frac{\partial^3 \bar{w}}{\partial X^2 \partial Y} \Big|_{Y=0,1} = 0 \quad \text{for } 0 \leq X \leq 1 \quad (17b)$$

$$\frac{\partial^2 \bar{w}}{\partial X \partial Y} \Big|_{\substack{X=1 \\ Y=0}} = 0, \quad \frac{\partial^2 \bar{w}}{\partial X \partial Y} \Big|_{\substack{X=1 \\ Y=1}} = 0 \quad (17c)$$

### 3. Differential quadrature method

Next, differential quadrature method is implemented for the numerical solution of the problem. A partial

derivative of the function  $\bar{w}(X, Y)$  at a sample point  $(X_i, Y_j)$  is expressed as a weighted linear sum of the function  $\bar{w}(X_i, Y_j) = \bar{w}_{ij}$  values at all the sample points chosen on the solution domain of spacial variable. The number of sample point is specified as  $N$  in the  $X$  direction and  $M$  in the  $Y$  direction. Thus,  $r^{th}$  order partial derivative of  $\bar{w}(X, Y)$  with respect to  $X$ ,  $s^{th}$  order partial derivative with respect to  $Y$  and  $(r+s)^{th}$  order mixed partial derivative with respect to  $X$  and  $Y$  at a given point  $(X_i, Y_j)$  are expressed as (Bert and Malik, 1996, Zong and Zhang, 2009):

$$\frac{\partial^r \bar{w}(X_i, Y_j)}{\partial X^r} = \sum_{k=1}^N A_{ik}^{(r)} W_{kj} \quad \text{for } i=1,2,\dots,N, \quad j=1,2,\dots,M-1 \quad (19)$$

$$\frac{\partial^s \bar{w}(X_i, Y_j)}{\partial X^s} = \sum_{l=1}^M B_{jl}^{(s)} W_{il} \quad \text{for } i=1,2,\dots,N, \quad j=1,2,\dots,M-1 \quad (20)$$

$$\frac{\partial^{r+s} \bar{w}(X_i, Y_j)}{\partial X^r \partial Y^s} = \sum_{k=1}^N A_{ik}^{(r)} \sum_{l=1}^M B_{jl}^{(s)} W_{kl} \quad (21)$$

where  $A_{ik}^{(r)}$  and  $B_{jk}^{(s)}$  are the weighting coefficients defined as (Tang and Chen, 2011)

$$A_{ik}^{(1)} = \begin{cases} \prod_{j=1, j \neq i}^N \frac{X_i - X_j}{(X_i - X_k) \prod_{j=1, j \neq k}^N (X_k - X_j)} & \text{for } i, k=1,2,\dots,N, i \neq k \\ \sum_{j=1, j \neq i}^N \frac{1}{X_i - X_j} & \text{for } i=1,2,\dots,N, i = k \end{cases} \quad (22)$$

$$B_{jl}^{(1)} = \begin{cases} \prod_{j=1, j \neq l}^M \frac{Y_j - Y_l}{(Y_j - Y_l) \prod_{j=1, j \neq l}^M (Y_j - Y_l)} & \text{for } l=1,2,\dots,M, j \neq l \\ \sum_{j=1, j \neq l}^M \frac{1}{Y_j - Y_l} & \text{for } j=1,2,\dots,M, j = l \end{cases} \quad (23)$$

for  $r = s = 1$  and

$$A_{ik}^{(r)} = \begin{cases} r \left( A_{ii}^{(r-1)} A_{ik}^{(1)} - \frac{A_{ik}^{(r-1)}}{X_i - X_k} \right) & \text{for } k=1,2,\dots,N, i \neq k \\ - \sum_{j=1, j \neq i}^N A_{ij}^{(r)} & \text{for } i=1,2,\dots,N, i = k \end{cases} \quad (24)$$

$$B_{jl}^{(s)} = \begin{cases} s \left( B_{jj}^{(s-1)} B_{jl}^{(1)} - \frac{B_{jl}^{(s-1)}}{Y_j - Y_l} \right) & \text{for } l=1,2,\dots,M, j \neq l \\ - \sum_{j=1, j \neq l}^M B_{jl}^{(s)} & \text{for } j=1,2,\dots,M, j = l \end{cases} \quad (25)$$

for  $r = 2,3,\dots,N-1$  and  $s = 2,3,\dots,M-1$ . The distributions of the grid points are taken following the approach developed in (Shu and Du, 1997) and we use the Coupling Boundary Conditions with General Equation (CBCGE) technique to implement the boundary conditions. Accordingly, the form of the grid points for CFFF plate is given by

$$X_i = 3\xi_i^2 - 2\xi_i^3, \quad Y_j = 3\eta_j^2 - 2\eta_j^3 \quad (26)$$

where

$$\xi_i = \frac{1}{2} \left[ 1 - \cos \left( \frac{i-1}{N-1} \pi \right) \right] \quad \text{for } i = 1, 2, \dots, N \quad (27a)$$

$$\eta_j = \frac{1}{2} \left[ 1 - \cos \left( \frac{j-1}{M-1} \pi \right) \right] \quad \text{for } j = 1, 2, \dots, M \quad (27b)$$

With the above considerations, Equation (13) is transformed into the following discretized form:

$$c_3 j^3 W_{ij} \omega^3 + \left[ c_2 j^2 S_{ij} + j^2 W_{ij} \right] \omega^2 + \left( c_1 j S_{ij} + c_3 j q \sum_{k=1}^N A_{ik}^{(2)} W_{kj} \right) \omega + S_{ij} + q(1-X) \sum_{i=1}^N A_{ik}^{(2)} W_{kj} = 0 \quad (29)$$

where

$$S_{ij} = \sum_{k=1}^N A_{ik}^{(4)} W_{kj} + 2\lambda^2 \sum_{l=1}^M B_{jl}^{(2)} \sum_{i=1}^N A_{ik}^{(2)} W_{kl} + \lambda^4 \sum_{i=1}^M B_{jl}^{(4)} W_{il} \quad (30)$$

The discretized form of the boundary conditions is given in the Appendix. The discretized equation (29) with the boundary conditions (17) (see Appendix) can be rearranged and written in the following form:

$$\left\{ \omega^3 [C_3] + \omega^2 [C_2] + \omega [C_1] + [C_0] \right\} \{W_{ij}\} = \{0\} \quad (31)$$

where  $[C_0]$ ,  $[C_1]$ ,  $[C_2]$  and  $[C_3]$  are the matrices and depend on dimensionless parameters delay time  $H$ , follower load  $q$ , and the aspect ratio  $\lambda$ . This equation may be viewed as the generalized eigenvalue problem describing the vibration of the plate.

## 4. Numerical results and discussion

### 4.1. Verification

To verify the method of solution Equation (13) is solved by DQ method for the case  $H = 0$ ,  $\lambda = 0$  and  $k = 0$  which corresponds to the problem studied in Lemaitre *et al.* (2005). The results are shown in Figure 2 which is the same as the one given Lemaitre *et al.* (2005) obtained by Galerkin method using 50 modes in the computation.

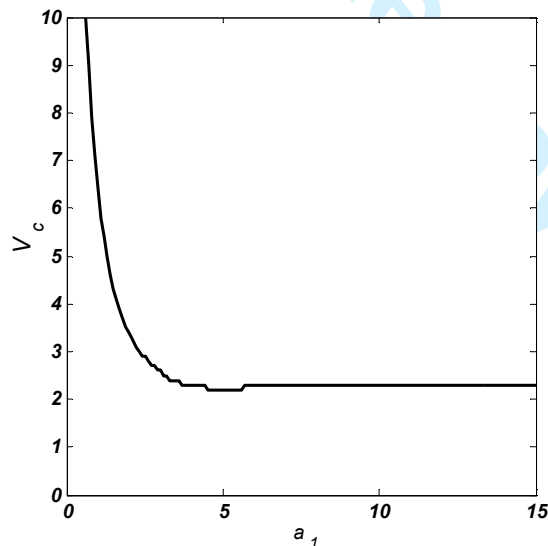


**Figure 2.**

Critical velocity vs dimensionless length with  
 $H = 0$ ,  $\lambda = 0$ ,  $k = 0$ ,  $\beta = 0.19$

#### 4.2 Influence of friction

The effect of the friction coefficient  $k$ , defined in equation (12), on the critical velocity is investigated for an elastic 1D plate, i.e., for  $H=0$  and  $\lambda=0$ , in Figure 3 by plotting the first three frequencies with respect to the flow velocity for various values of  $k$ . As the friction constant  $k$  increases from  $k=0.01$  to  $k=0.3$ , the critical velocity, the dimensionless critical velocity, as determined by the fundamental frequency  $\omega_1$  becoming zero, increases from  $V_c=6.2$  to  $V_c=9.7$ . This indicates that the friction has an appreciable effect on critical velocity.

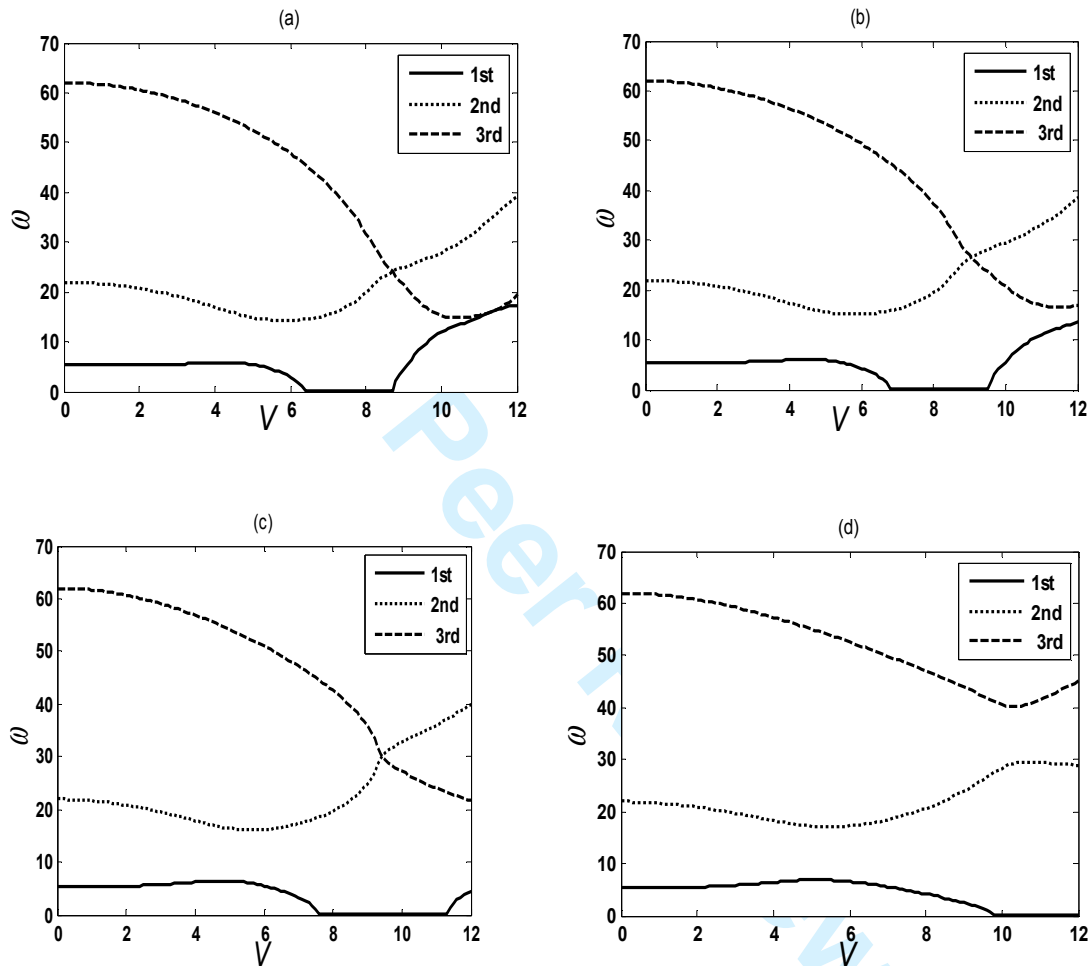


**Figure 3.**  
First three natural frequencies vs flow velocity with  
 $H=0$ ,  $\lambda=0$ ,  $a_1=1$ ,  $\beta=0.19$ ,  
(a)  $k=0.01$ , (b)  $k=0.1$ , (c)  $k=0.2$ , (d)  $k=0.3$

In Figure 4 the critical velocity  $V_c$  is plotted against the dimensionless length  $a_1$  for  $k=0.01$ ,  $k=0.1$ , and  $k=0.3$  for an elastic 1D plate ( $H=0$ ,  $\lambda=0$ ). When  $k$  increases from 0.01 to 0.3, the asymptotic value of critical velocity increases slightly from 2 to 2.2 indicating that as the length of the plate increases, effect of the friction coefficient  $k$  decreases, and in particular, its effect on the critical asymptotic velocity is observed to be minor.

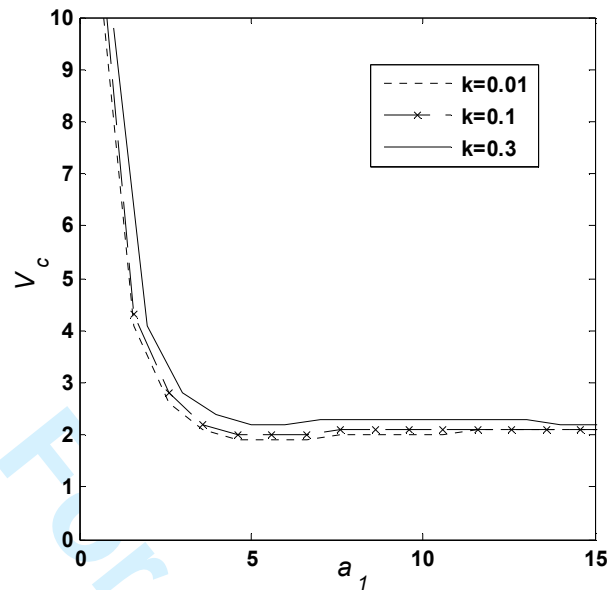


**Figure 4.**  
Critical velocity vs dimensionless length for  $H=0$ ,  $\lambda=0$ ,  $\beta=0.19$  and for various values of  $k$ .

#### 4.3 Effect of added mass on critical velocity

The effect of added mass for one and two-dimensional cases is studied in Figure 5 by plotting added mass parameter  $\beta$  against the critical velocity for 1D and 2D elastic plates. It is observed that the critical velocity decreases with increasing added mass as expected, however the decrease is higher in the case of 2D plate as compared to the one-dimensional model.

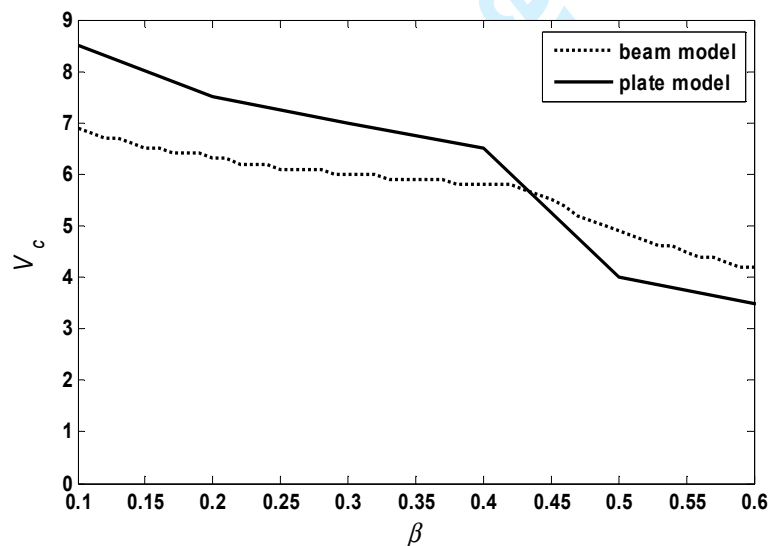


**Figure 5.**  
Effect of mass ratio  $\beta$  on critical velocity using one dimensional model ( $H=0$ ,  $\lambda=0$ ,  $a_1=1$ ,  $k=0$ ) and two dimensional model ( $H=0$ ,  $\lambda=1$ ,  $a_1=1$ ,  $k=0$ ).

#### 4.4 Effect of aspect ratio and friction

Real and imaginary parts of the first three frequencies of a viscoelastic plate are plotted against the flow velocity  $V$  in Figure 6 and 7 for the aspect ratios  $\lambda = 0.5$  and  $\lambda = 1$ , respectively, with friction coefficients  $k = 0.01$  and  $k = 0.4$  with the dimensionless viscoelastic coefficient  $H = 10^{-5}$ . Figures 6a, 6c, 7a and 7c show that an increase in the friction coefficient  $k$  does not affect the real part of the frequency which remains the same for different  $k$  values. The real part of the first frequency becomes zero for  $V = 6.5$  for  $\lambda = 0.5$  (Figures 6a, 6c) and the imaginary parts remain positive (Figures 6b, 6d). However, the imaginary parts of the frequencies are affected by an increase in  $k$  (see Figures 6b, 6d and 7b, 7d). To assess the effect of the aspect ratio we compare Figure 6 ( $\lambda = 0.5$ ) and Figure 7 ( $\lambda = 1$ ). An important difference is that the imaginary part of the third frequency becomes negative for  $\lambda = 1$  (Figure 7b, d), leading to single-mode flutter instability for  $V \geq 5$ . Thus instability depends on the aspect ratio with the high aspect ratios leading to flutter instabilities.

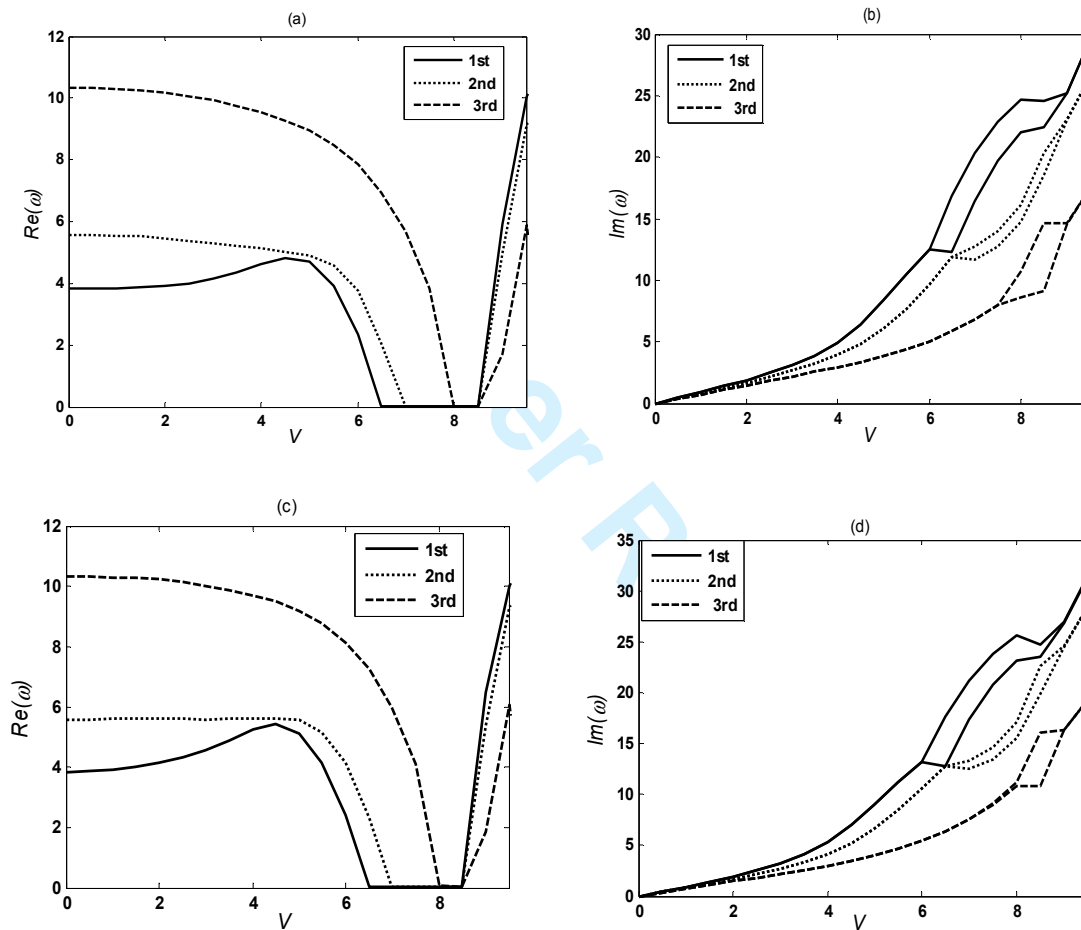


**Figure 6.**  
Real and imaginary parts of first three frequencies  $\omega$  vs flow velocity  $V$  for  $H = 10^{-5}$ ,  $a_1 = 1$ ,  $\beta = 0.19$ ,  $\lambda = 0.5$ , (a, b)  $k = 0.01$ , (c, d)  $k = 0.4$ .

# Dynamic Stability of Viscoelastic Plates under Axial Flow by Differential Quadrature Method

## Part 2

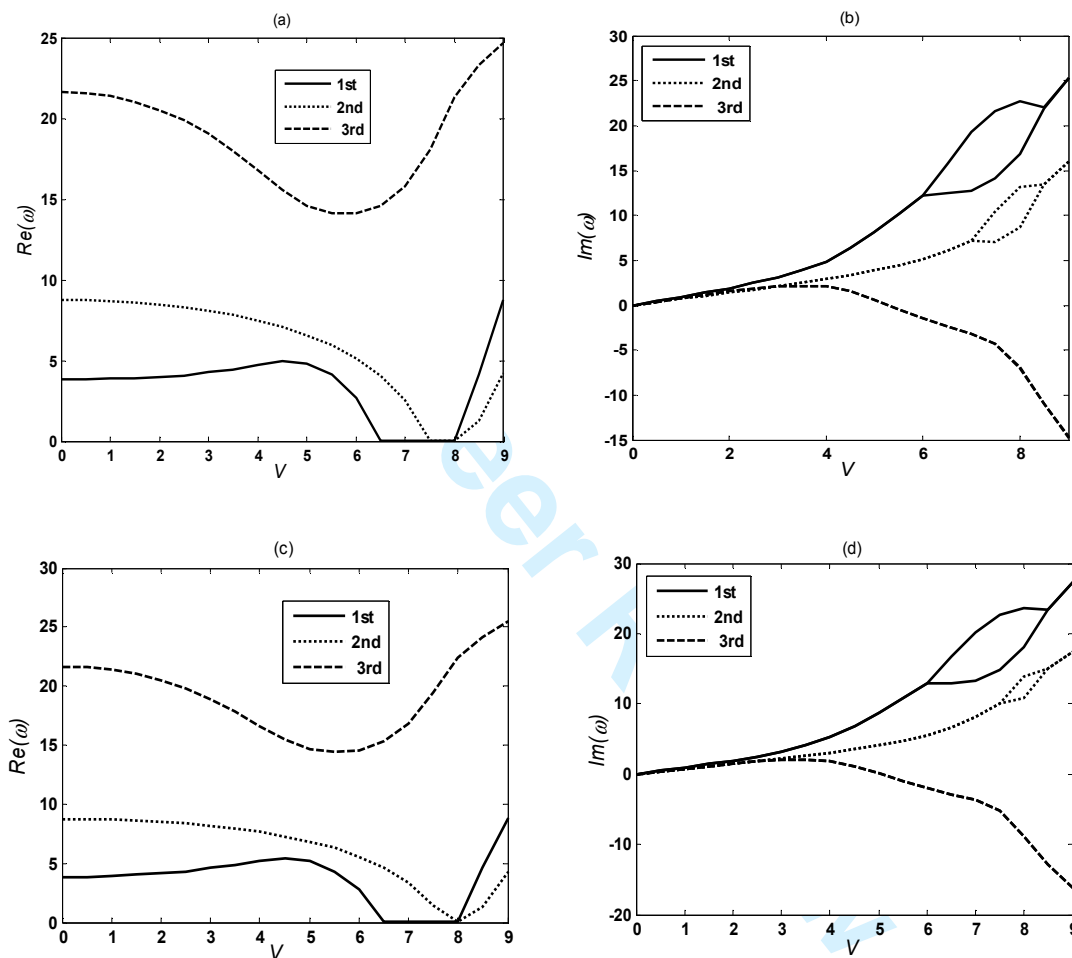


**Figure 7.** Real and imaginary parts of first three frequencies  $\omega$  vs flow velocity  $V$  for  $H = 10^{-5}$ ,  $a_1 = 1$ ,  $\beta = 0.19$ ,  $\lambda = 1$ , (a, b)  $k = 0.01$ , (c, d)  $k = 0.4$ .

The corresponding results for increased viscoelastic damping with  $H = 10^{-3}$  are given in Figures 8 and 9 for the aspect ratios  $\lambda = 0.5$  and  $\lambda = 1$ , respectively. The real part of the first frequency first increases, then decrease for  $\lambda = 0.5$  (Figures 8a, c), but does not become zero. As the imaginary parts of the frequencies remain positive, the plate stays stable due to increased damping of the viscoelastic material. For  $\lambda = 1$ , the real parts of the first and second frequencies become zero for flow velocity  $V > 7$ , however the imaginary part of the third frequency becomes negative for  $V > 5$  ( $k = 0.01$ ) and  $V > 5.6$  ( $k = 0.4$ ), leading to single-mode flutter instability as was

the case for  $H = 10^{-5}$  in Figure 7. Thus the aspect ratio has a direct effect on the stability of viscoelastic plates and the friction coefficient  $k$  affects the magnitude of the critical velocity.

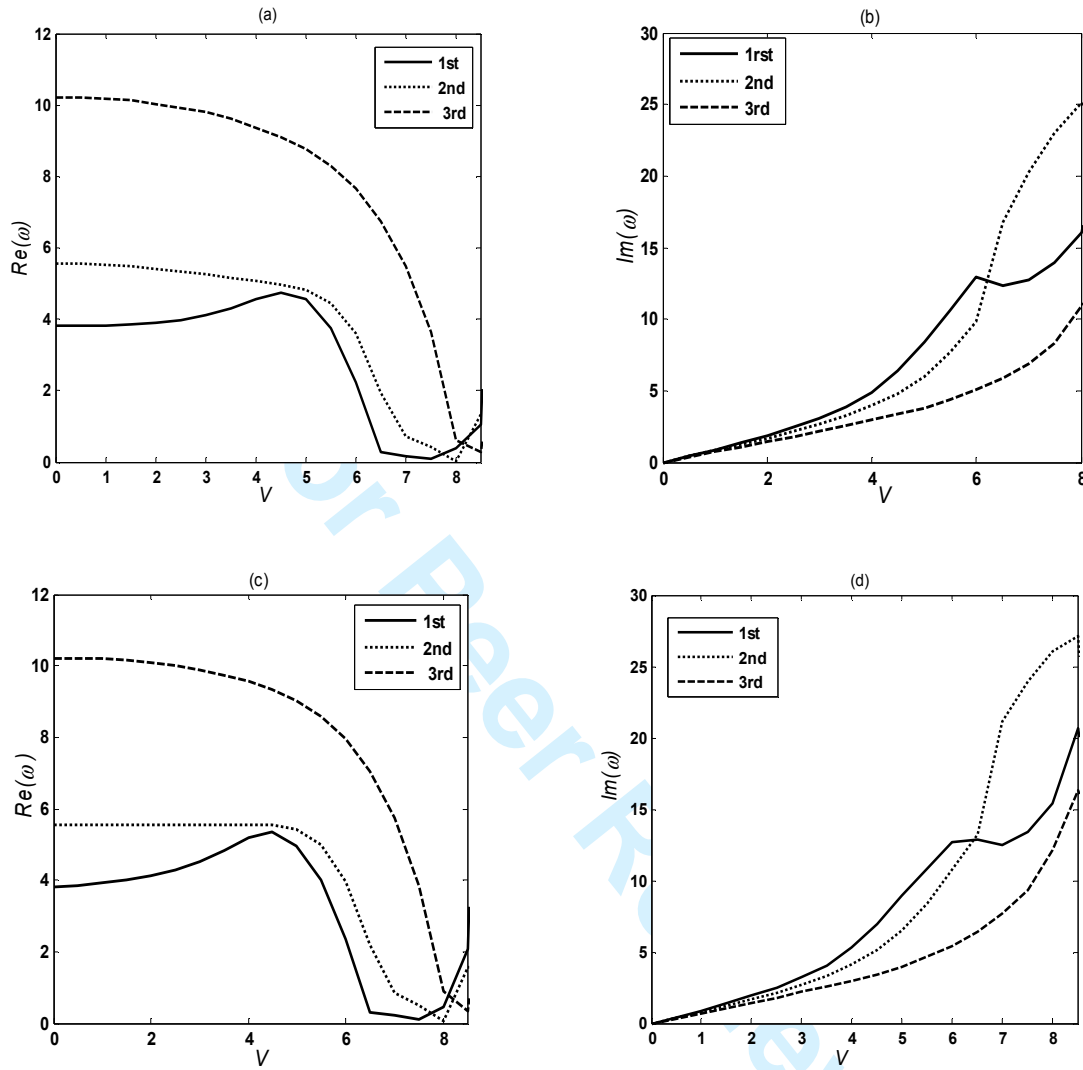


**Figure 8.** Real and imaginary parts of first three frequencies  $\omega$  vs. flow velocity  $V$  for  $H = 10^{-3}$ ,  $a_1 = 1$ ,  $\beta = 0.19$ ,  $\lambda = 0.5$ , (a, b)  $k = 0.01$ , (c, d)  $k = 0.4$ .

1  
2  
3  
4  
5  
6  
7  
8  
9  
10  
11  
12  
13  
14  
15  
16  
17  
18  
19  
20  
21  
22  
23  
24  
25  
26  
27  
28  
29  
30  
31  
32  
33  
34  
35  
36  
37  
38  
39  
40  
41  
42  
43  
44  
45  
46  
47  
48  
49  
50  
51  
52  
53  
54  
55  
56  
57  
58  
59  
60

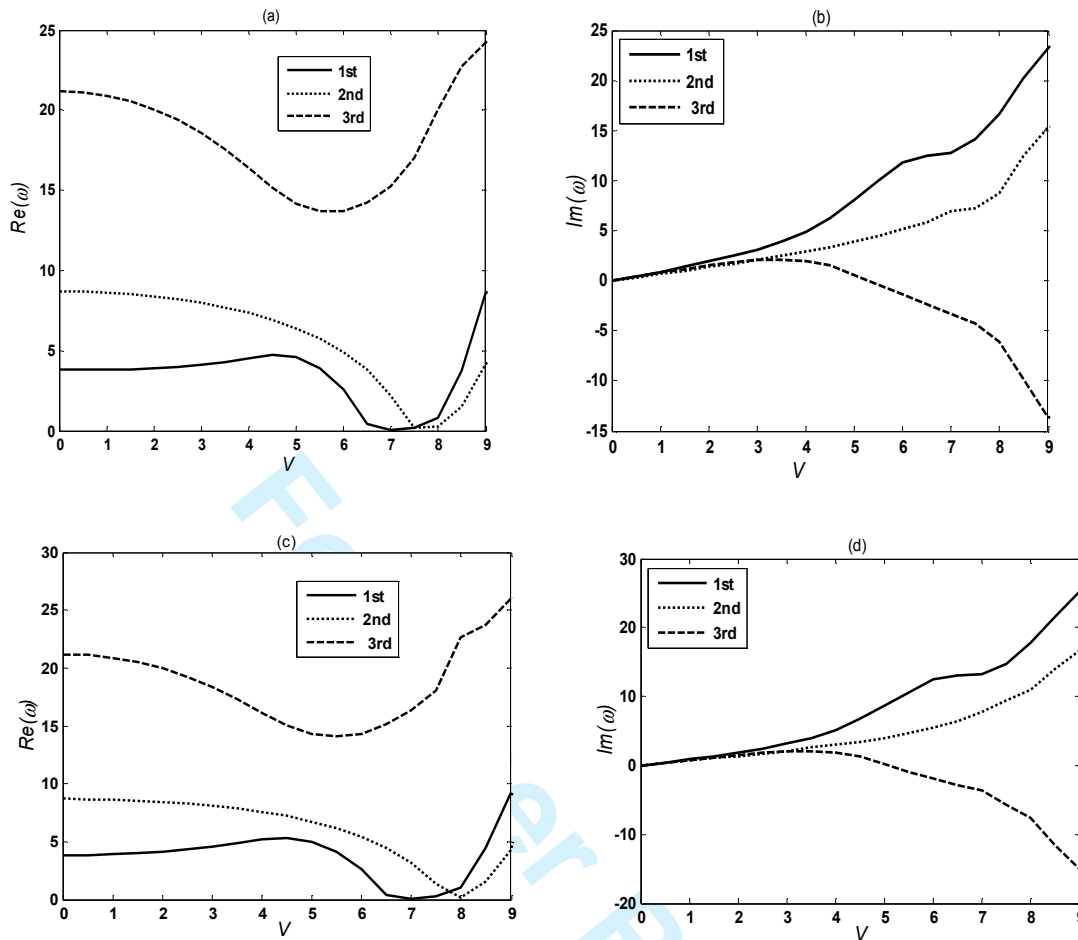


**Figure 9.**  
 Real and imaginary parts of first three frequencies  $\omega$  vs flow velocity  $V$  for  $H = 10^{-3}$ ,  $a_1 = 1$ ,  $\beta = 0.19$ ,  $\lambda = 1$ ,  
 (a, b)  $k = 0.01$ , (c, d)  $k = 0.4$ .

## 5. Conclusions

Dynamic stability of a cantilever viscoelastic plate subject to axial flow is studied using the differential quadrature method for numerical solutions. The viscoelastic material is defined as Kelvin-Voigt type and the equation of motion is derived by using inverse Laplace transformation. The method of solution is verified by applying it to a known solution in the literature.

It is observed that the aspect ratio and the viscoelastic coefficient directly affect the stability of the plate in axial flow. At low aspect ratios and viscoelastic coefficients, flutter instability does not occur as the real parts of the frequencies decrease with increasing flow velocity until they become zero while the imaginary parts remain positive (Figure 6). However, high aspect ratios cause the plate to lose stability by undergoing flutter as can be observed from Figures 7 and 9. Another observation is that increased viscoelasticity at low aspect ratios convert divergence stability to a simple stability and the plate remains stable (see Figures 8a, c).

An interesting phenomenon is the fact that the flutter instability at high aspect ratios is caused by the imaginary part of the third frequency becoming negative for high enough flow velocities rather than the first frequency (see Figures 7b, d, 9b, d). Numerical results indicate that the effect of laminar friction coefficient of the flowing fluid on the stability behaviour is minor, however, increasing friction leads to higher critical velocity for flutter instability.

### Appendix

For  $X = 0$  and  $X = 1$ , discretized form of boundary conditions (17) are given by

$$\begin{aligned}
 W_{1,j} &= 0 \quad \text{for } j = 1, 2, \dots, M \\
 \sum_{k=1}^N A_{1k}^{(1)} W_{kj} &= 0 \quad \text{for } j = 2, 3, \dots, M-1 \\
 \sum_{k=1}^N A_{Nk}^{(2)} W_{kj} + \nu \lambda^2 \sum_{l=1}^M B_{jl}^{(2)} W_{Nl} &= 0 \quad \text{for } j = 2, 3, \dots, M-1 \\
 \sum_{k=1}^N A_{Nk}^{(3)} W_{kj} + (2-\nu) \lambda^2 \sum_{k=l=1}^N \sum_{l=1}^M A_{Nk}^{(1)} B_{jl}^{(2)} W_{kl} &= 0 \quad \text{for } j = 2, 3, \dots, M-1
 \end{aligned}$$

For  $Y = 0$  and  $Y = 1$ , the corresponding equations are

$$\begin{aligned}
 \lambda^2 \sum_{l=1}^M B_{il}^{(2)} W_{il} + \nu \sum_{k=1}^N A_{ik}^{(2)} W_{k1} &= 0 \quad \text{for } i = 2, 3, \dots, N-1 \\
 \lambda^2 \sum_{l=1}^M B_{il}^{(3)} W_{il} + (2-\nu) \sum_{k=l=1}^N \sum_{l=1}^M A_{ik}^{(2)} B_{il}^{(1)} W_{kl} &= 0 \quad \text{for } i = 3, 4, \dots, N-2 \\
 \lambda^2 \sum_{l=1}^M B_{Ml}^{(2)} W_{il} + \nu \sum_{k=1}^N A_{ik}^{(2)} W_{kM} &= 0 \quad \text{for } i = 2, 3, \dots, N-1 \\
 \lambda^2 \sum_{l=1}^M B_{Ml}^{(3)} W_{il} + (2-\nu) \sum_{k=l=1}^N \sum_{l=1}^M A_{ik}^{(2)} B_{Ml}^{(1)} W_{kl} &= 0 \quad \text{for } i = 3, 4, \dots, N-2
 \end{aligned}$$

At two free corners

$$\sum_{k=l=1}^N \sum_{l=1}^M A_{ik}^{(1)} B_{jl}^{(1)} W_{kl} = 0 \quad \text{for } i = N, j = 1, M$$

### References

- Allen, J.J. and Smits, A. J. (2001), "Energy harvesting eel", *Journal of Fluids and Structures*, Vol. 15, pp. 629-640.
- Amabili, M. (2008), "Nonlinear Vibrations and Stability of Shells and Plates", *Cambridge University Press*, Cambridge, UK.
- Axisa, F. and Antunes J. (2007), "Modelling of Mechanical Systems-Fluid Structure Interaction", Vol. 3, *Elsevier*, Oxford, UK.
- Baliant, T. and Lucey, A. D. (2005), "Instability of a cantilevered flexible plate in viscous channel flow", *Journal of Fluids and Structures*, Vol. 20, pp. 893-912.
- Bert, C. W. and Malik M. (1996), "Implementing multiple boundary conditions in the DQ solution of higher-order PDE's: Application to free vibration of plates", *International Journal for Numerical Methods in Engineering*, Vol. 39, 1237-1258.
- Bryant, M. and Garcia, E. (2011), "Modeling and testing of a novel aeroelastic flutter energy harvester", *Journal of Vibration and Acoustics*, Vol. 133, pp. 1-11.
- Chen, M., Jia L., Wu, Y., Yin, X. and Ma Y. (2014a), "Bifurcation and chaos of a flag in an inviscid flow", *Journal of Fluids and Structures*, Vol. 45, pp. 124-137.
- Chen, M., Jia L.-B., Chen X.-P. and Yin X.-Z. (2014b), "Flutter analysis of a flag of fractional viscoelastic material", *Journal of Sound and Vibration*, Vol. 333, pp. 7183-7197.
- Cheng, Z.B., Xu, Y.G. and Zhang, L.L. (2015), "Analysis of flexural wave bandgaps in periodic plate structures using differential quadrature element method", *International Journal of Mechanical Sciences*, Vol. 100, pp. 112-125.
- Connell, B.S.H. and Yue D.K.P. (2006), "Flapping dynamics of a flag in a uniform stream", *Journal of Fluid Mechanics*, Vol. 581, pp. 33-68.

- 1  
2  
3 Datta, S.K. and Gottenberg, W. G. (2007), "Instability of an elastic strip hanging in an airstream", *ASME Journal of Applied Mechanics*, Vol. 42, pp. 195-198.
- 4  
5 De Rosa, M.A. and Lippiello, M. (2016), "Nonlocal frequency analysis of embedded single-walled carbon nanotube using the  
6 differential quadrature method", *Composites Part B: Engineering*, Vol. 84, pp. 41-51.
- 7 Doaré, O., Sauzade M. and Eloy C. (2011), "Flutter of an elastic plate in a channel flow: Confinement and finite-size effects",  
8 *Journal of Fluids and Structures*, Vol. 27, pp.76-88.
- 9 Eloy, C., Kofman N. and Schouveiler, L. (2012), "The origin of hysteresis in the flag instability", *Journal of Fluid Mechanics*,  
10 Vol. 691, pp. 583-593.
- 11 Eloy, C., Lagrange, R., Souilliez, C. and Schouveiler, L. (2008), "Aeroelastic instability of cantilevered flexible plates in  
12 uniform flow", *Journal of Fluid Mechanics*, Vol. 611, pp. 97-106.
- 13 Eloy, C., Souilliez, C. and Schouveiler, L. (2007), "Flutter of a rectangular plate", *Journal of Fluids and Structures*, Vol. 23,  
14 pp. 904-919.
- 15 Favier, J., Revell, A. and Pinelli, A. (2015), "Numerical study of flapping filaments in a uniform fluid flow", *Journal of Fluids  
16 and Structures*, Vol. 53, pp. 26-35.
- 17 Forouzesf, F. and Jafari, A.A. (2015), "Radial vibration analysis of pseudoelastic shape memory alloy thin cylindrical shells  
18 by the differential quadrature method", *Thin-Walled Structures*, Vol. 93, pp. 158-168.
- 19 Howell, R.M., Lucey, A.D., Carpenter, P.W. and Pitman, M.W. (2009), "Interaction between a cantilevered-free flexible plate  
20 and ideal flow", *Journal of Fluids and Structures*, Vol. 25, pp. 544-566.
- 21 Huang, L. (1995), "Mechanical modelling of palatal snoring", *Journal of the Acoustical Society of America*, Vol. 97, pp. 3642-  
22 3648.
- 23 Huang, L. (1995), "Flutter of cantilevered plates in axial flow", *Journal of Fluids and Structures*, Vol. 9, pp. 127-147.
- 24 Huang, L. and Zhang, C. (2013) "Modal analysis of cantilever plate flutter", *Journal of Fluids and Structures*, Vol. 38, pp.  
25 273-289.
- 26 Ilyasov, M. and Ilyasova, N. (2006), "Flutter of viscoelastic strips", *Mechanics of Time-Dependent Materials*, Vol. 10, pp. 201-  
27 213.
- 28 Khudayarov, B. A. (2005), "Numerical analysis of the nonlinear flutter of viscoelastic plates", *International Journal of Applied  
29 Mechanics*, Vol. 41, pp. 538-542.
- 30 Khudayarov, B.A. (2010), "Flutter of a viscoelastic plate in a supersonic gas flow", *International Journal of Applied  
31 Mechanics*, Vol. 46, pp. 455-460.
- 32 Kiiko, I.A. (1996), "Flutter of a viscoelastic plate", *Journal of Applied Mathematics and Mechanics*, Vol. 60, pp. 167-170.
- 33 Kiiko, I. A. and Pokazeev, V.V. (2013), "Flutter of a viscoelastic strip", *Moscow University Mechanics Bulletin*, Vol. 68, pp.  
34 25-27.
- 35 Korkmaz, A. and Dağ, I. (2013), "Cubic B-spline differential quadrature methods and stability for Burgers' equation",  
36 *Engineering Computations*, Vol. 30, pp. 320-344.
- 37 Kumar, V., Jiwari, R. and Gupta, R.K. (2013), "Numerical simulation of two dimensional quasilinear hyperbolic equations by  
38 polynomial differential quadrature method", *Engineering Computations*, Vol. 30, pp.892 – 909.
- 39 Lemaitre, C., Hémon, P. and Delangre, E. (2005), "Instability of long ribbon in axial flow", *Journal of Fluids and Structures*,  
40 Vol. 20, pp. 913-925.
- 41 Merrett, C.G. and Hilton, H.H. (2010), "Elastic and viscoelastic panel flutter in incompressible, subsonic and supersonic  
42 flows", *ASD Journal*, Vol. 2, pp. 53-80.
- 43 Mittal, R.C., Jiwari, R. and Sharma, K.K. (2013), "A numerical scheme based on differential quadrature method to solve time  
44 dependent Burgers' equation", *Engineering Computations*, Vol. 30, pp. 117-131.
- 45 Païdoussis, M.P. (2004), "Fluid-Structure Interactions: Slender Structures and Axial Flow", *Elsevier, Academic Press,  
46 London*, Vol. 2.
- 47 Pang, Z., Jia, L.B. and Yin, X. Z. (2010), "Flutter instability of rectangle and trapezoid flags in uniform flow", *Physics of  
48 Fluids*, Vol. 22, No. 121701.
- 49 Perez, M., Boisseau, S., Gasnier, P., Willemin, J. and Reboud, J.L. (2015), "An electret-based aeroelastic flutter energy  
50 harvester", *Smart Materials and Structures*, Vol. 24, No. 035004.
- 51 Pokazeyev, V. (2008), "Flutter of a cantilevered elastic and viscoelastic strip", *Journal of Applied Mathematics and  
52 Mechanics*, Vol. 72, pp. 446-451.
- 53 Potapov, V.D. (1995), "Stability of viscoelastic plates in supersonic flow under random loading", *AIAA Journal*, Vol. 33, pp.  
54 712-715.
- 55  
56  
57  
58  
59  
60

- 1  
2  
3 Potapov, V.D. (2004), "Stability of elastic and viscoelastic plates in a gas flow taking into account shear strains", *Journal of*  
4 *Sound and Vibration*, Vol. 276, pp. 615–626.
- 5 Robinson, M.T.A. (2013), "Nonlinear vibration of 2d viscoelastic plates subjected to tangential follower force", *Engineering*  
6 *Mechanics*, Vol. 20, No. 1, pp 59–74
- 7 Robinson, M.T.A. and Adali, S. (2016), "Nonconservative stability of viscoelastic rectangular plates with free edges under  
8 uniformly distributed follower force", *International Journal of Mechanical Sciences*, Vol. 107, pp. 150-159.
- 9 Robinson, M.T.A. and Adali, S. (Under review) "Dynamic stability of viscoelastic rectangular plates subjected to triangular  
10 tangential follower loads", Submitted to *Journal of Mechanical Science and Technology*.
- 11 Rossi, R., Oñate, E. (2010), "Analysis of some partitioned algorithms for fluid-structure interaction", *Engineering*  
12 *Computations*, Vol. 27, pp. 20-56.
- 13 Shu, C. (2000), *Differential Quadrature and Its Applications in Engineering*, Springer-Verlag, London.
- 14 Shu, C. and Du, H. (1997), "A generalized approach for implementing general boundary conditions in the GDQ free vibration  
15 analysis of plates", *International Journal of Solids Structures*, Vol. 34, pp. 837-846.
- 16 Taneda, S. (1968), "Waving motions of flags", *Journal Physical Society of Japan*, Vol. 24, pp. 392-401.
- 17 Tang, D.M. and Dowell, E. H. (2004), "Effects of geometric structural nonlinearity of flutter and limit cycle oscillations of  
18 high-aspect-ratio wings", *Journal of Fluids and Structures*. Vol. 19, pp. 291-306.
- 19 Tang, L. and Païdoussis, M.P. (2007), "On the stability and the post-critical behaviour of two-dimensional cantilevered flexible  
20 plates in axial flow", *Journal of Sound and Vibration*, Vol. 305, pp. 97-115.
- 21 Tang, L., Païdoussis, M.P. and Jiang, J. (2009), "Cantilevered flexible plates in axial flow: Energy transfer and the concept of  
22 flutter-mill", *Journal of Sound and Vibration*, Vol. 326, pp. 263-276.
- 23 Tang, L., Païdoussis, M.P. and Jiang, J. (2009), "The dynamics of variants of two-dimensional cantilevered flexible plates in  
24 axial flow", *Journal of Sound and Vibration*, Vol. 323, pp. 214–231.
- 25 Tang, Y.-Q. and Chen, L.-Q. (2011), "Nonlinear free transverse vibration of in-plane moving plate: Without and with internal  
26 resonances", *Journal of Sound and Vibration*, Vol. 330, pp. 110-126.
- 27 Vadim, D. and Potapov, V.D. (1995), "Stability of viscoelastic plates in supersonic flow under random loading", *AIAA*  
28 *Journal*, Vol. 33, pp. 712-715.
- 29 Virost, E., Amandolese, X. and Hémon, P. (2013), "Fluttering flags: an experimental study of fluid forces", *Journal of Fluids*  
30 *and Structures*, Vol. 43, pp. 385–401.
- 31 Wang, D.-A. and Ko, H.-H. (2010), "Piezoelectric energy harvesting from flow-induced vibration", *Journal of*  
32 *Micromechanics and Microengineering*, Vol. 20, No. 025019.
- 33 Wang, Z.-M., Zhou, Y.-F. and Wang Y. (2007), "Dynamic stability of non-conservative viscoelastic rectangular plate",  
34 *Journal of Sound and Vibration*, Vol. 307, pp. 250-264.
- 35 Watanabe, Y., Suzuki, S., Sugihara, M. and Sueoka, Y. (2002a), "An experimental study of paper flutter", *Journal of Fluids*  
36 *and Structures*, Vol. 16, pp. 529–542.
- 37 Watanabe, Y., Isogai, K., Suzuki, S. and Sugihara, M. (2002b), "A theoretical study of paper flutter", *Journal of Fluids and*  
38 *Structures*, Vol. 16, pp. 543–560.
- 39 Yamaguchi, N., Yokota, K. and Tsujimoto, Y. (2000a), "Flutter limits and behaviour of a flexible thin sheet in high-speed  
40 flow-I: Analytical method for prediction of the sheet behaviour", *ASME Journal of Fluids Engineering*, Vol.122, pp.  
41 65-73.
- 42 Yamaguchi, N., Sekiguchi Y., Yokota, K. and Tsujimoto, Y. (2000b), "Flutter limits and behaviours of a flexible thin sheet in  
43 high-speed flow-II: Experimental results and predicted behaviours for low mass ratios", *ASME Journal of Fluids*  
44 *Engineering*, Vol. 122, pp. 74-83.
- 45 Yadykin, Y., Tenetov V. and Levin D. (2001), "The flow-induced vibration of a flexible strip hanging vertically in a parallel  
46 flow part 1: Temporal aeroelastic instability", *Journal of Fluids and Structures*, Vol. 15, pp. 1167–1185.
- 47 Zhao, W., Païdoussis M.P., Tang, L., Liu, M. and Jiang, J. (2012), "Theoretical and experimental investigations of the  
48 dynamics of cantilevered flexible plates subjected to axial flow", *Journal of Sound and Vibration*, Vol. 331, pp. 575–  
49 587.
- 50 Zhi Zong, Z. and Zhang, Y. (2009), *Advanced Differential Quadrature Methods*, Chapman & Hall/CRC, Boca Raton, FL.  
51  
52  
53  
54  
55  
56  
57  
58  
59  
60

## LIST OF FIGURE CAPTIONS

Fig. 1. Geometry of the cantilever plate in axial flow

Fig. 2. Critical velocity vs dimensionless length with  $H = 0$ ,  $\lambda = 0$ ,  $k = 0$ ,  $\beta = 0.19$

Fig. 3. First three natural frequencies vs flow velocity with  $H = 0$ ,  $\lambda = 0$ ,  $a_1 = 1$ ,  $\beta = 0.19$ ,  
(a)  $k = 0.01$ , (b)  $k = 0.1$ , (c)  $k = 0.2$ , (d)  $k = 0.3$

Fig. 4. Critical velocity vs. dimensionless length for  $H = 0$ ,  $\lambda = 0$ ,  $\beta = 0.19$  for various values of  $k$ .

Fig. 5. Effect of mass ratio  $\beta$  on critical velocity using one dimensional model ( $H = 0$ ,  $\lambda = 0$ ,  $a_1 = 1$ ,  $k = 0$ )  
and two dimensional model ( $H = 0$ ,  $\lambda = 1$ ,  $a_1 = 1$ ,  $k = 0$ ).

Fig. 6. Real and imaginary parts of first three frequencies  $\omega$  vs flow velocity  $V$  for  $H = 10^{-5}$ ,  $a_1 = 1$ ,  
 $\beta = 0.19$ ,  $\lambda = 0.5$ , (a, b)  $k = 0.01$ , (c, d)  $k = 0.4$ .

Fig. 7. Real and imaginary parts of first three frequencies  $\omega$  vs flow velocity  $V$  for  $H = 10^{-5}$ ,  $a_1 = 1$ ,  
 $\beta = 0.19$ ,  $\lambda = 1$ , (a, b)  $k = 0.01$ , (c, d)  $k = 0.4$ .

Fig. 8. Real and imaginary parts of first three frequencies  $\omega$  vs. flow velocity  $V$  for  $H = 10^{-3}$ ,  $a_1 = 1$ ,  
 $\beta = 0.19$ ,  $\lambda = 0.5$ , (a, b)  $k = 0.01$ , (c, d)  $k = 0.4$ .

Fig. 9. Real and imaginary parts of first three frequencies  $\omega$  vs. flow velocity  $V$  for  $H = 10^{-3}$ ,  $a_1 = 1$ ,  
 $\beta = 0.19$ ,  $\lambda = 1$ , (a, b)  $k = 0.01$ , (c, d)  $k = 0.4$ .

## CHAPTER 7 : BUCKLING OF NON LOCAL NANOBEAMS

### 7.1-Introduction

This chapter is devoted to study on Carbon Nanotubes (CNT) from basic definitions to the formulation of the buckling of nanotubes including its synthesis. To carry on the task, the author first defines the basic concepts around CNTs, then gives the reasons for its modelling as a nanobeam. The establishment of the governing equation for the CNT considered as an Euler-Bernoulli nanobeam and subjected to distributed forces and point loads are performed. Weak formulation and the Rayleigh-Ritz method are explained in detail in order to understand the method of solution employed in the solutions of the problems in chapters 8 and 9.

### 7.2-The basic definitions and origin of Carbon nanotubes

The term Nanotechnology was introduced firstly by Japanese researcher Norio Taniguchi, in 1974, but, only became popular later in 1986 with Eric Drexler, an American engineer from MIT (Massachusetts Institute of Technology) through his famous book titled: "Engines of Creation: The Coming Era of Nanotechnology" [1]. In fact, the nanoparticles have always been present in the composition of some natural materials. They can't be then considered as invented by human beings. The terminology "nanotechnology" itself became more popular after the discovery of a particular nano structure, called Carbon Nanotubes in 1991 by Japanese researcher S. Iijima. They are defined as Cylindrical tubes, generally made of carbon with diameters on nanometer scale (one fifty thousandth of human hair's thickness). Their length can be as much as a few centimeters. They physically exist in two principal categories, namely, Single walled nanotube (SWNT) and Multi-walled nanotube (MWNT) as presented in Figure 7.1 .

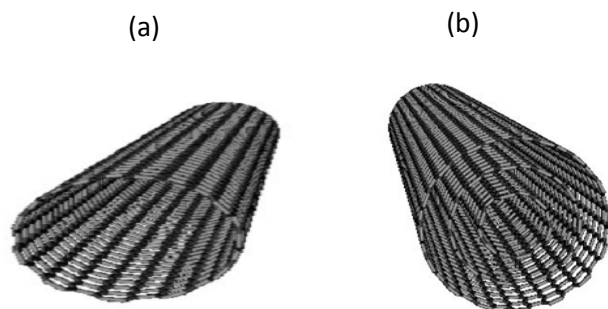


Fig 7.1: Schematic diagrams of (a) single-wall nanotube (SWNT) and (b) multi-wall nanotube (MWNT) [2]

Many methods have been developed for synthesis of CNTs [3, 4]. Among them, one can name Chemical vapour deposition (CVD), Arc discharge, Laser ablation, Flame pyrolysis, Bottom-up organic approach. After the synthesis, it is very important to be able to characterize mechanically the carbon nanotubes as well as their material responses. Two methods have been developed in this regards, which are experimental, and theoretical methods. Experiments have shown that CNTs have very high Young's modulus, a characteristic which makes them strong materials. Other experiments have demonstrated their excellent thermal and electrical conductivity, comparing to existing well known conductors (Table1).

Tab. 7.1. Comparison of thermal and electrical conductivity of CNT with some materials [5]

Material	Thermal Conductivity (W/m.k)	Electrical Conductivity
Carbon Nanotubes	> 3000	10 <sup>6</sup> - 10 <sup>7</sup>
Copper	400	6 x 10 <sup>7</sup>
Carbon Fiber - Pitch	1000	2 - 8.5 x 10 <sup>6</sup>
Carbon Fiber - PAN	8 - 105	6.5 - 14 x 10 <sup>6</sup>

All these great characteristics made CNTs very useful in many technological domains. These domains include: Electronics, optics or material sciences. For example, because they are very reactive and interact with their surrounding milieu, they have been demonstrated to be very useful for water purification. Precisely, nano filters have ceramic nano pores which are used for water filtration and eliminate bacteria and virus from water. Nano filters can then be an alternative way of water purification as Chlorine. Carbon nanotubes can be used to create reinforced steel or concrete for civil and mechanical engineering. The obtained composite materials will be more stiff, and resistant. These composites are very useful in automobile industry (production of composites trunks, car bodies...), aerospace industry, sport industry (cyclists using bicycle whose frame is a composite material containing nanotubes, tennis players using carbon nanotube racket, hockey players using sticks doped carbon nanotubes). CNTs are also very important in Nanoelectromechanical systems, for manufacturing devices such as RAM (random access memory), TV and computer screens.

Facing the difficulties of implementing and controlling experiments at nanoscale, theoretical approach is widely developed. These theoretical methods include atomistic

approach and continuum mechanic analysis. Due to being computationally expensive, especially for large-scale carbon nanotubes with high number of walls, the atomistic approach is used less in preference to continuum mechanic which is preferred, especially by large number of researchers who use the existing continuum mechanics beam theory or shell theory to model the CNTs .

In fact, beams are one dimensional bar structures, capable of carrying loads in bending. Beam theory was also extensively used to model the behavior of many existing structures such as pipes, columns, wood-made posts, concrete-made posts, long bridges,...etc.

Mathematically, beams behavior can be modelled by many theories. The first one is Euler-Bernoulli theory. Sometimes called Bernoulli (1700-1782) theory or Euler theory (1707-1783), it is the simplest beam theory as shear and rotary effects are not taken into account in the constitutive relationship. Only membrane and displacement effect are considered. To include the above cited effects neglected in Bernoulli theory, Rayleigh beam theory (1877) takes the rotary effect into account in their constitutive relation while Timoshenko theory includes shear and rotary effects. Other theories include Reddy beam theory, Hu-Thai-Tai theory... etc.

The utilization of beam theory on the modelling of carbon nanotubes is widely nowadays, following the shell theory, formerly used for mathematical modeling of CNTs. The reason is that, in classical continuum theory, size effect plays an important role in the modeling of small size devices because, if they are not taken into account, the behavior of such materials could be overestimated or underestimated. The beam theory has shown its capacity of producing high precision results compared to shell theory. Many size-based beam theories have been developed in this regard. Those theories include couple stress theory, strain gradient theory and nonlocal theory. Eringen Nonlocal theory will be used in this thesis to model CNT as it appears to be the best mathematical model for studying vibration, bending and buckling.

The term “buckling” means a deformation process in which a structure subjected to high stress undergoes a sudden change in morphology at a critical load [6]. Also known as static reaction of a structure, when subjected to compressive-type forces like follower forces, and considered in the design of structural members, such as bridges and machineries, buckling appears to be also very important at nanoscale. It can be created on CNT's by bending, torsional deformation, thermal deformation, and also due to their long and hollow tube-like

form. Buckling can appear during their preparation processes, and has been discovered not to be only noxious but sometimes also very important as it may increase the thermal conductivity of the obtained CNTs [7]. The buckling may also depend of other parameters such as Chirality.

### 7.3-Equation of buckling of the CNT s considered as a nanobeam

In this section the equation governing the buckling of CNTs as nanobeam will be established by using the free body diagram.

#### 7.3.1-Displacement and stress distribution on the beam

The figure below shows a free body diagram of the on nanobeam.

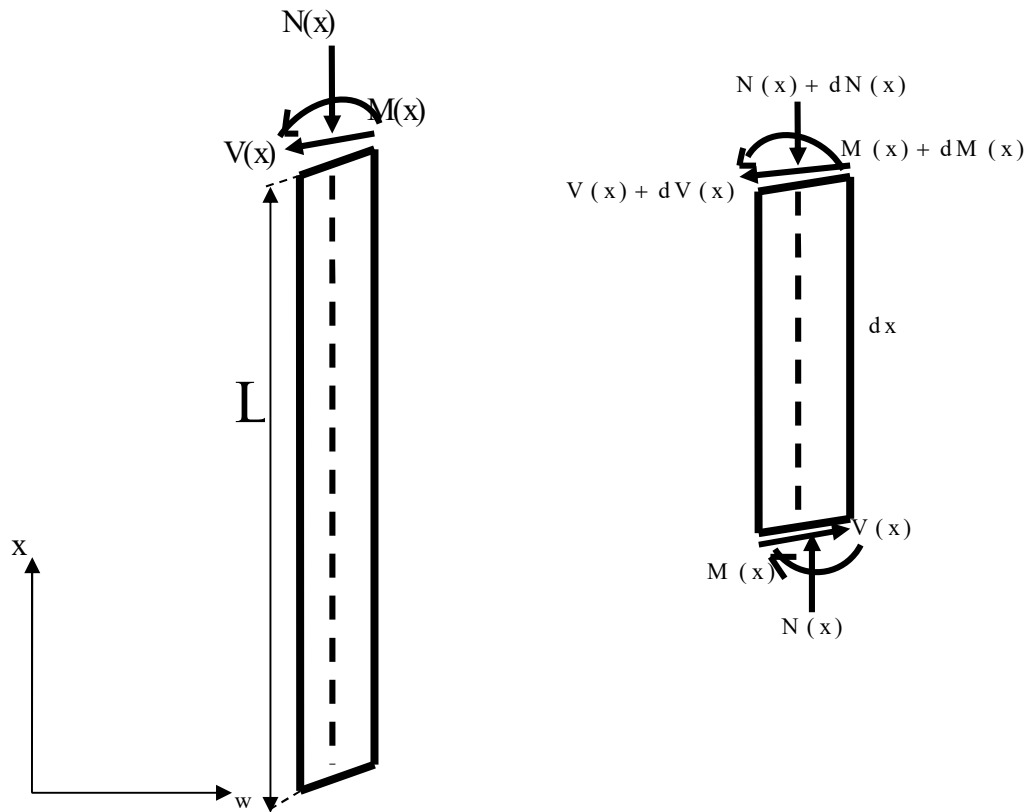


Fig. 7.2: Free body diagram of nanobeam

#### 7.3.1a-The displacement

The displacement field of nanobeam in this study is the one adopted by Euler-Bernoulli

$$u = -z \frac{\partial w}{\partial x}, \quad v = 0, \quad w = w(x) \quad (7.1)$$

Here,  $u$  and  $w$  are axial (along  $x$ ) and transverse displacement (along  $w$ ) axis, respectively.

### 7.3.1b-The stress of nanobeam

The nonlocal theory was developed by Eringen et al [8-11] to overcome the drawbacks of local theory of elasticity. Based on atomic theory of lattice dynamics and experimental observations on phonon dispersion, this approach assumes that the nonlocal stress tensor at a point within one or multidimensional domain of structure is not only affected by the strain at that local point, but also by strains at all other points of the entire domain in an integral manner. This consideration takes into account the size effect, which is not taken into consideration by local theory and consequently, the local Hooke's law constitutive relation is replaced by integration. Mathematically it's written as:

$$\sigma_{ij,i} + \rho f_j = 0 \quad (7.2)$$

with

$$\sigma_{ij}(\mathbf{x}) = \int_V \alpha(|\mathbf{x}' - \mathbf{x}|, \mu) \sigma'_{ij}(\mathbf{x}') dV(\mathbf{x}') \quad (7.3)$$

where

$$\sigma'_{ij}(\mathbf{x}') = \lambda_L e_{kk}(\mathbf{x}') \delta_{ij} + 2\mu_L e_{ij}(\mathbf{x}') \quad (7.4)$$

and

$$e_{ij}(\mathbf{x}') = \frac{1}{2} \left( \frac{\partial u_i(\mathbf{x}')}{\partial x'_j} + \frac{\partial u_j(\mathbf{x}')}{\partial x'_i} \right) \quad (7.5)$$

$\sigma_{ij}(\mathbf{x})$ ,  $f_j$ ,  $u_i$ ,  $\rho$  stand, respectively, for nonlocal stress tensor, body force density, mass density, and displacement vector at the reference point  $\mathbf{x}$  in the body  $V$ ,  $i, j = 1, 2$  or  $3$  depending on chosen dimension.  $\lambda_L$  and  $\mu_L$  are Lamé parameters. The weight is specified by nonlocal Kernel function  $\alpha(|\mathbf{x}' - \mathbf{x}|, \mu)$  which depends on a dimensionless length nanoscale

$$\mu = \frac{e_0 a}{L} \quad (7.6)$$

where  $e_0$  stands for a material constant, which can be determined either experimentally by using vibration or buckling load measurements, or by the use of atomic dispersion relation. The constant  $a$  represents an internal characteristic length such as granular distance, lattice parameter while  $L$  is an external characteristic length. The nonlocal parameter can be

determined by conducting experiments and a comparison of dispersion curves from nonlocal continuum mechanics and molecular dynamics simulations as suggested by [12,13]. In general, a conservative estimate of nonlocal parameter is  $e_0 a \sim 2\text{nm}$  for SWCNT [13]. Its value depends on many parameters such as boundary conditions, chirality, mode shape, number of walls and type of motion [14].

In a macroscopic analysis when the effects of nanoscale becomes infinitely insignificant in the limit  $\mu \rightarrow 0$ , the effects of strains at points  $x \neq x'$  are negligible, the nonlocal modulus approaches the Dirac delta function and hence  $\sigma'_{ij}(x) = \sigma'_{ij}(x')$ . Consequently, the classical elasticity for continuum mechanics should be recovered in the limit of vanishing nonlocal nanoscale. Eq.(7.2) is an integro-partial differential equation and it is extremely difficult mathematically to obtain the solutions in terms of displacement field in nonlocal elasticity due to the presence of spatial derivatives inside the integral. However, by using Green's function with certain approximation error, Eringen [8] transformed the integro-partial differential equation to the following form:

$$\sigma - (e_0 a)^2 \nabla^2 \sigma = \sigma' \quad (7.7)$$

where  $\nabla^2 \equiv \frac{\partial^2}{\partial x^2}$  is a Laplacian operator helping on writing the nonlocal stress-strain relation of nanobeams as:

$$\sigma_{xx} - (e_0 a)^2 \frac{d^2 \sigma_{xx}}{dx^2} = E \varepsilon_{xx} \quad (7.8)$$

where the strain is given by

$$\varepsilon_{xx} = -z \frac{d^2 w(x)}{dx^2} \quad (7.9)$$

#### 7.4-Equilibrium equation for axially loaded nanobeam

By applying the Newton's third law on Fig. 7.2, one can obtain the equilibrium equation of the beam, relating forces and moments as follow:

$$\sum F_z = 0: \quad -\frac{dV}{dx} = 0 \quad (7.10)$$

$$\sum M = 0: \quad Nd w + V dx - \frac{dM}{dx} dx = 0 \quad (7.11)$$

Differentiating Eq.(7.11) with respect to  $x$  and introducing it into Eq.(7.10), one obtains:

$$\frac{d^2M}{dx^2} - \frac{d}{dx} \left( N \frac{dw}{dx} \right) = 0 \quad (7.12)$$

and

$$V = \frac{dM}{dx} - N \frac{dw}{dx} \quad (7.13)$$

By using the definition of bending moment given by:

$$M = \int_A z \sigma dA \quad (7.14)$$

we could get from Eq.(7.12) the bending moment equation for the nonlocal beam as:

$$M - (e_0 a)^2 \frac{d^2M}{dx^2} + EI \frac{d^2w}{dx^2} = 0 \quad (7.15)$$

where

$$M(x) = -EI \frac{d^2w}{dx^2} + (e_0 a)^2 \frac{d}{dx} \left( N \frac{dw}{dx} \right) \quad (7.16)$$

Combining the previous equations, viz. (7.16) into (7.15), we get:

$$EI \frac{d^4w}{dx^4} + \frac{d}{dx} \left( N \frac{dw}{dx} \right) - (e_0 a)^2 \frac{d^2}{dx^2} \left[ \frac{d}{dx} \left( N \frac{dw}{dx} \right) \right] = 0 \quad (7.17)$$

#### 7.5-Weak form derivati on for axially loaded elastically restr ained nan obeam

The Eq. (7.17) is called a strong formulation of the buckling of nanobeam. In other to transform to a form which can be solved using the weighted residual method, a weak formulation must be used. The weak formulation of differential equation of problem is a weighted-integral form that is equivalent to both the governing differential equation as well as the associated natural boundary conditions. The first step consists on multiplying Eq. (7.17) with a test function  $\phi$  as follows

$$\int_0^L \phi \left\{ EI \frac{d^4w}{dx^4} + \frac{d}{dx} \left( N \frac{dw}{dx} \right) - (e_0 a)^2 \frac{d^2}{dx^2} \left[ \frac{d}{dx} \left( N \frac{dw}{dx} \right) \right] \right\} dx = 0 \quad (7.18)$$

That test function must be smooth enough and must satisfy the homogeneous essential boundary conditions. After this, an integration by part is done on Eq.(7.18), producing therefore the weak form of Eq. (7.17) and the associated boundary conditions as:

$$\int_0^L \left[ EI \frac{d^2 \phi}{dx^2} \frac{d^2 w}{dx^2} - N \frac{d\phi}{dx} \frac{dw}{dx} - (e_0 a)^2 \left( \frac{dN}{dx} \frac{d^2 \phi}{dx^2} \frac{dw}{dx} + N \frac{d^2 \phi}{dx^2} \frac{d^2 w}{dx^2} \right) \right] dx + [V\phi]_0^L + \left[ M \frac{d\phi}{dx} \right]_0^L = 0 \quad (7.19)$$

## 7.6-The Rayleigh -Ritz method for solving the buckling problem

The Ritz method has been widely used to solve buckling problems. It is employed for obtaining the solutions of structural problems governed by differential equations by the use of principle of minimum potential energy. It assumes a shape function  $W(x, y)$  for the solution in the form of a series which can be expressed as

$$W(x) = \sum_{j=1}^n C_j \phi_j(x) \quad (7.20)$$

where  $n$  is the number of terms needed in the displacement function to reach the desired accuracy.

Functions  $\phi_j(x)$  are the approximating functions which should satisfy the geometric boundary conditions. These functions have to be orthogonal [15] or transformed to an orthogonal function set by the use of Gram-Schmidt process [16,17]. The unknowns  $C_j$  ( $j = 1, 2, \dots, n$ ) are obtained by minimizing the Rayleigh quotient [18].

The above described process transforms a Rayleigh quotient to a set of inhomogeneous linear equations expressed in terms of the coefficients  $C_j$ . In this way, the problem can be reduced to solving the eigenvalue equation:

$$([K] - q[F])\{C\} = 0 \quad (7.21)$$

where  $[K]$  and  $[F]$  are  $n \times n$  order coefficient matrices,  $q$  is the unknown buckling load and  $\{C\} = \{C_1 \ C_2 \ \dots \ C_n\}^T$  is a vector of unknown constants to be determined.

## 7.7-References

- [1] Eric Drexler (1987). Engines of Creation: The Coming Era of Nanotechnology
- [2] R. Purohit, K. Purohit, R. S. Rana, V. Patel (2014). Carbon Nanotubes and Their Growth Methods Procedia Materials Science (6) 716 -728

- [3] M. S. Dresselhaus, Y. M. Lin, O. Rabin, A. Jorio, A. G. Souza Filho, M. A. Pimenta, R. Saito, G. G. Samsonidze, G. Dresselhaus (2003). Nanowires and nanotubes. *Material Sciences. Engineering C.*, 23 129–140
- [4] J. P. Jana, Bohlavova, J. Chomoucka, J. Hubalek, O. Jasek, V. Adam, R. Kizek (2011). Methods for carbon nanotubes synthesis—review, *Journal of Dynamic Journal of Materials Chemistry*, 21, 15872
- [5] J. Choi and Y. Zhang. Properties and applications of single-, double- and multi-walled carbon nanotubes Aldrich Materials Science, Sigma-Aldrich Co. LLC
- [6] D. O Brush, B. O. Almroth (1975). *Buckling of Bars, Plates, and Shells*, McGraw-Hill: New York, USA
- [7] A. N. Volkov, T. Shiga, D. Nicholson, J. Shiomi, L. V. Zhigilei (2012). Effect of bending buckling of carbon nanotubes on thermal conductivity of carbon nanotube materials, *Journal of Applied Physics* 111, 053501
- [8] A. C. Eringen (1983). On differential equations of nonlocal elasticity and solutions of screw dislocation and surface waves. *Journal of Applied Physics* 54 4703–4710
- [9] A. C. Eringen (1972). Nonlocal polar elastic continua, *International Journal of Engineering Sciences*. 10 1–16
- [10] A. C. Eringen. (2002). *Nonlocal Continuum Field Theories*. Springer-Verlag, New York
- [11] A. C. Eringen, D. G. B. Edelen. (1972). On nonlocal elasticity. *International Journal of Engineering Sciences*. 10, 233–248
- [12] B. Arash, R. Ansari (2010). Evaluation of nonlocal parameter in the vibrations of single-walled carbon nanotubes with initial strain. *Physica E: Low-dimensional Systems and Nanostructures*, 42(8), pp. 2058–2064
- [13] Q. Wang, C. M. Wang (2007). The constitutive relation and small scale parameter of nonlocal continuum mechanics for modelling carbon nanotubes. *Nanotechnology*.18:07570
- [14] B. Arash, Q. Wang (2012). A review on the application of nonlocal elastic models in modeling of carbon nanotubes and graphenes. *Computational Materials Science* Vol 51, 1 303–313
- [15] S. A. M. Ghannadpour, B. Mohammadi, J. Fazilati (2013). Bending, buckling and vibration problems of nonlocal Euler beams. *Composite Structures*, 96584–589
- [16] S. Chakraverty, L. Behera (2015). Free vibration of non-uniform nanobeams using Rayleigh–Ritz method, *Physica E*, 6738–46
- [17] L. Behera, S. Chakraverty (2014). Free vibration of Euler and Timoshenko nanobeams using boundary characteristic orthogonal polynomials. *Applied Nanosciences* 4:347–358
- [18] S. Adali (2008). Variation principles for multi-walled carbon nanotubes undergoing buckling based on nonlocal elasticity theory. *Physics Letters A*. Volume 372, Issue 35, 25 pp 5701–5705

CHAPTER 8-PAPER 4:  
VARIATIONAL SOLUTION FOR BUCKLING OF NONLOCAL CARBON  
NANOTUBES UNDER UNIFORMLY AND TRIANGULARLY DISTRIBUTED  
AXIAL LOADS. published in Composite Structures .



# Variational solution for buckling of nonlocal carbon nanotubes under uniformly and triangularly distributed axial loads



Mouafo Teifouet Armand Robinson<sup>a,b</sup>, Sarp Adali<sup>a,\*</sup>

<sup>a</sup> Discipline of Mechanical Engineering, University of KwaZulu-Natal, Durban 4041, South Africa

<sup>b</sup> Department of Physics, University of Dschang, Cameroon

## ARTICLE INFO

### Article history:

Available online 8 January 2016

### Keywords:

Buckling of nanotubes  
Distributed axial loads  
Variational formulation  
Nonlocal model  
Rayleigh quotient

## ABSTRACT

In the present study buckling loads are computed for carbon nanotubes subject to a combination of concentrated and axially distributed loads. Distributed axial loads are taken as uniformly distributed and triangularly distributed. Carbon nanotubes are modeled as nonlocal Euler–Bernoulli beams. Variational formulation of the problem is derived and variationally consistent boundary conditions are obtained. The Rayleigh quotients for the distributed axial loads are formulated. Numerical solutions are obtained by Rayleigh–Ritz method and employing orthogonal Chebyshev polynomials. Results are given in the form of counter plots for a combination of simply supported, clamped and free boundary conditions. It is observed that the sensitivity of the buckling loads to small scale parameter depends on the specific boundary conditions.

© 2016 Elsevier Ltd. All rights reserved.

## 1. Introduction

Advanced properties of carbon nanotubes (CNT) such as high stiffness to weight ratio, large failure strain, to name a few, make them materials of choice in a large number of technologically advanced applications [1,2]. An expanding area of application for their use is as reinforcing materials in polymer matrix composites leading to the development of nano-composites with superior properties [3–5]. One limiting factor in the use of CNTs is their low buckling strength due to their slenderness. Buckling of CNTs is also of interest in a number of applications such as nano-mechanical devices and drug delivery. The modeling approach often employed in the study of carbon nanotubes is nonlocal continuum mechanics [6] to take into account the nano-scale effects [7–9]. Recent studies provide further elaboration of the nonlocal models [10] and employ the integral formulation of the nonlocal elasticity [11]. Due to the importance of the subject, buckling of carbon nanotubes has been studied extensively and the reviews of the subject can be found in [12–14]. Recent studies on the buckling of single-walled nanotubes involving a concentrated tip load include [15–19]. In a number of nano applications, the stability of a nanotube under its own weight becomes important and the problem has been studied in [20,21].

The present study is directed to investigating the buckling characteristics of single-walled nanotubes via nonlocal Euler beam theory with the compressive loads taken as a combination of concentrated and distributed axial loads. In particular, two types of distributed axial loads are considered, namely, uniformly distributed load which corresponds to self-weight and triangularly distributed load. Stability under triangularly distributed axial loads has not been studied for nanotubes although it was studied extensively for columns based on local elastic theory. In particular, columns under conservative triangularly distributed axial loads were studied in [22–29]. Corresponding studies involving the buckling of columns subject to non-conservative triangularly distributed loads were given in [30–32].

In the present study, first the variational formulation of the problem is derived and variationally consistent boundary conditions are obtained. The Rayleigh quotients are obtained from the variational formulations. Variational formulation of a local column under distributed loads is given in [33]. Variational formulations for carbon nanotubes subject to buckling loads have been obtained for a number of cases [34–38].

The numerical solutions are given for various boundary conditions employing Rayleigh–Ritz approximation and using orthogonal Chebyshev polynomials. It is observed that the sensitivity of the buckling load to small scale parameter depends on the specific boundary conditions with highest sensitivity displaced by the clamped–simply supported and clamped–clamped boundary conditions and the lowest by clamped–free boundary condition.

\* Corresponding author. Tel.: +27 31 2603203.

E-mail address: [adali@ukzn.ac.za](mailto:adali@ukzn.ac.za) (S. Adali).

**2. Variational formulation**

We consider a single-walled carbon nanotube of length  $L$  subject to a concentrated load  $P$  and a distributed axial load  $q(x)$  as shown in Fig. 1. Both uniformly distributed axial load given by  $q_1(x) = Q_1(L - x)$  (Fig. 1a) and triangularly distributed axial load given by  $q_2(x) = \frac{1}{2}Q_2(L^2 - x^2)$  (Fig. 1b) are studied. In the case of a column subject to its own weight,  $q_1$  represents the weight per unit length of the column. The axial load can be expressed as

$$N = P + q(x), \quad 0 \leq x \leq L \tag{1}$$

The equation governing the buckling of a nanotube is given in terms of moment  $M(x)$  and deflection  $w(x)$  as

$$\frac{d^2 M}{dx^2} - \frac{d}{dx} \left( N \frac{dw}{dx} \right) = 0 \tag{2}$$

The constitutive relation based on the nonlocal theory of elasticity can be expressed as

$$M - (e_0 a)^2 \frac{d^2 M}{dx^2} = -EI \frac{d^2 w}{dx^2} \tag{3}$$

where  $e_0 a$  is the small scale parameter,  $E$  is the Young’s modulus and  $I$  is the moment of inertia of the cross-section. The expression for  $M(x)$  is obtained from Eqs. (2) and (3) as

$$M(x) = -EI \frac{d^2 w}{dx^2} + (e_0 a)^2 \left[ -\frac{d}{dx} \left( N \frac{dw}{dx} \right) \right] \tag{4}$$

Substituting Eq. (4) into Eq. (2), the differential equation governing the buckling of a nanotube is obtained as

$$D(w) = EI \frac{d^4 w}{dx^4} + \frac{d}{dx} \left( N \frac{dw}{dx} \right) - (e_0 a)^2 \left[ \frac{d^2}{dx^2} \left( \frac{dN}{dx} \frac{dw}{dx} \right) + \frac{d^2}{dx^2} \left( N \frac{d^2 w}{dx^2} \right) \right] = 0 \tag{5}$$

Noting that

$$\int_0^L D(w) w dx = 0 \tag{6}$$

we proceed to obtain the variational formulation for the problem. Let

$$U(w) = \sum_{i=1}^4 U_i(w) \tag{7}$$

where

$$U_1(w) = \int_0^L EI \frac{d^4 w}{dx^4} w dx, \quad U_2(w) = \int_0^L \frac{d}{dx} \left( N \frac{dw}{dx} \right) w dx \tag{8}$$

$$U_3(w) = -(e_0 a)^2 \int_0^L \frac{d^2}{dx^2} \left( \frac{dN}{dx} \frac{dw}{dx} \right) w dx,$$

$$U_4(w) = -(e_0 a)^2 \int_0^L \frac{d^2}{dx^2} \left( N \frac{d^2 w}{dx^2} \right) w dx \tag{9}$$

Thus Eq. (6) can be expressed as

$$\sum_{i=1}^4 U_i(w) = 0 \tag{10}$$

By integration by parts, the following relations can be obtained

$$U_1(w) = \int_0^L EI \left( \frac{d^2 w}{dx^2} \right)^2 dx + EI \left( \frac{d^3 w}{dx^3} w - \frac{d^2 w}{dx^2} \frac{dw}{dx} \right) \Big|_{x=0}^{x=L} \tag{11}$$

$$U_2(w) = - \int_0^L N \left( \frac{dw}{dx} \right)^2 dx + N \frac{dw}{dx} w \Big|_{x=0}^{x=L} \tag{12}$$

$$U_3(w) = -(e_0 a)^2 \int_0^L \frac{dN}{dx} \frac{dw}{dx} \frac{d^2 w}{dx^2} dx - (e_0 a)^2 \left[ \frac{d}{dx} \left( \frac{dN}{dx} \frac{dw}{dx} \right) w - \frac{dN}{dx} \left( \frac{dw}{dx} \right)^2 \right] \Big|_{x=0}^{x=L} \tag{13}$$

$$U_4(w) = -(e_0 a)^2 \int_0^L N \left( \frac{d^2 w}{dx^2} \right)^2 dx - (e_0 a)^2 \left[ \frac{d}{dx} \left( N \frac{d^2 w}{dx^2} \right) w - N \frac{d^2 w}{dx^2} \frac{dw}{dx} \right] \Big|_{x=0}^{x=L} \tag{14}$$

Let

$$V(x) = EI \frac{d^3 w}{dx^3} + N \frac{dw}{dx} - (e_0 a)^2 \left[ \frac{d}{dx} \left( \frac{dN}{dx} \frac{dw}{dx} \right) + \frac{d}{dx} \left( N \frac{d^2 w}{dx^2} \right) \right] \tag{15}$$

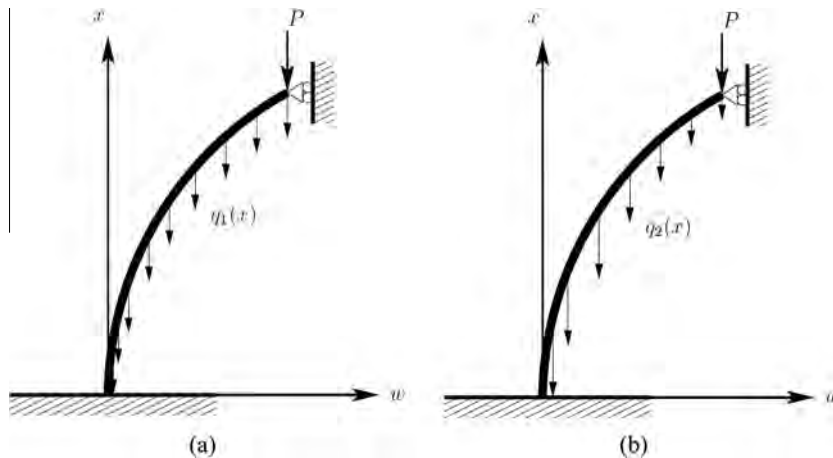


Fig. 1. Nanocolumn under concentrated and distributed axial loads, (a) uniform, (b) triangular.

Then Eq. (10) can be expressed as

$$\int_0^L \left\{ EI \left( \frac{d^2 w}{dx^2} \right)^2 - N \left( \frac{dw}{dx} \right)^2 - (e_0 a)^2 \left[ \frac{dN}{dx} \frac{dw}{dx} \frac{d^2 w}{dx^2} + N \left( \frac{d^2 w}{dx^2} \right)^2 \right] \right\} dx + \left( V(x)w + M(x) \frac{dw}{dx} \right)_{x=0}^{x=L} = 0 \tag{16}$$

where  $M(x)$  is given by Eq. (4) and  $V(x)$  by Eq. (15). Eq. (16) corresponds to the weak formulation of the problem. Next the boundary conditions are given for various cases.

Simply supported boundary conditions:

$$w(0) = 0, \quad M(0) = 0, \quad w(L) = 0, \quad M(L) = 0 \tag{17}$$

Clamped–clamped boundary conditions:

$$w(0) = 0, \quad \left. \frac{dw}{dx} \right|_{x=0} = 0, \quad w(L) = 0, \quad \left. \frac{dw}{dx} \right|_{x=L} = 0 \tag{18}$$

Clamped–simply supported boundary conditions:

$$w(0) = 0, \quad \left. \frac{dw}{dx} \right|_{x=0} = 0, \quad w(L) = 0, \quad M(L) = 0 \tag{19}$$

Clamped–free supported boundary conditions:

$$w(0) = 0, \quad \left. \frac{dw}{dx} \right|_{x=0} = 0, \quad M(L) = 0, \quad V(L) = 0 \tag{20}$$

### 3. Rayleigh quotients

First the Rayleigh quotient is derived for a nanotube subject to a concentrated axial load  $N = P$  only and  $q(x) = 0$ . In this case

$$\begin{aligned} M(x) &= -EI \frac{d^2 w}{dx^2} + P(e_0 a)^2 \frac{d^2 w}{dx^2}, \\ V(x) &= EI \frac{d^3 w}{dx^3} + P \left( \frac{dw}{dx} + (e_0 a)^2 \frac{d^3 w}{dx^3} \right) \end{aligned} \tag{21}$$

Eq. (16) can be written as

$$\int_0^L \left\{ EI \left( \frac{d^2 w}{dx^2} \right)^2 - P \left[ \left( \frac{dw}{dx} \right)^2 + (e_0 a)^2 \left( \frac{d^2 w}{dx^2} \right)^2 \right] \right\} dx + [b_0(x) + P b_1(x)]_{x=0}^{x=L} = 0 \tag{22}$$

where

$$\begin{aligned} b_0(x) &= EI \left( \frac{d^3 w}{dx^3} w - \frac{d^2 w}{dx^2} \frac{dw}{dx} \right), \\ b_1(x) &= \frac{dw}{dx} w - (e_0 a)^2 \left( \frac{d^3 w}{dx^3} w - \frac{d^2 w}{dx^2} \frac{dw}{dx} \right) \end{aligned} \tag{23}$$

Thus the Rayleigh quotient follows from Eq. (22) as

$$P = \frac{u_1 + b_0(L) - b_0(0)}{u_2 - b_1(L) + b_1(0)} \tag{24}$$

where

$$u_1 = \int_0^L EI \left( \frac{d^2 w}{dx^2} \right)^2 dx, \quad u_2 = \int_0^L \left[ \left( \frac{dw}{dx} \right)^2 + (e_0 a)^2 \left( \frac{d^2 w}{dx^2} \right)^2 \right] dx \tag{25}$$

Next the Rayleigh quotients for the distributed loads are derived. Let

$$N = P + q(x) = P + Q_i S_i(x) \tag{26}$$

where  $S_1(x) = L - x$  for a uniformly distributed load and  $S_2(x) = \frac{1}{2}(L - x)^2$  for a triangularly distributed load. We express  $M(x)$  and  $V(x)$  given by Eqs. (4) and (15) in the following form

$$M(x) = m_0(x) + Q_i m_i(x), \quad V(x) = v_0(x) + Q_i v_i(x) \tag{27}$$

where

$$\begin{aligned} m_0(x) &= -EI \frac{d^2 w}{dx^2} + P(e_0 a)^2 \frac{d^2 w}{dx^2}, \\ v_0(x) &= EI \frac{d^3 w}{dx^3} + P \left( \frac{dw}{dx} - (e_0 a)^2 \frac{d^3 w}{dx^3} \right) \end{aligned} \tag{28}$$

$$m_i(x) = (e_0 a)^2 \left( \frac{dS_i}{dx} \frac{dw}{dx} + S_i(x) \frac{d^2 w}{dx^2} \right), \quad i = 1, 2 \tag{29}$$

$$v_i(x) = S_i \frac{dw}{dx} - (e_0 a)^2 \left( \frac{d^2 S_i}{dx^2} \frac{dw}{dx} + 2 \frac{dS_i}{dx} \frac{d^2 w}{dx^2} + S_i \frac{d^3 w}{dx^3} \right), \quad i = 1, 2 \tag{30}$$

From Eqs. (16), (27)–(30), the buckling load parameter  $Q_i$  can be expressed in the form of a Rayleigh quotient as

$$Q_i = \frac{u_3 + (m_0(x) \frac{dw}{dx} + v_0(x)w)_{x=0}^{x=L}}{u_4 + (-m_i(x) \frac{dw}{dx} + v_i(x)w)_{x=0}^{x=L}} \tag{31}$$

where

$$u_3 = \int_0^L \left[ EI \left( \frac{d^2 w}{dx^2} \right)^2 - P \left( \frac{dw}{dx} \right)^2 - P(e_0 a)^2 \left( \frac{d^2 w}{dx^2} \right)^2 \right] dx \tag{32}$$

$$u_4 = \int_0^L \left\{ S_i(x) \left( \frac{dw}{dx} \right)^2 + (e_0 a)^2 \left[ \frac{dS_i(x)}{dx} \frac{dw}{dx} \frac{d^2 w}{dx^2} + S_i(x) \left( \frac{d^2 w}{dx^2} \right)^2 \right] \right\} dx \tag{33}$$

Non-dimensional form of the formulation can be obtained by introducing dimensionless variables

$$X = \frac{x}{L}, \quad W = \frac{w}{L}, \quad \mu = \frac{e_0 a}{L}, \quad p = \frac{PL^2}{EI}, \quad q_i = \frac{Q_i L^{2+i}}{EI} \tag{34}$$

Non-dimensional forms of the Rayleigh quotients (24) and (31) are given in the Appendix A.

### 4. Method of solution

The numerical solution of the problem is obtained by Rayleigh–Ritz method [39]. Deflection function  $W(X)$  is expressed in terms of Chebyshev polynomials multiplied by a function to satisfy the geometric boundary conditions [40–43]. Thus the essential boundary conditions are satisfied and the Chebyshev polynomials provide a complete and orthogonal set leading to a relatively fast convergence. The deflection function  $W(X)$  is defined as

$$W(X) = X^r (1 - X)^s \sum_{j=1}^N c_j f_{j-1}(X) \tag{35}$$

where  $r$  and  $s$  take the values 0, 1 or 2 for free, simply supported and clamped boundaries, respectively, and  $c_j$  is determined to minimize the Rayleigh quotient. Thus for a simply supported column  $r = s = 1$  and for a clamped–free column  $r = 2$  and  $s = 0$ . Minimization of the Rayleigh quotient with respect to  $c_j$  leads to a generalized eigenvalue problem and the buckling load corresponds to the minimum eigenvalue of this problem. By taking the number of terms  $N$  sufficiently large, an accurate solution of the problem is obtained. In Eq. (35),  $f_j(X)$  is the  $j$ th Chebyshev polynomial with  $f_0(X) = 1$  and  $f_1(X) = X$ . The remaining terms are obtained by using the following recursive relationship:

**Table 1**  
Comparison of buckling loads  $p$  ( $q(x) = 0$ ) with existing results for four boundary conditions.

BC	$\mu = 0$			$\mu = 0.2$		$\mu = 1$		
	Present	Reference [40]	Reference [46]	Present	Reference [40]	Present	Reference [40]	Reference [46]
SS	9.870	9.870	9.870	7.076	7.076	0.895	0.908	0.908
CS	20.191	20.191	20.191	11.170	11.170	0.921	0.953	0.953
CC	39.478	39.478	39.478	15.307	15.307	0.975	0.975	0.975
CF	2.467	2.467	2.465	2.246	2.246	0.712	0.712	0.712

**Table 2**  
Comparison of buckling loads  $q_1$  and  $q_2$  ( $p = 0$ ) with existing results for  $\mu = 0$  (local theory).

BC	$q_1$		$q_2/2$		
	Present	Reference [47]	Reference [48]	Present	Reference [23]
SS	18.569	18.569	18.58	23.239	23.239
CS	52.504	52.501	53.91	78.983	78.983
CC	74.643	74.629	78.96	107.823	107.823
CF	7.837	7.837	7.84	16.101	16.101

**Table 3**  
Convergence of buckling load  $q_1$  ( $p = 0$ ) with the number of trial functions for  $\mu = 0.4$ .

Number of polynomials (N)	SS	CS	CC	CF
2	5.4864	8.9957	7.7170	4.9348
4	5.6558	6.8480	6.7589	4.6922
6	5.6909	6.5772	6.5416	4.6619
8	5.6925	6.4059	6.4442	4.6962
10	5.6925	6.4059	6.4442	4.6962

**Table 4**  
Convergence of buckling load  $q_1$  ( $p = 0$ ) with the number of trial functions for  $\mu = 1.0$ .

Number of polynomials (N)	SS	CS	CC	CF
2	1.0595	1.6665	1.3328	1.6167
4	1.0071	1.1574	1.1131	1.1574
6	1.0028	1.0742	1.0590	1.0803
8	1.0015	1.0439	1.0367	1.0485
10	1.0009	1.0292	1.0251	1.0323
12	1.0006	1.0207	1.0182	1.0285

$$f_{j+1}(X) = 2Xf_j(X) - f_{j-1}(X) \tag{36}$$

which are Chebyshev orthogonal polynomials of the first kind [44,45].

Method of solution is first applied to buckling problems available in the literature to verify its accuracy. The first problem is the buckling of a nonlocal nanotube subject to a concentrated axial load only, i.e.,  $p > 0$  and  $q(x) = 0$ . The results are given in Table 1. It is observed that the present method implemented by using Chebyshev polynomials give accurate results. Next the method is applied to columns subject to distributed axial loads and the results are shown in Table 2. The present method is observed to be accurate also in the case of buckling with distributed axial loads.

The convergence of the present method is studied in Table 3 which gives the buckling load for the case of a uniformly distributed axial load and  $\mu = 0.4$  with the convergence reached with 10 trial functions. When  $\mu = 1.0$ , convergence is observed to be slower as demonstrated in Table 4.

### 5. Numerical results

Numerical results are given for the four boundary conditions of SS, CS, CC and CF which are given by Eqs. (17)–(20). The range of the small scale parameter  $\mu$  is taken as  $0 \leq \mu \leq 0.4$ . The contour plots of the buckling loads  $q_1$  and  $q_2$  with respect to  $p$  and  $\mu$  are shown in Fig. 2 for a simply supported nanotube. It is observed that the buckling load decreases as the small-scale parameter increases. The corresponding results for the clamped–simply supported nanotubes are shown in Fig. 3. In this case the effect of the small-scale parameter is more pronounced, indicating that boundary

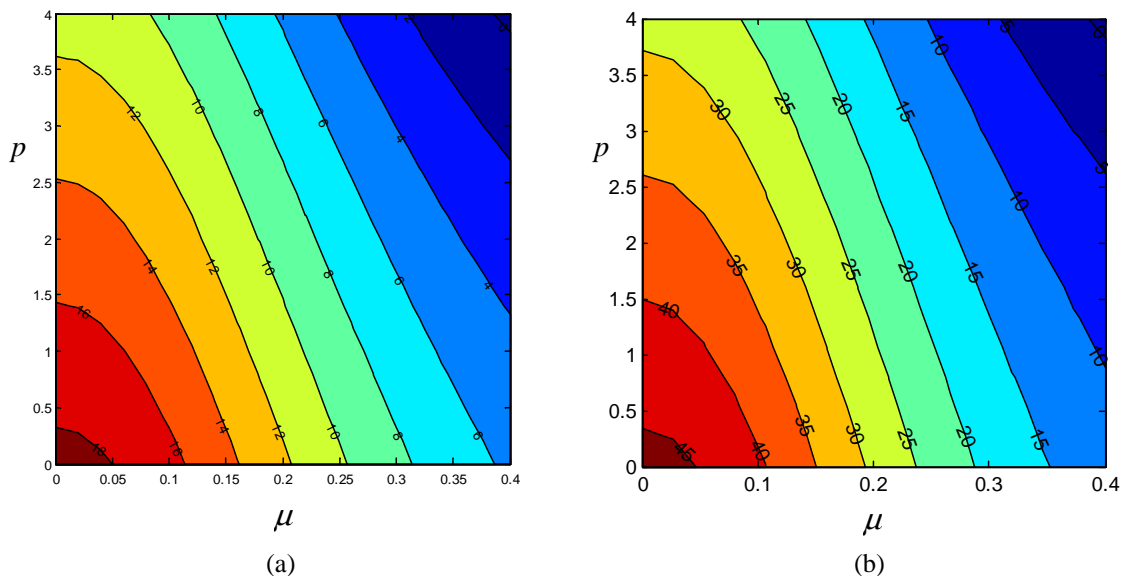


Fig. 2. Contour plots of  $q_i$  with respect to  $p$  and  $\mu$  for SS nanocolumns, (a)  $q_1$ , (b)  $q_2$ .

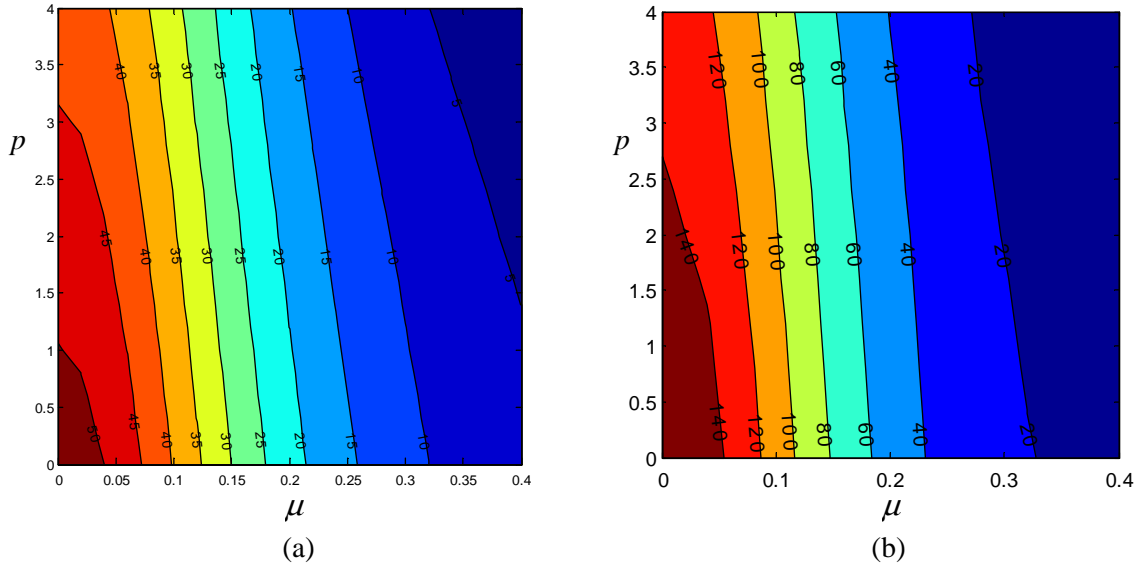


Fig. 3. Contour plots of  $q_i$  with respect to  $p$  and  $\mu$  for CS nanocolumns, (a)  $q_1$ , (b)  $q_2$ .

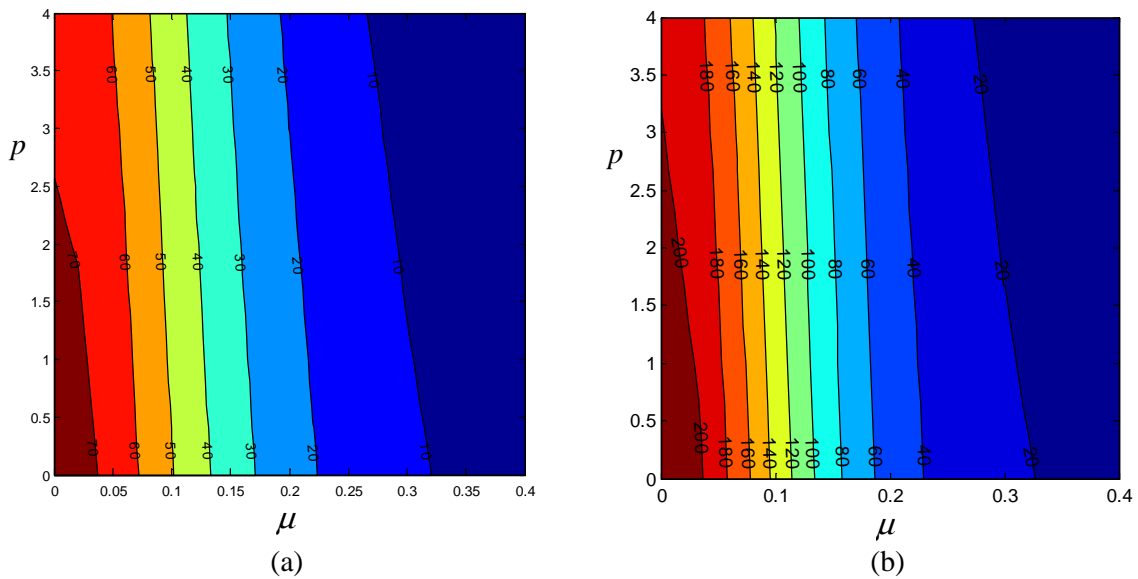


Fig. 4. Contour plots of  $q_i$  with respect to  $p$  and  $\mu$  for CC nanocolumns, (a)  $q_1$ , (b)  $q_2$ .

conditions affect the sensitivity of the buckling load to the small scale parameter for distributed axial loads.

The contour plots for clamped–clamped nanotubes are shown in Fig. 4 which shows increased sensitivity of the buckling load to the small scale parameter. Contour plots for clamped–free nanotubes are shown in Fig. 5. In this case the buckling loads are more sensitive to the tip load  $p$  and less sensitive to  $\mu$ . In Fig. 5, the stability boundary between the tip load  $p$  and the distributed loads can be observed, i.e., the line on which  $q_1 = 0$  (Fig. 5a) and  $q_2 = 0$  (Fig. 5b). Above these lines the distributed load  $q$  becomes tensile indicated by negative numbers.

### 6. Conclusions

The buckling loads for carbon nanotubes were obtained with the axial loads taken as a combination of concentrated tip load

and distributed axial loads. Two types of distributed loads were investigated, namely, uniformly distributed axial load which can model the own weight of the nanotube and triangularly distributed axial load. The results were obtained by Rayleigh–Ritz method employing Chebyshev polynomials of first kind as the approximating functions. The variational formulation of the problem based on nonlocal Euler–Bernoulli beam theory was derived and the corresponding Rayleigh quotients for the tip load and the distributed axial loads were obtained. Variationally consistent boundary conditions were derived for various boundary conditions and the numerical results were given for a combination of simple, clamped and free supports.

The effect of the small-scale parameter on the buckling loads was investigated by means of contour plots of the distributed loads with respect to the tip load and the small scale parameter. These plots indicate the sensitivity of the buckling load and it was

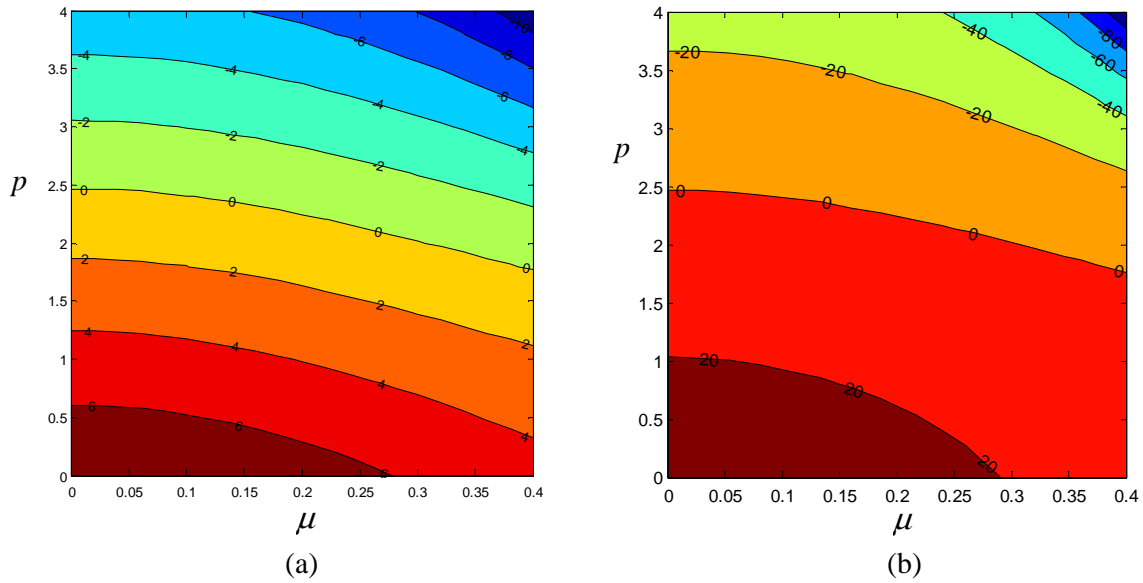


Fig. 5. Contour plots of  $q_i$  with respect to  $p$  and  $\mu$  for CF nanocolumns, (a)  $q_1$ , (b)  $q_2$ .

observed that buckling load becomes sensitive to the magnitude of the small scale parameter for the clamped–simply supported and clamped–clamped boundary conditions. On the other hand buckling load is more sensitive to the magnitude of the tip load for the clamped–free boundary conditions.

Nondimensional form of the Rayleigh quotient for the case of a nanotube subject to a uniformly distributed axial load  $q_1(1 - X)$  and tip load  $p$  is given by

$$q_1 = \frac{\int_0^L [W''^2 - p(W'^2 + \mu^2 W''^2)] dX + (M_1(X)W' + V_1(X)W)|_{X=0}^{X=1}}{\int_0^L [(1 - X)W'^2 + \mu^2(-W'W''^2 + (1 - X)W''^2)] dX + (M_2(X)W' - V_2(X)W)|_{X=0}^{X=1}} \tag{A4}$$

**Acknowledgements**

The research reported in this paper was supported by research grants from the University of KwaZulu-Natal (UKZN) and from National Research Foundation (NRF) of South Africa. The authors gratefully acknowledge the supports provided by UKZN and NRF.

**Appendix A**

$$q_2 = \frac{\int_0^L [W''^2 - p(W'^2 + \mu^2 W''^2)] dX + (M_1(X)W' + V_1(X)W)|_{X=0}^{X=1}}{\int_0^L [F(X)W'^2 + \mu^2(-XW'W''^2 + F(X)W''^2)] dX + (M_3(X)W' - V_3(X)W)|_{X=0}^{X=1}} \tag{A7}$$

Nondimensional form of the Rayleigh quotient for the case of a nanotube subject to a concentrated axial load  $p$  only with  $q(x) = 0$  is given by

$$p = \frac{\int_0^1 W''^2 dX + B_0(1) - B_0(0)}{\int_0^1 (W'^2 + \mu^2 W''^2) dX - B_1(1) + B_1(0)} \tag{A1}$$

where

$$W' = \frac{dW}{dX}, W'' = \frac{d^2W}{dX^2}, W''' = \frac{d^3W}{dX^3} \tag{A2}$$

$$B_0(X) = W'''W - W''W', B_1(x) = W'W - \mu^2(W'''W - W''W') \tag{A3}$$

where

$$M_1(X) = W''(-1 + p\mu^2), M_2(X) = \mu^2(-W' + (1 - X)W'') \tag{A5}$$

$$V_1(X) = W''' + p(W' - \mu^2 W'''), \tag{A6}$$

$$V_2(X) = (1 - X)W' + \mu^2(2W'' - (1 - X)W''') \tag{A6}$$

Nondimensional form of the Rayleigh quotient for the case of a nanotube subject to a triangularly distributed axial load  $\frac{1}{2}q_2(1 - X)^2$  and tip load  $p$  is given by

where

$$F(X) = \frac{1}{2}(1 - X)^2, M_3(X) = \mu^2[-(1 - X)W' + F(X)W''] \tag{A8}$$

$$V_3(X) = F(X)W' - \mu^2(W' - 2(1 - X)W'' + F(X)W'''). \tag{A9}$$

**References**

[1] Meyyappan M, editor. Carbon nanotubes: science and applications. CRC Press; 2005.  
 [2] O’Connell M, editor. Carbon nanotubes: properties and applications. CRC Press; 2006.

- [3] Grady BP. Carbon nanotube–polymer composites: manufacture, properties, and applications. New Jersey: John Wiley & Sons; 2011.
- [4] Tserpes KI, Silvestre N, editors. Modeling of carbon nanotubes, graphene and their composites. Switzerland: Springer International Publishing; 2014.
- [5] Mittal V, editor. Polymer nanotube nanocomposites. Scrivener Publishing; 2014.
- [6] Zhang YY, Wang CM, Duan WH, Xiang Y, Zong Z. Assessment of continuum mechanics models in predicting buckling strains of single-walled carbon nanotubes. *Nanotechnology* 2009;20:395707. 8pp.
- [7] Arash B, Wang Q. A review on the application of nonlocal elastic models in modeling of carbon nanotubes and graphenes. *Comput Mater Sci* 2012;51(1):303–13.
- [8] Reddy JN. Nonlocal theory for bending, buckling and vibration of beams. *Int J Eng Sci* 2007;45:288–307.
- [9] Reddy JN, Pang SD. Nonlocal continuum theories of beams for the analysis of carbon nanotubes. *J Appl Phys* 2008;103. 023511-1-16.
- [10] Challamel N, Zhang Z, Wang CM, Reddy JN, Wang Q, Michelitsch T, et al. On nonconservativeness of Eringen's nonlocal elasticity in beam mechanics: correction from a discrete-based approach. *Arch Appl Mech* 2014;84:1275–92.
- [11] Fernández-Sáez J, Zaera R, Loya JA, Reddy JN. Bending of Euler–Bernoulli beams using Eringen's integral formulation: a paradox resolved. *Int J Eng Sci* 2016;99:107–16.
- [12] Wang CM, Zhang YY, Xiang Y, Reddy JN. Recent studies on buckling of carbon nanotubes. *Appl Mech Rev* 2010;63:030804–18.
- [13] Shima H. Buckling of carbon nanotubes: a state of the art review. *Materials* 2012;5:47–84.
- [14] Eltaher MA, Khater ME, Emam SA. A review on nonlocal elastic models for bending, buckling, vibrations, and wave propagation of nano scale beams. *Appl Math Model* 2015;00:1–20.
- [15] Senthilkumar V. Buckling analysis of a single-walled carbon nanotube with nonlocal continuum elasticity by using differential transform method. *Adv Sci Lett* 2010;3:337–40.
- [16] Pradhan S, Reddy GK. Buckling analysis of single walled carbon nanotube on Winkler foundation using nonlocal elasticity theory and DTM. *Comput Mater Sci* 2011;50:1052–6.
- [17] Ansari R, Sahmani S, Rouhi H. Rayleigh–Ritz axial buckling analysis of single-walled carbon nanotubes with different boundary conditions. *Phys Lett A* 2011;375:1255–63.
- [18] Hosseini-Ara R, Mirdamadi HR, Khademyzadeh H. Buckling analysis of short carbon nanotubes based on a novel Timoshenko beam model. *J Theor Appl Mech* 2012;50:975–86.
- [19] Xu SP, Xu MR, Wang CM. Stability analysis of nonlocal elastic columns with initial imperfection. *Math Prob Eng* 2013;2013:12. Article ID 341232.
- [20] Wang GW, Zhao YP, Yang GT. The stability of a vertical single-walled carbon nanotube under its own weight. *Mater Des* 2004;25:453–7.
- [21] Mustapha KB, Zhong ZW. Stability of single-walled carbon nanotubes and single-walled carbon nanocones under self-weight and an axial tip force. *Int J Eng Sci* 2012;50:268–78.
- [22] Glück J. The buckling load of an elastically supported cantilevered column with continuously varying cross section and distributed axial load. *Ing Arch* 1973;42:355–9.
- [23] Eisenberger M. Buckling loads for variable cross-section members with variable axial forces. *Int J Solids Struct* 1991;27(2):135–44.
- [24] Lee K. Buckling of fibers under distributed axial load. *Fibers Polym* 2008;9(2):200–2.
- [25] Wang CM, Wang CY, Reddy JN. Exact solutions for buckling of structural members. Florida, Boca Raton: CRC Press; 2004.
- [26] Li QS. Exact solutions for the generalized Euler's problem. *J Appl Mech* 2009;76. 041015-1-041015-9.
- [27] Li X-F, Xi L-Y, Huang Y. Buckling load of tapered fibers subjected to axially distributed load. *Fibers Polym* 2010;11:1193–7.
- [28] Wei D, Yan S, Zhang Z, Li X. Critical load for buckling of non-prismatic columns under self weight and tip force. *Mech Res Commun* 2010;37(6):554–8.
- [29] Sun D-L, Li X-F, Wang CY. Buckling of standing tapered Timoshenko columns with varying flexural rigidity under combined loadings. *Int J Struct Stab Dyn* 2016;16:1550017. 14 pages.
- [30] Leipholz H, Bhalla K. On the solution of the stability problems of elastic rods subjected to triangularly distributed tangential follower forces. *Ing Arch* 1977;46:115–24.
- [31] Sugiyama Y, Mladenov KA. Vibration and stability of elastic columns subjected to triangularly distributed sub-tangential forces. *J Sound Vib* 1983;88:447–57.
- [32] Ryu BJ, Sugiyama Y, Yim KB, Lee GS. Dynamic stability of an elastically restrained column subjected to triangularly distributed subtangential forces. *Comput Struct* 2000;76:611–9.
- [33] Tabarrok B, Xiong Y. Application of a new variational formulation for stability analysis of columns subjected to distributed loads. *ZAMM Z Angew Math Mech* 1989;69:435–40.
- [34] Adali S. Variational principles for multi-walled carbon nanotubes undergoing buckling based on nonlocal elasticity theory. *Phys Lett A* 2008;372(35):5701–5.
- [35] Phadikar JK, Pradhan S. Variational formulation and finite element analysis for nonlocal elastic nanobeams and nanoplates. *Comput Mater Sci* 2010;49:492–9.
- [36] Yang Y, Lim CW. A variational principle approach for buckling of carbon nanotubes based on nonlocal Timoshenko beam models. *Nano* 2011;6(4):363–77.
- [37] Adali S. Variational formulation for buckling of multi-walled carbon nanotubes modelled as nonlocal Timoshenko beams. *J Theor Appl Mech* 2012;50(1):321–33.
- [38] Xu X-J, Deng Z-C. Variational principles for buckling and vibration of MWCNTs modeled by strain gradient theory. *Appl Math Mech (Engl Ed)* 2014;35(9):1115–28.
- [39] Reddy JN. Energy principles and variational methods in applied mechanics. Hoboken, New Jersey: John Wiley & Sons, Inc.; 2002.
- [40] Ghannadpour SAM, Mohammadi B, Fazilat J. Bending, buckling and vibration problems of nonlocal Euler beams using Ritz method. *Compos Struct* 2013;96:584–9.
- [41] Behera L, Chakraverty S. Free vibration of Euler and Timoshenko nanobeams using boundary characteristic orthogonal polynomials. *Appl Nanosci* 2014;4:347–58.
- [42] Ghannadpour SAM, Mohammadi B. Buckling analysis of micro- and nano-rods/tubes based on nonlocal Timoshenko beam theory using Chebyshev polynomials. *Adv Mater Res* 2010;123–125:619–22.
- [43] Ghannadpour SAM, Mohammadi B. Vibration of nonlocal Euler beams using Chebyshev polynomials. *Key Eng Mater* 2011;471:1016–21.
- [44] Qu Y, Long X, Li H, Meng G. A variational formulation for dynamic analysis of composite laminated beams based on a general higher-order shear deformation theory. *Compos Struct* 2013;102:175–92.
- [45] Jeffrey A, Dai H-H. Handbook of mathematical formulas and integrals. Burlington, MA, USA: Academic Press; 2008.
- [46] Pradhan SC, Phadikar JK. Bending, buckling and vibration analyses of nonhomogeneous nanotubes using GDQ and nonlocal elasticity theory. *Struct Eng Mech* 2009;33:193–213.
- [47] Duan WH, Wang M. Exact solution for buckling of columns including self-weight. *ASCE J Eng Mech* 2008;134(1):116–9.
- [48] Wang CM, Ang KK. Buckling capacities of braced heavy columns under axial loads. *Comput Struct* 1988;28(5):563–71.

**CHAPTER 9-PAPER 5:**  
**BUCKLING OF NONUNIFORM CARBON NANOTUBES UNDER**  
**CONCENTRATED AND DISTRIBUTED AXIAL LOADS WITH**  
**APPLICATION TO NANOCONES. Submitted to *Mechanics Research***  
***Communications***

<b>Mechanics Research Communications.</b> <b>Year</b>	Publication Office: <b>Elsevier UK</b>
<b>Editor-in-Chief: A. Rosato</b> New Jersey Institute of Technology, Newark, New Jersey, USA Anthony.Rosato@njit.edu	

# Buckling of nonuniform carbon nanotubes under concentrated and distributed axial loads with applications to nanocones

Mouafo Teifouet Armand Robinson<sup>a,b</sup> and Sarp Adali<sup>a,\*</sup>

<sup>a</sup>*Discipline of Mechanical Engineering, University of KwaZulu-Natal, Durban 4041, South Africa*

<sup>b</sup>*Department of Physics, University of Dschang, Cameroon*

\* e-mail address: adali@ukzn.ac.za

Corresponding author. Tel.: +27 31 2603203

## Abstract

Buckling of nonuniform carbon nanotubes are studied with the axial load taken as a combination of concentrated and axially distributed loads. Distributed axial loads are specified as uniformly distributed and triangularly distributed. Nonlocal continuum modelling of the carbon nanotubes is implemented to obtain the governing equations. The solution is obtained by employing a weak formulation of the problem and the Rayleigh-Ritz method which is implemented using orthogonal Chebyshev polynomials. Counter plots are given of the buckling loads for a combination of simply supported, clamped and free boundary conditions.

© 2016 The Authors. Published by Elsevier Ltd.

*Keywords:* Nonuniform nanotubes; Buckling of nanotubes; Distributed axial loads; Nonlocal model .

## 1. Introduction

Superior properties of carbon nanotubes (CNT) led to their use in a number of technologically advanced fields such as biotechnology, nanocomposites and nanoelectronics. Even though CNTs have high stiffness and large failure strain, they are prone to buckling under compressive loads due to their slenderness which results in limiting their use in applications involving compressive axial loads. Thus, in many applications of CNTs, buckling is of primary interest as this could be the dominant failure mode. Such applications include nano-mechanical devices, drug delivery and nanocomposites. This resulted in buckling of CNTs being an active area of research for a number of years and the subject has been investigated extensively due to its importance [1-3]. Recent works on the buckling of CNTs with uniform cross-sections include [4-8]. In particular, stability of CNTs under its own weight has been studied in [9-11] and under distributed axial loads in [12]. Nonuniform CNTs are employed in the design of nanostructures such as nanoscale sensors and actuators and their vibration characteristics have been studied in [13-16]. Studies on the buckling of nonuniform nanotubes seem to have been restricted to nanocones which are of interest in

atomic force microscopy and electroanalysis [17, 18] as the tip structure of nanocones can be used to achieve mechanical properties which cannot be obtained by uniform nanotubes. A number of studies have been directed to elucidating the mechanical and physical properties of nanocones [19, 20]. Buckling and post-buckling behaviors of nanocones have been studied in [21, 22]. Molecular mechanics was employed in [23] to investigate the buckling behavior of nanocones and a computational approach was used in [24] to compute the buckling loads of nanocones. Buckling of nanocones under self weight and concentrated loads have been studied in [25].

Present study involves the buckling of nonuniform nanotubes under variable axial loads employing a nonlocal continuum model and extends the results of [12] to nonuniform nanotubes. Axial loads acting on the nanotube are a combination of concentrated and distributed loads. Distributed loads can be uniform corresponding to self-weight or triangular. The method of solution involves the weak variational formulation of the problem and employing the Rayleigh-Ritz method using orthogonal Chebyshev polynomials. Numerical results are given for various combination of boundary conditions to study the effect of small-scale parameter on buckling.

**2. Problem formulation**

We consider a nonuniform single-walled carbon nanotube of length  $L$  and cross sectional area  $A(x)$ . A combination of compressive axial loads  $P$  (concentrated load) and  $q(x)$  (distributed load) act on the nanotube as shown in Fig. 1.

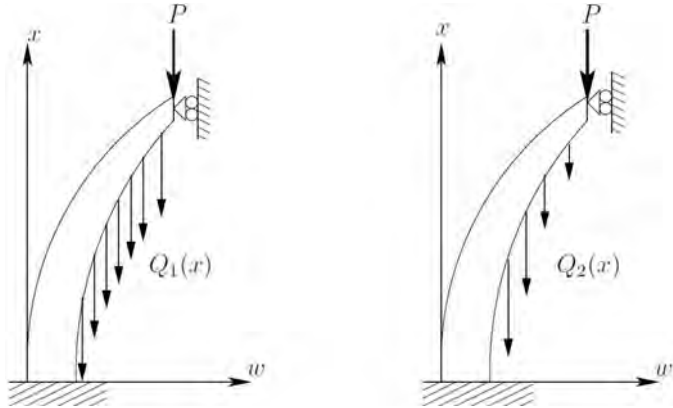


**Fig. 1.** Columns under tip loads distributed axial loads

Distributed loads can be uniformly distributed given by  $Q_1(x) = \bar{q}_1(L - x)$  (Fig. 1a) or triangularly distributed given by  $Q_2(x) = \frac{1}{2}\bar{q}_2(L - x)^2$  (Fig. 1b). The axial load can be expressed as

$$N_i(x) = P + Q_i(x), \quad 0 \leq x \leq L \tag{1}$$

The equation governing the buckling of a nanotube is in terms of moment  $M(x)$  and deflection  $w(x)$  can be expressed as

$$M'' - (N_i(x)w')' = 0 \tag{2}$$

where a prime denotes differentiation with respect to  $x$ . The constitutive relation based on nonlocal Euler-Bernoulli theory is given by

$$M - (e_0a)^2 M'' = -EI(x)w'' \tag{3}$$

where  $e_0a$  is the small scale parameter,  $E$  is the Young's modulus and  $I(x)$  is the moment of inertia of the nonuniform cross-section. Combining Eqs. (2) and (3), we obtain  $M(x)$  as

$$M = -EI(x)w'' + (e_0a)^2 (N_i(x)w')' \tag{4}$$

From Eqs. (2) and (4), the differential equation governing the buckling of a nonuniform nanotube can be obtained as

$$D(w) = (EI(x)w'')'' + (N_i w')' - (e_0a)^2 (N_i' w' + N_i w'')'' = 0 \tag{5}$$

where  $N_i = N_i(x)$  and  $N_i' = dN_i / dx$ . The weak form of Eq. (5) can be derived by noting that

$$\int_0^L D(w) w \, dx = 0 \tag{6}$$

Eq. (6) is expressed as

$$\sum_{i=1}^4 U_i(w) = 0 \tag{7}$$

where

$$U_1(w) = \int_0^L (EI(x)w'')'' w \, dx, \quad U_2(w) = \int_0^L (N_i w')' w \, dx \tag{8}$$

$$U_3(w) = -(e_0a)^2 \int_0^L (N_i' w')'' w \, dx \tag{9a}$$

$$U_4(w) = -(e_0a)^2 \int_0^L (N_i w'')'' w \, dx \tag{9b}$$

Expressions for  $U_i(w)$  are transformed to integral and boundary terms by integration by parts, viz.,

$$U_1(w) = \int_0^L EI(x)(w'')^2 \, dx + \left[ (EI(x)w'')' w - EI(x)w''w' \right]_{x=0}^{x=L} \tag{10}$$

$$U_2(w) = -\int_0^L N_i (w')^2 \, dx + N_i w'w \Big|_{x=0}^{x=L} \tag{11}$$

$$U_3(w) = -(e_0a)^2 \int_0^L N_i' w'w'' \, dx - (e_0a)^2 \left[ (N_i'w')' w - N_i'w''w' \right]_{x=0}^{x=L} \tag{12}$$

$$U_4(w) = -(e_0a)^2 \int_0^L N_i w''^2 \, dx - (e_0a)^2 \left[ (N_i w'')' w - N_i w''w' \right]_{x=0}^{x=L} \tag{13}$$

The moment expression is given by Eq. (4) and the shear force by

$$V(x) = (EI(x)w'')' + N_i w' - (e_0a)^2 \left[ (N_i'w')' + (N_i w'')' \right] \tag{14}$$

Then Eq. (7) can be expressed as

$$\int_0^L \left\{ EI(x)w''^2 - N_i w'^2 - (e_0a)^2 \left[ N_i' w'w'' + N_i w''^2 \right] \right\} dx + (V(x)w + M(x)w') \Big|_{x=0}^{x=L} = 0 \tag{15}$$

where  $M(x)$  and  $V(x)$  are defined by Eqs. (4) and (14), respectively. Boundary conditions for various cases can be expressed as follows:

Simply supported boundary conditions:

$$w(0) = 0, \quad M(0) = 0, \quad w(L) = 0, \quad M(L) = 0 \tag{17}$$

Clamped-clamped boundary conditions:

$$w(0) = 0, \quad \frac{dw}{dx} \Big|_{x=0} = 0, \quad w(L) = 0, \quad \frac{dw}{dx} \Big|_{x=L} = 0 \tag{18}$$

Clamped-simply supported boundary conditions:

$$w(0) = 0, \quad \frac{dw}{dx} \Big|_{x=0} = 0, \quad w(L) = 0, \quad M(L) = 0 \tag{19}$$

Clamped-free supported boundary conditions:

$$w(0) = 0, \quad \left. \frac{dw}{dx} \right|_{x=0} = 0, \quad M(L) = 0, \quad V(L) = 0 \quad (20)$$

Let  $I(x) = I_0 g(x)$  where  $I_0$  is a dimensional reference constant and  $g(x)$  is a nondimensional function of  $x$ . Nondimensional form of the formulation can be obtained by introducing the dimensionless variables defined as

$$X = \frac{x}{L} \quad W = \frac{w}{L} \quad \mu = \frac{e_0 a}{L} \quad p = \frac{PL^2}{EI_0}$$

$$q_i = \frac{\bar{q}_i L^{2+i}}{EI_0} \quad n_i = \frac{N_i L^2}{EI_0} \quad (21)$$

Nondimensional form of eq. (16) can be expressed as

$$\int_0^1 \left\{ g(X) W''^2 - \eta_i W'^2 - \mu^2 \left[ \eta_i' W' W'' + \eta_i W''^2 \right] \right\} dX$$

$$+ (v(X)W + m(X)W') \Big|_{X=0}^{X=1} = 0 \quad (22)$$

where

$$m(X) = \frac{L}{EI_0} M = -g(X)W'' + \mu^2 (n_i W')' \quad (23)$$

$$v(X) = \frac{L^2}{EI_0} V(x) = (g(X)W'')' + \eta_i W'$$

$$- \mu^2 \left[ (\eta_i' W')' + (\eta_i W'')' \right] \quad (24)$$

$$n_2(X) = p + \frac{1}{2} q_2 (1-X)^2, \quad n_1(X) = p + q_1 (1-X) \quad (25)$$

### 3. Method of solution

To obtain the solution by Rayleigh-Ritz method as outlined in [26], Chebyshev polynomials are introduced to approximate the deflection  $W(X)$ . Geometric boundary conditions are satisfied by multiplying the polynomials by suitable functions [27-30] and  $W(X)$  is expressed as

$$W(X) = X^r (1-X)^s \sum_{j=1}^N c_j f_{j-1}(X) \quad (26)$$

where  $r$  and  $s$  take the values 0, 1 or 2 for free, simply supported and clamped boundaries, respectively. Parameters  $c_j$  are determined as part of the solution of an eigenvalue problem which yields the buckling load as the minimum eigenvalue. In eq. (26),  $f_j(X)$  is the  $j^{th}$  Chebyshev polynomial with  $f_0(X) = 1$  and  $f_1(X) = X$ . The remaining terms are obtained from

$$f_{j+1}(X) = 2X f_j(X) - f_{j-1}(X) \quad (27)$$

To verify the accuracy of the present method, it was applied to the buckling of a nonuniform column subject to a tip load only, i.e.,  $p > 0$  and  $q(x) = 0$ , as given in [32]. The column has a square cross-section and its stiffness is given by  $EI(x) = EI_0(1 - \beta x^4)$  [32]. The results are given in Table 1.

It is observed that the present method implemented by using Chebyshev polynomials give accurate results. Next the method is applied to columns subject to distributed axial loads and the results are shown in Table 2. The present method is observed to be accurate also in the case of buckling with distributed axial loads.

**Table 1:** Comparison of buckling loads  $p$  ( $q(x) = 0$ ) with existing results for four boundary conditions with  $EI(x) = EI_0(1 - \beta x^4)$  and  $\mu = 0$  (local beam).

$\beta$	S-S		C-S		C-C		C-F	
	Present	Ref. [32]						
0.0	9.869	9.870	20.191	20.191	39.478	39.478	2.467	2.467
0.2	6.317	6.317	12.922	12.922	25.266	25.266	1.883	1.884
0.4	3.553	3.553	7.269	7.269	14.212	14.212	1.309	1.309
0.6	1.579	1.579	3.231	3.230	6.317	6.316	0.7567	0.757
0.8	0.398	0.395	0.815	0.807	1.583	1.547	0.265	0.265

### 4. Numerical results

Numerical results are given for the boundary conditions SS, CS, CC and CF which are given by Eqs. (17)-(20). The range of the small scale parameter  $\mu$  is taken as  $0 \leq \mu \leq 0.4$ . The cross-section is specified as a square and the moment of inertia is taken as  $I(x) = I_0(1 - \beta x^4)$ . The contour plots of the buckling load  $p$  with respect to  $\mu$  and  $\beta$  are shown in Fig. 2 for simply supported and clamped-hinged nanocolumns. It is observed that the buckling load decreases as the small-scale parameter increases. The corresponding results for uniformly distributed axial load and triangularly distributed axial load are shown in Fig. 3 and Fig. 4, respectively. It is observed that, the effect of the non-uniformity parameter  $\beta$  on the buckling load is more pronounced for the concentrated load  $p$ .

Next the buckling under the combined axial loads of a concentrated load  $p$  and a distributed load is investigated. Contour plots for the buckling load  $q_1$  corresponding to the uniformly distributed axial load are given in Fig. 5 with respect to  $p$  and  $\beta$  for simply supported and clamped-hinged nanocolumns and in Fig. 6 for clamped-clamped and clamped-free nanocolumns with  $\mu = 0.1$ . Corresponding results for  $q_2$  (triangularly distributed axial load) are given in Figs. 7 and 8. Figs. 5-8 show the numerical differences in the buckling loads in the case of uniformly and triangularly distributed axial loads for nonuniform nanocolumns. The effect of the boundary conditions on the buckling loads can be observed from these figures. Buckling parameters  $q_1$  and  $q_2$  are least affected by the change in the stiffness  $EI(x)$  as indicated by  $\beta$  in the case of clamped-free columns (Figs. 6b and 8b) and most affected in the case of clamped-clamped

columns (Figs. 6a and 8a). Similarly, the buckling loads  $q_1$  and  $q_2$  decrease most by an increase in the tip load  $p$  in the case of clamped-free columns as expected (Figs. 6b and 8b). In fact  $q_1$  and  $q_2$  become negative, i.e., change from

compression to tension, above a certain value of  $p$  (Figs. 6b and 8b).

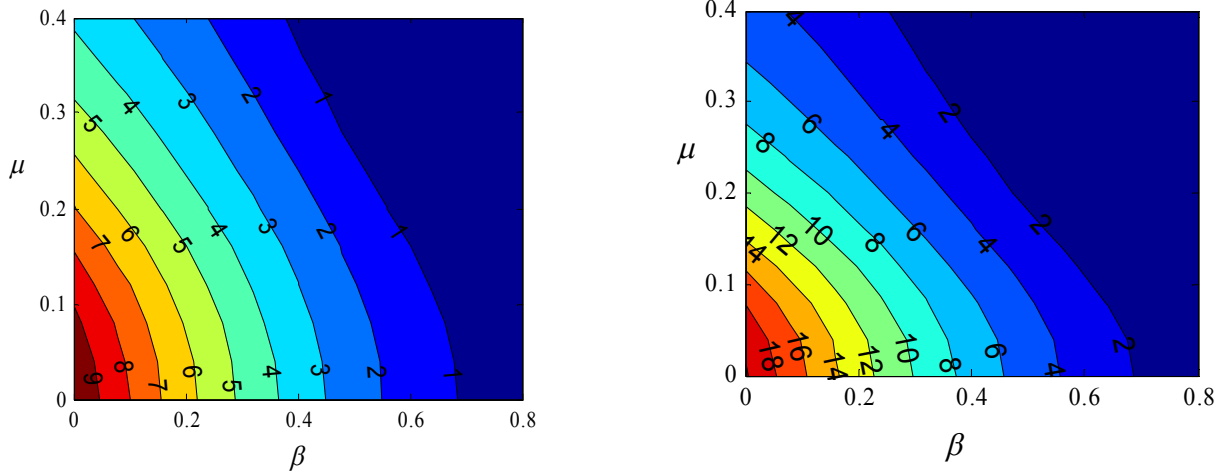


Fig. 2. Contour plot of  $p$  with respect to  $\beta$  and  $\mu$ , a) SS, b) CS

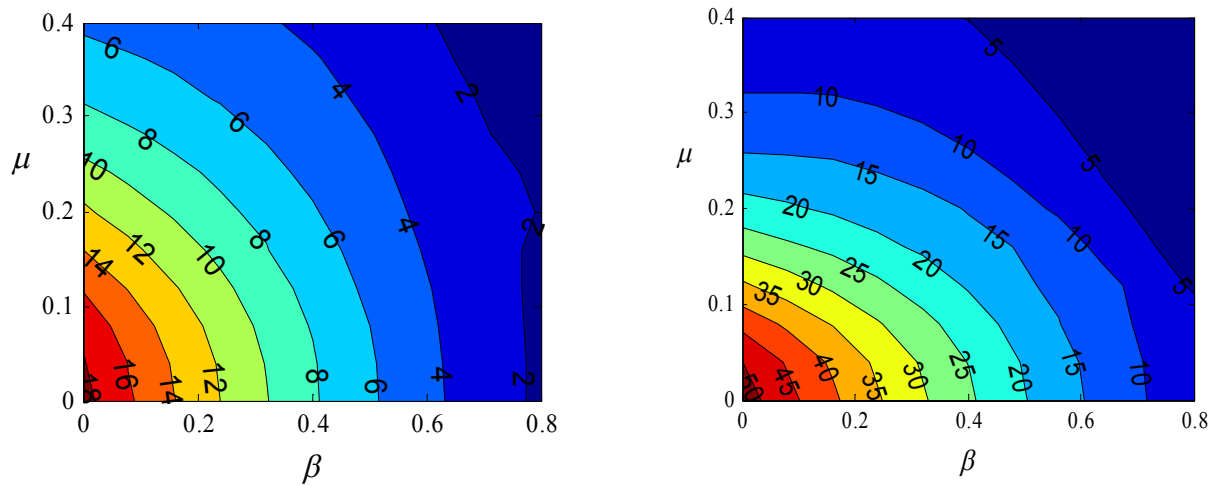


Fig. 3. Contour plot of  $q_1$  with respect to  $\beta$  and  $\mu$ , a) SS, b) CS

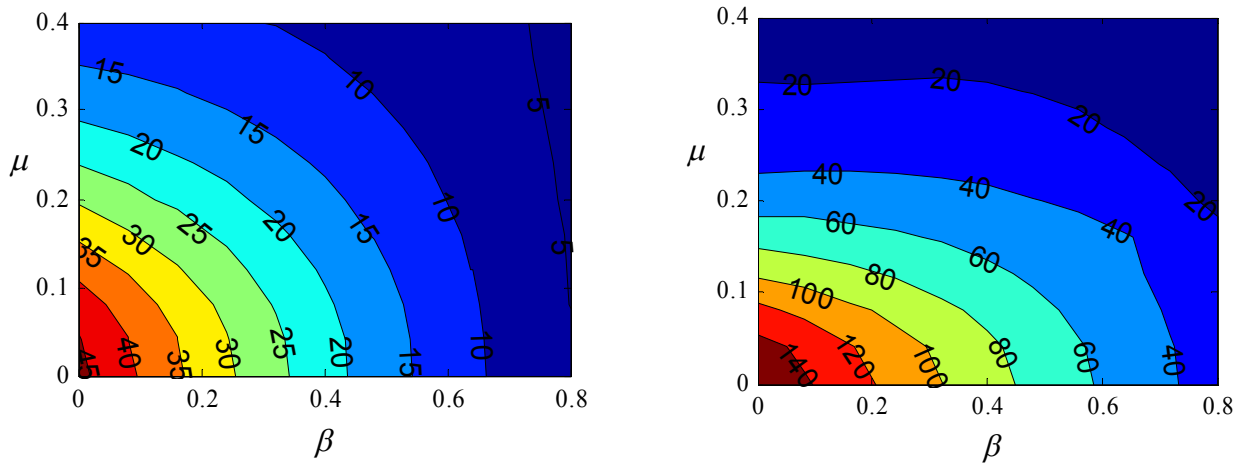


Fig. 4. Contour plot of  $q_2$  with respect to  $\beta$  and  $\mu$ , a) SS, b) CS

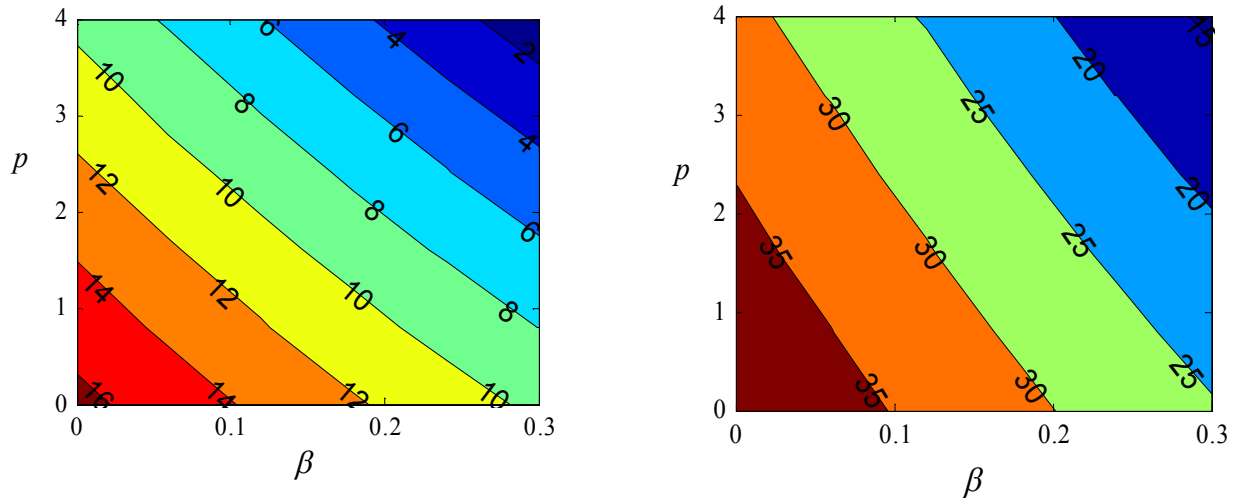


Fig. 5. Contour plot of  $q_1$  with respect to  $\beta$  and  $p$  with  $\mu = 0.1$ , a) SS, b) CS

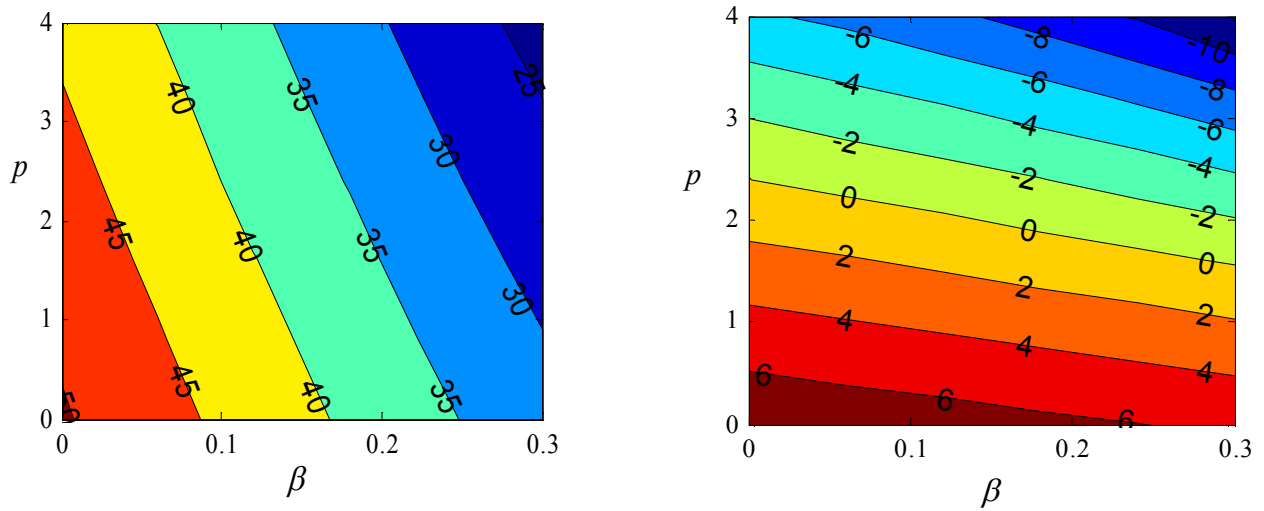


Fig. 6. Contour plot of  $q_1$  with respect to  $\beta$  and  $p$  with  $\mu = 0.1$ , a) CC, b) CF

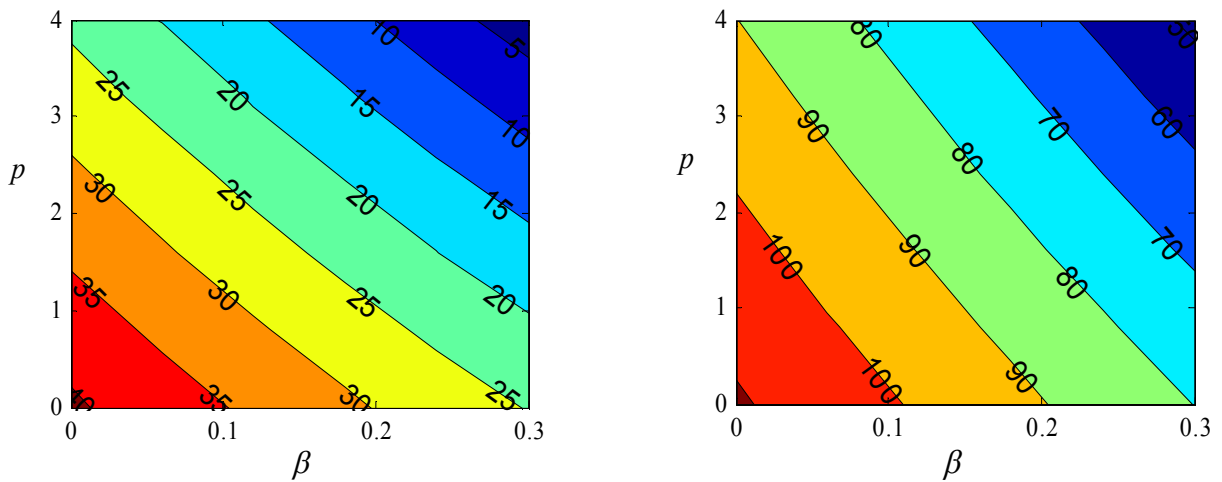


Fig. 7. Contour plot of  $q_2$  with respect to  $\beta$  and  $p$  with  $\mu = 0.1$ , a) SS, b) CS

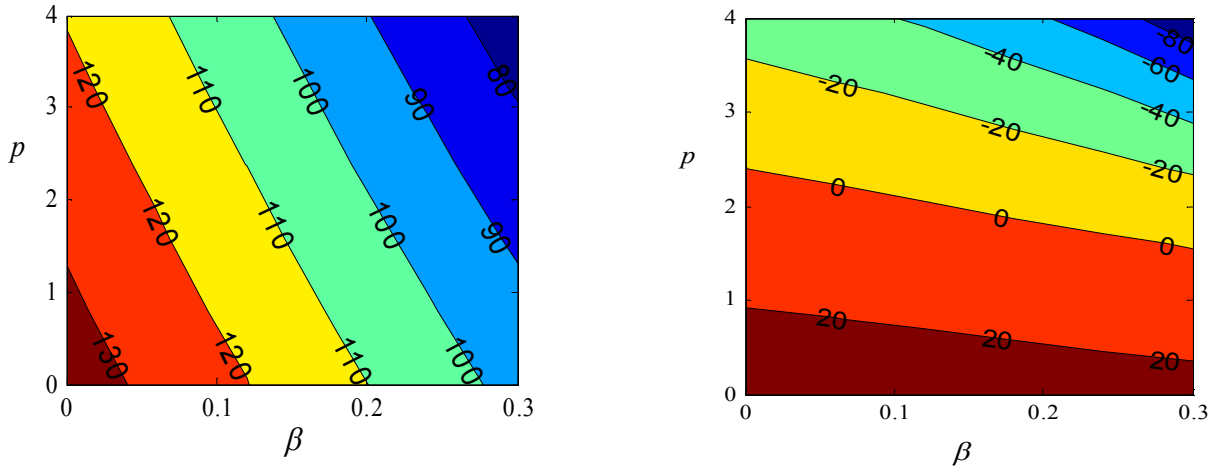


Fig. 8. Contour plot of  $q_2$  with respect to  $\beta$  and  $p$  with  $\mu = 0.1$ , a) CC, b) CF

4.1. Application to horn-shaped nanotubes

Cross-sectional shape of a horn-shaped nanotube of constant wall thickness  $\delta$  is defined as a circle with radius  $r$  which varies linearly from  $r_0$  to  $r_L$ . Thus the moment of inertia of the nanohorn is given by  $I = I_0 g(X)$  where  $g(X)$  is

$$g(X) = \frac{\pi}{4} \left[ \left( 1 - \left( 1 - \frac{r_L}{r_0} \right) X + \frac{\delta}{2r_0} \right)^4 - \left( 1 - \left( 1 - \frac{r_L}{r_0} \right) X - \frac{\delta}{2r_0} \right)^4 \right] \tag{28}$$

and  $r_0 \leq X \leq r_0 + \delta = r_L$ . This nonuniform cross-section is the same as the cross-section of the nanohorn studied in [33]. Numerical results are given for  $r_0 = 0.8$  nm and  $\delta = 0.34$  nm for concentrated and uniformly distributed axial loads. Buckling loads for simply supported nanotubes are plotted

against  $r_L / r_0$  in Fig. 9 for various values of the small scale parameter  $\mu$ . Corresponding results for clamped-simply supported nanotubes are given in Fig. 10. It is observed that the increase in the buckling load is steeper in the case of the concentrated tip load  $p$  as  $r_L / r_0$  increases (Figs. 9a and 10a) as compared to the increase in the buckling parameter  $q_1$  of the distributed load indicating higher sensitivity of  $p$  to non-uniformity of the cross-section. The effect of the small scale parameter on the buckling load is shown in Fig. 11 for simply supported nanotubes for various values of  $r_L / r_0$ . The corresponding results for clamped-simply supported nanotubes are given in Fig. 12. It is observed that small scale parameter  $\mu$  reduces the buckling load but its effect tapers off as  $\mu$  becomes larger. Buckling load due to  $p$  is observed to be more sensitive to small scale parameter  $\mu$ .

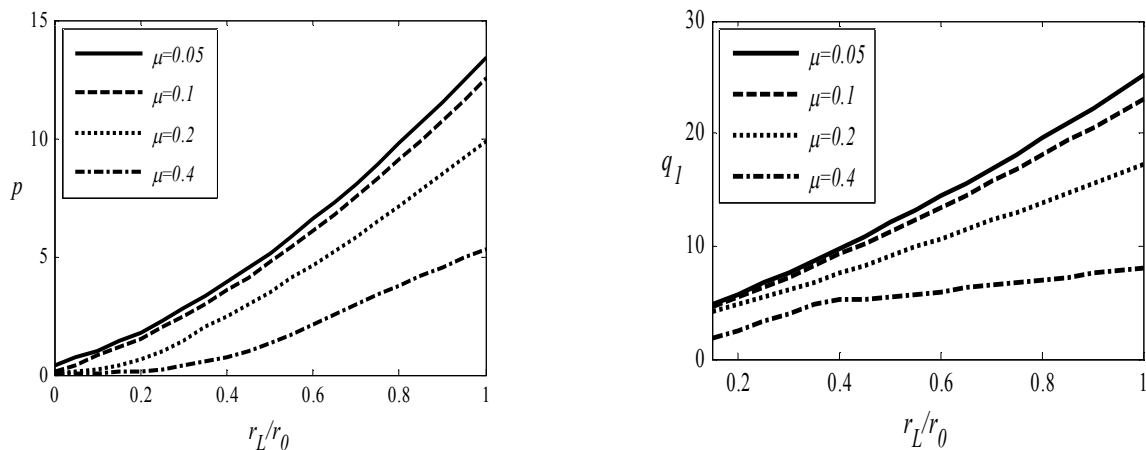
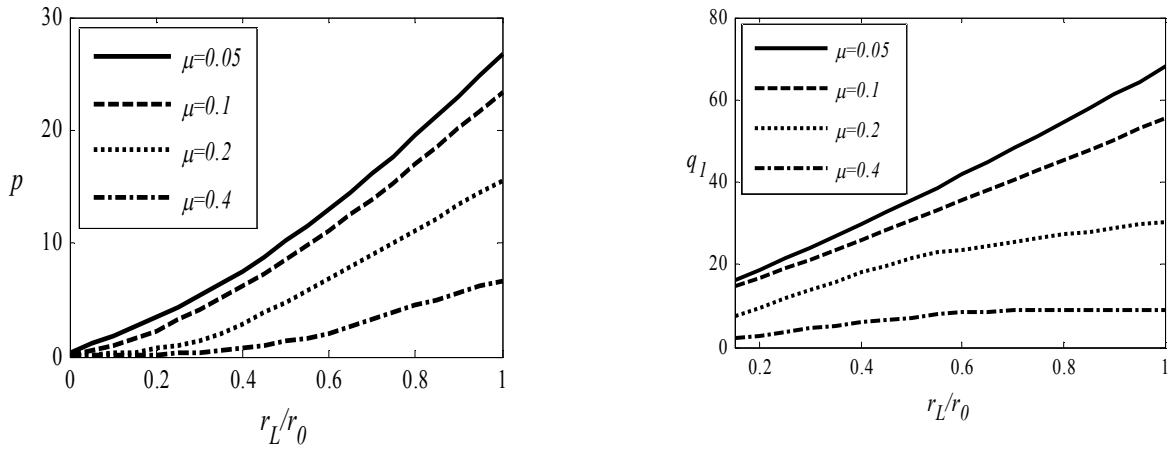
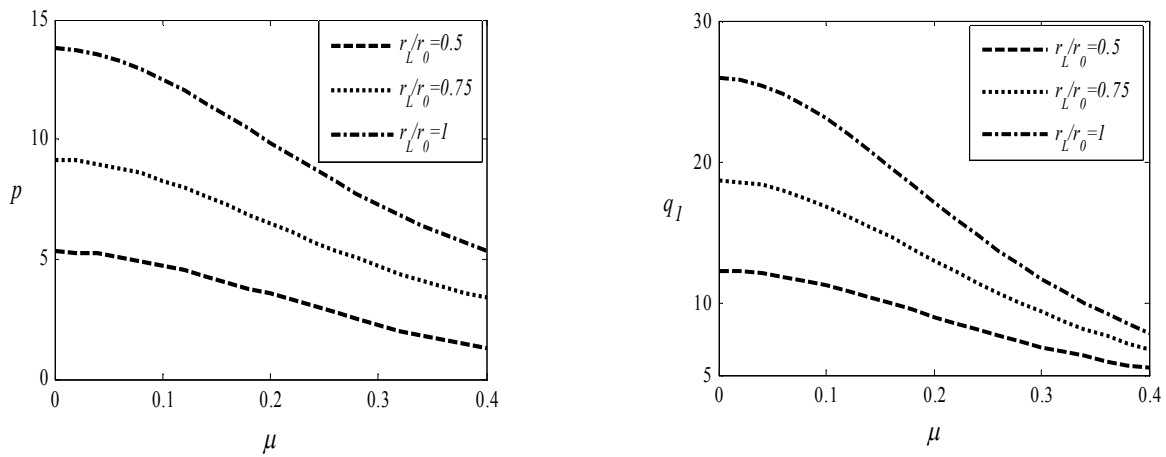


Fig. 9. Buckling loads plotted against the ratio of radii for SS nanotubes for different values of  $\mu$ , a) tip load  $p$ , b) uniformly distributed load  $q_1$



**Fig. 10.** Buckling loads plotted against the ratio of radii for CS nanotubes for different values of  $\mu$ , a) tip load  $p$ , b) uniformly distributed load  $q_1$



**Fig. 11.** Buckling loads plotted against the small scale parameter for SS nanotubes for different ratios of radii, a) tip load  $p$ , b) uniformly distributed load  $q_1$

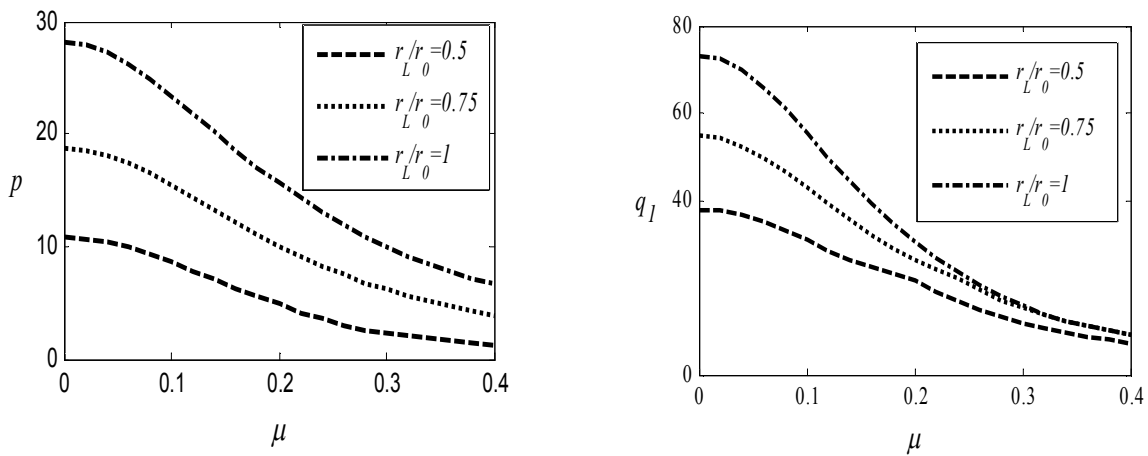


**Fig. 12.** Buckling loads plotted against the small scale parameter for CS nanotubes for different ratios of radii, a) tip load  $p$ , b) uniformly distributed load  $q_1$

## 5. Conclusions

Buckling of nonuniform nanotubes subject to concentrated and variable axial loads was studied. In particular, uniformly distributed and triangularly distributed axial loads and nonuniform shapes with moment of inertia proportional to  $(1-\beta X)^4$  were investigated. The results are obtained by Rayleigh-Ritz method employing Chebyshev polynomials of first kind as the approximating functions for a combination of simply supported, clamped and free boundary conditions. The accuracy of the method was verified by comparing the solutions with available results in the literature.

The effects of non-uniformity of the cross-section and the small-scale parameter on the buckling loads were investigated by means of contour plots. These plots indicate the sensitivity of the buckling loads to problem parameters and it was observed that buckling load under concentrated tip load is more sensitive to the change in the cross-section. On the other hand buckling load is more sensitive to the magnitude of the tip load for the clamped-free boundary conditions.

## Acknowledgement

The research reported in this paper was supported by research grants from the University of KwaZulu-Natal (UKZN) and from National Research Foundation (NRF) of South Africa. The authors gratefully acknowledge the supports provided by UKZN and NRF.

## References

- [1] I. Elishakoff, D. Pentaras, K. Dujat, C. Versaci, G. Muscolino, J. Storch, S. Bucas, N. Challamel, T. Natsuki, Y.Y. Zhang, C.M. Wang, G. Ghyselinck, Carbon Nanotubes and Nanosensors: Vibrations, Buckling and Ballistic impact, ISTE, London and John Wiley, New Jersey, 2012.
- [2] H. Shima, Buckling of carbon nanotubes: A state of the art review, *Materials*, 5 (2012) 47-84.
- [3] C.M. Wang, Y.Y. Zhang, Y. Xiang, J.N. Reddy, Recent studies on buckling of carbon nanotubes, *Appl. Mech. Reviews* 63 (2010) 030804–030818.
- [4] S. Pradhan, G.K. Reddy, Buckling analysis of single walled carbon nanotube on Winkler foundation using nonlocal elasticity theory and DTM, *Comput. Mater. Sci.* 50 (2011) 1052–56.
- [5] R. Ansari, S. Sahmani, H. Rouhi, Rayleigh–Ritz axial buckling analysis of single-walled carbon nanotubes with different boundary conditions, *Physics Letters A* 375 (2011) 1255–1263.
- [6] R. Hosseini-Ara, H.R. Mirdamadi, H. Khademyzadeh, Buckling analysis of short carbon nanotubes based on a novel Timoshenko beam model, *J. Theoretical Appl. Mech.* 50 (2012) 975-986.
- [7] M. Zidour, T. H. Daouadji, K. H. Benrahou, A. Tounsi, El A. Adda Bedia, and L. Hadji, Buckling analysis of chiral single-walled carbon nanotubes by using the nonlocal Timoshenko beam theory, *Mech. Composite Mat.* 50 (2014) 95-104.
- [8] F. Ebrahimi, G.R. Shaghghi, M. Boreiry, A semi-analytical evaluation of surface and nonlocal effects on buckling and vibrational characteristics of nanotubes with various boundary conditions, *Int. J. Struct. Stability Dynamics*, 16 (2016) 1550023 (20 pages).
- [9] G.W. Wang, Y.P. Zhao, G.T. Yang, The stability of a vertical single-walled carbon nanotube under its own weight, *Mater. Des.* 25 (2004) 453–457.
- [10] K.B. Mustapha, Z.W. Zhong, Stability of single-walled carbon nanotubes and single-walled carbon nanocones under self-weight and an axial tip force, *Int. J. Eng. Sci.* 50 (2012) 268–278.
- [11] C.M. Wang, H. Zhang, N. Challamel, Y. Xiang, Buckling of nonlocal columns with allowance for selfweight, *ASCE J. Eng. Mech.* (2016) 04016037.
- [12] M.T.A. Robinson, S. Adali, Variational solution for buckling of nonlocal carbon nanotubes under uniformly and triangularly distributed axial loads, *Compos. Struct.* (2016).
- [13] T. Murmu, S.C. Pradhan, Small-scale effect on the vibration of nonuniform nano cantilever based on nonlocal elasticity theory, *Physica E* 41 (2009) 1451–1456.
- [14] H.L. Lee, W.J. Chang, Surface and small-scale effects on vibration analysis of a nonuniform nanocantilever beam, *Physica E* 43(1) (2010) 466–469.
- [15] H.-L. Lee, W.-J. Chang, Surface effects on axial buckling of nonuniform nanowires using non-local elasticity theory, *Micro Nano Letters*, 6 (2011) 19–21.
- [16] H.L. Tang, Z.B. Shen, D.K. Li, Vibration of nonuniform carbon nanotube with attached mass via nonlocal Timoshenko beam theory, *J. Mech. Sci. Technol.* 28 (2014) 3741–3747.
- [17] C. Chen, L.H. Chen, X. R. Ye, C. Daraio, S. Jin, C.A. Orme, A. Quist, R. Lal, Extreme sharp carbon nanocone probe for atomic force microscopy imaging, *Appl. Physics Letters*, 88 (2006) 153102.
- [18] J. Sripirom, S. Noor, U. Köhler, A. Schulte, Easy made and handled carbon nanocones for scanning tunneling microscopy and electroanalysis, *Carbon*, 49 (2011) 2402-2412.
- [19] J.X. Wei, K.M. Liew, X.Q. He, Mechanical properties of carbon nanocones. *Appl. Physics Letters*, 91 (2007) 261906.
- [20] R. Ansari, E. Mahmoudinezhad, Characterizing the mechanical properties of carbon nanocones using an accurate spring-mass model, *Comput. Mat. Sci.* 101 (2015) 260-266.
- [21] K.M. Liew, J.X. Wei, X.Q. He, Carbon nanocones under compression: Buckling and post-buckling behaviors, *Physical Review B*, 75 (2007) 195435.
- [22] J.W. Yan, K.M. Liew, L.H. He, Buckling and post-buckling of single-wall carbon nanocones upon bending, *Comp. Struct.* 106 (2013) 793-798.
- [23] M.M.S. Fakhraabadi, N. Khani, R. Omidvar, A. Rastgoo, Investigation of elastic and buckling properties of carbon nanocones using molecular mechanics approach, *Comput. Mat. Sci.* 61 (2012) 248–256.
- [24] J.W. Yan, K.M. Liew, L.H. He, A mesh-free computational framework for predicting buckling behaviors of single-walled carbon nanocones under axial compression based on the moving Kriging interpolation, *Comput. Methods Appl. Mech. Eng.* 247–248 (2012) 103-112.
- [25] C. M. Wang, H. Zhang, N. Challamel, Y. Xiang, Buckling of Nonlocal Columns with Allowance for Selfweight, *ASCE J. Eng. Mech.* 04016037 (20 pages)
- [26] Reddy JN. *Energy Principles and Variational Methods in Applied Mechanics*. 2002, John Wiley and Sons, Inc., Hoboken, New Jersey.
- [27] S.A.M. Ghannadpour, B. Mohammadi, Buckling analysis of micro- and nano-rods/tubes based on nonlocal Timoshenko beam theory using Chebyshev polynomials, *Adv. Mater. Res.* 123-125 (2010) 619–622.
- [28] S.A.M. Ghannadpour, B. Mohammadi, Vibration of nonlocal Euler beams using Chebyshev polynomials, *Key Eng. Mater.* 471 (2011) 1016–1021.
- [29] S.A.M. Ghannadpour, B. Mohammadi, J. Fazilati, Bending, buckling and vibration problems of nonlocal Euler beams using Ritz method, *Compos. Struct.* 96 (2013) 584–589.
- [30] L. Behera, S. Chakraverty, Free vibration of Euler and Timoshenko nanobeams using boundary characteristic orthogonal polynomials, *Appl. Nanosci.* 4 (2014) 347–358.
- [31] X.-F. Li, L.-Y. Xi, Y. Huang, Stability analysis of composite columns and parameter optimisation against buckling, *Composites: Part B* 42 (2011) 1337-1345.
- [32] D.J. Wei, S.X. Yan, Z.P. Zhang, X.-F. Li, Critical load for buckling of non-prismatic columns under self-weight and tip force, *Mechanics Research Communications* 37 (2010) 554–558.
- [33] H.-L. Tang, D.-K. Li, S.-M. Zhou, Vibration of horn-shaped carbon nanotube with attached mass via nonlocal elasticity theory, *Physica E* 56 (2014) 306–311.

## LIST OF FIGURE CAPTIONS

**Fig. 1.** Columns under tip loads distributed axial loads

**Fig. 2.** Contour plot of  $p$  with respect to  $\beta$  and  $\mu$ , a) SS, b) CS

**Fig. 3.** Contour plot of  $q_1$  with respect to  $\beta$  and  $\mu$ , a) SS, b) CS

**Fig. 4.** Contour plot of  $q_2$  with respect to  $\beta$  and  $\mu$ , a) SS, b) CS

**Fig. 5.** Contour plot of  $q_1$  with respect to  $\beta$  and  $p$  with  $\mu = 0.1$ , a) SS, b) CS

**Fig. 6.** Contour plot of  $q_1$  with respect to  $\beta$  and  $p$  with  $\mu = 0.1$ , a) CC, b) CF

**Fig. 7.** Contour plot of  $q_2$  with respect to  $\beta$  and  $p$  with  $\mu = 0.1$ , a) SS, b) CS

**Fig. 8.** Contour plot of  $q_2$  with respect to  $\beta$  and  $p$  with  $\mu = 0.1$ , a) CC, b) CF

**Fig. 9.** Buckling loads plotted against the ratio of radii for SS nanotubes for different values of  $\mu$ , a) tip load  $p$ , b) uniformly distributed load  $q_1$

**Fig. 10.** Buckling loads plotted against the ratio of radii for CS nanotubes for different values of  $\mu$ , a) tip load  $p$ , b) uniformly distributed load  $q_1$

**Fig. 11.** Buckling loads plotted against the small scale parameter for SS nanotubes for different ratios of radii, a) tip load  $p$ , b) uniformly distributed load  $q_1$

**Fig. 12.** Buckling loads plotted against the small scale parameter for CS nanotubes for different ratios of radii, a) tip load  $p$ , b) uniformly distributed load  $q_1$

## CHAPTER 10 : CONCLUSION AND FUTURE PROSPECTS

### 10.1-Conclusion

The main aim of the present work was to study the effect of distributed follower forces on the dynamic stability of viscoelastic rectangular plates and the effect of axial and point loads on the buckling of carbon nanotubes modelled as nonlocal nanobeams. For plate, differential quadrature method was employed whereas for the study of the buckling of nanobeams, Rayleigh-Ritz method was used. For both cases the obtained results were compared with those available in the literature with good satisfaction. The present chapter presents firstly the main results obtained in each paper and secondly the resulting prospective research topics.

In paper 1, the nonconservative stability of viscoelastic rectangular plate under uniform follower force was studied. Kelvin-Voigt model for viscoelastic materials was used for the stress-strain relation of the plate. The constitutive equation of vibration of the viscoelastic rectangular plate was determined, and it depends on several parameters such as plate dimensions, Young's modulus, Poisson's coefficient, transverse displacement and viscoelastic coefficient. The assumption that the plate was undergoing harmonic vibrations permitted the elimination of the time in the final equation. The space and frequency dependent equation was solved by the method of differential quadrature. Here the considered boundary conditions of the plate was one edge clamped and three others free (CFFF), two opposite edges free and two others simply supported (SFSF) and one edge clamped and three others simply supported (CSSS). The method of coupling boundary conditions with general equation (CBCGE) was used to introduce the boundary conditions into the problem's solution while the delta-technics was for discretization. The obtained generalized eigenvalues equation was solve with high precision. The critical loads values obtained agreed well with those calculated by others after comparisons. The graphs of frequencies versus loads were plotted for both CFFF and SFSF boundaries. The CFFF plate presented only the coupled mode flutter instability which disappears when the delay time increases while the SFSF presented the static instability. The aspect ratio appeared to qualitatively increase the critical values of loads without changing the nature of the instability.

Remark: The results presented in this paper were original as, no works was done previously, concerning the differential quadrature discretization of viscoelastic rectangular plate with

free edges. The results obtained here agreed well when compared to the existing ones. This is the reason why the same numerical method was used in the Papers 2 and 3

In paper 2, the stability of nonconservative viscoelastic rectangular plates subjected to triangularly distributed tangential follower loads was studied, extending the results of paper 1. The boundary conditions were simply supported (SSSS) and two opposite edges clamped and others simply supported (CSCS). After the derivation of the equation of vibration exactly as it was done in the paper 1, DQM is used to solve the generalized eigenvalue equation and the main observations were that, the simply supported plate presented divergence instability while the plate with two opposite edges simply supported and others clamped underwent flutter instability. For SSSS plate, delay time slightly changes the imaginary part of frequency without modifying qualitatively the instability. For the CSCS plate, the increase of aspect ratio increases the value of flutter load. Also, the increase of delay time nullifies the instability apart from the aspect ratio.

Remark: The values of the critical loads obtained for the triangular follower force are higher than those obtained for the uniform follower loads. Also the increase of aspect ratio doesn't change the instability type. It was observed for CSCS plate that, for square plate, only flutter instability occurs when triangular follower force acts contrarily of mixed (flutter+dynamic) instability observed for uniform follower forces.

Paper 3 investigated the dynamic stability of viscoelastic plates under axial flow by differential quadrature method. The forces to which the plate was subjected include the fluid force and the local tensile force. The same procedure used in paper 1 and paper 2 was utilized to derive the final equation of the plate considered as a cantilever. Firstly the verification of the differential quadrature method is done for 1D problem by zeroing the aspect ratio. The results obtained were in good agreement with those available in previous works. Secondly, the effect of friction coefficient on the frequency of 1D plate was shown in details, proving that it cannot be neglected, especially when it goes up to 0.3. Finally, the instability of 2D plate was studied, by plotting the evolution of vibrating frequency vs flow velocity. For low aspect ratio, dynamic instability did not occur when the delay time was lower or equal to  $10^{-5}$  and for the first three modes of vibration. The instability appeared for high aspect ratio and only on third mode of vibration as its imaginary frequency branch was negative. When the

delay increases, the instability disappears for small aspect ratio while it is still present when the aspect ratio is greater than one.

Remark: It was shown that, laminar friction coefficient of the flowing fluid increases the critical fluid velocity, but its effect on the instability behavior is minor. Higher aspect ratios lead to single-mode flutter instability. It was found that increasing viscoelasticity can lead to divergence instability, especially for square plate.

Paper 4 investigated variational solution for the buckling of nonlocal carbon nanotubes under uniformly and triangularly distributed axial loads. The Euler-Bernoulli beam theory was used to derive the displacement field of CNTs, and Eringen nonlocal theory was employed to determine the stress-strain constitutive equations. The forces acting on the nanobeams were tip load and uniformly distributed or triangular distributed forces. The variational principle was used to derive the weak formulation of the differential equation, followed by the Rayleigh quotients and the derivation of the boundary conditions. Using the Rayleigh-Ritz method, based on the Chebyshev polynomials, characteristic equation was derived and the values of buckling loads were obtained for all three types of forces. The comparison of the obtained results and those existing in the literature was done with good satisfaction. It was observed that the increase of the nonlocal small scale parameter decreases the buckling load.

Remark: The contour plots of the distributed loads with respect to the tip load and the small scale parameter was shown. It was observed that buckling was more sensitive to the magnitude of the tip load for the clamped-free boundary conditions.

Paper 5 studied the buckling of nonuniform carbon nanotubes under concentrated and distributed axial loads with application to nanocones were carried out. we considered a nonuniform carbon nanotube with varying cross sectional area. The inertia was taken as fourth order linear polynomial and the results obtained were compared with those found in the literature. Contour plots of tip, uniformly distributed and triangularly distributed loads were plotted with respect to small scale parameter and the non-uniformity parameter for SS and CS boundary conditions. The effect of non-uniform parameter appeared to be more pronounced for the concentrated load, especially when the nanobeam is simply supported. Secondly the contour plots of distributed loads with respect to tip load and non-uniformity parameter was shown for a nanobeam with fixed nonlocal parameter. The sensitivity here was

more observable for clamped-clamped column. Moreover, buckling values for uniform and triangular loads decreased the most when the tip load increased in the case of clamped-free columns.

Remark. The application of the present theory to a nanocone permitted the plotting of the axial forces vs radius ratio. The results showed that the buckling loads increase with the radius ratio and decreases with increasing small scale constant.

## 10.2-Future prospects

The Love-Kirchhoff theory was used in order to derive the equations of plates in this thesis, although there exist many other theories. These theories include von Karman or Mindlin models of rectangular plate, which can be explored for future research. Also, composite rectangular plate subjected to follower forces have not yet been studied and could therefore be considered as potential extension of the present work. Nonlocal theory could be applied in order to derive the equation of a nanoplate under nonuniformly distributed axial loads and the same analysis can be applied to compute the buckling loads following exactly the same procedure utilized in this dissertation.

Carbon nanotubes were considered as nanobeams in the present work. The work can be extended to nanorods which are modelled as cylindrical shells. The study of nonlinear viscoelastic CNTs could also represent a very good and interesting prospect, as this work could be used as starting point.